Lysophosphatidic Acid: Role in CXCL12-Mediated Vascular Repair and Atherogenic Monocyte Recruitment

Von der Fakultät für Mathematik, Informatik und Naturwissenschaften der RWTH Aachen Universität zur Erlangung des akademischen Grades einer Doktorin der Naturwissenschaften genehmigte Dissertation

vorgelegt von
M.Sc. Biotechnology
Pallavi Subramanian
aus
Pondicherry, India

Berichter:
Universitätsprofessor Dr. med. Andreas Schober
Universitätsprofessor Dr. rer. nat. Jürgen Bernhagen

Tag der mündlichen Prüfung: 12.06.2012

To my father

The results of this work were in part published in:

Subramanian P*, Karshovska E*, Reinhard P, Megens RT, Zhou Z, Akhtar S, Schumann U, Li X, van Zandvoort M, Ludin C, Weber C, Schober A. Lysophosphatidic acid receptors LPA_1 and LPA_3 promote CXCL12-mediated smooth muscle progenitor cell recruitment in neointima formation. Circ Res. 2010;107:96-105. * Equal contribution

Zhou Z*, **Subramanian P***, Sevilmis G, Globke B, Soehnlein O, Karshovska E, Megens RT, Heyll K, Chun J, Saulnier-Blache J, Reinholz M, van Zandvoort M, Weber C, Schober A. Lipoprotein-derived lysophosphatidic acid promotes atherosclerosis by releasing CXCL1 from the endothelium. Cell Metabolism, 2011;13:592-600. * Equal contribution

Table of contents

Abbreviations

Ab	Antibody
AC	Adenylyl cyclase
ALT	Alanine transaminase
ApoE	Apolipoprotein E
ApoB100	Apolipoprotein B100
ARNT	Aryl hydrocarbon receptor nuclear translocator
ATX	Autotaxin
BM	Bone marrow
CAD	Coronary artery disease
CCA	Common carotid artery
CRP	C-reactive protein
DAG	Diacylglycerol
DAPI	4',6-Diamidino-2-phenylindol
DGPP	Dioctylglycerol pyrophosphate
DGK	Diacylglycerol kinase
DMSO	Dimethyl sulfoxide
DMEM	Dulbecco’s modified eagle medium
EC	Endothelial cell
ECA	External carotid artery
EDG	Endothelial differentiation gene
EEL	external elastic lamina
ELR	Glutamate-leucine-arginine

ELISA	Enzyme-linked immunosorbant assay
ESAM	Endothelial cell-selective adhesion molecule
EVG	Elastica van gieson
FDA	Food and Drug Administration
FDG	Di-β-d-galactopyranoside
FIH	Factor inhibiting HIF-1α
FSC	Forward scatter
GAG	Glycosaminoglycan
GDP	Guanosine diphosphate
GPCR	G protein-coupled receptor
GRO	Growth-regulated oncogene
GTP	Guanosine triphosphate
HBSS	Hanks balanced salt solution
HFD	High fat diet
HIF	Hypoxia inducible factor
HRE	HIF response element
HRP	Horse radish peroxidase
HUVECS	Human umbilical endothelial cells
ICA	Internal carotid artery
ICAM-1	Inter-cellular adhesion molecule-1
IEL	Internal elastic lamina
Ig	Immunoglobulin
IP	Intraperitoneal
IVM	Intravital microscopy

IV	Intravenous
JAM	Junctional adhesion molecule
KC	Keratinocyte-derived chemokine
LCAT	Lecithin-cholesterol acyltransferase
LDL	Low density lipoprotein
LDLr	Low density lipoprotein receptor
LFA1	Leukocyte functional antigen 1
lin	Lineage
LPA	Lysophosphatidic acid
LPL	Lysophospholipids
LPC	Lysophosphatidylcholine
LPE	Lysophosphatidylethanolamine
LPS	Lysophosphatidylserine
LPA_1	Lysophosphatidic acid receptor 1
LPA_2	Lysophosphatidic acid receptor 2
LPA_3	Lysophosphatidic acid receptor 3
LPA20:4	1-arachidonoyl-2-lyso-*sn*-glycero-3-phosphate
LPA18:0	1-stearoyl-2-lyso-sn-glycero-3-phosphate
MAC1	Macrophage receptor 1
MADCAM1	Mucosal vascular addressin cell-adhesion molecule 1
MC	Monoclonal
M-CSF	Macrophage colony stimulating factor
MIF	Macrophage migration inhibitory factor
MIP-2	Macrophage inflammatory protein-2

MM6	Mono mac6
mmLDL	Minimally modified low density lipoprotein
moxLDL	Mildly oxidised LDL
MPC	Monocyte chemotactic protein
nLDL	Native LDL
ON	Overnight
oxLDL	Oxidised LDL
PA	Phosphatidic acid
PBS	Phosphate buffered saline
PC	Polyclonal
PCR	Polymerase chain reaction
PDGF	Platelet derived growth factor
PE	Phycoerythrin
PECAM1	Platelet/endothelial cell adhesion molecule 1
PETG	Phenylethyl β-D-thiogalactopyranoside
PFA	Paraformaldehyde
PI	Percutaneous interventions
PK	Protein kinase
PLD	Lysophospholipase D
PL	Phospholipase
PLC	Phospholipase C
PPAR	Peroxisome proliferator activated receptor
PS	Phosphatidylserine
PSGL1	P-selectin glycoprotein ligand 1

PTM	Photomultiplier tube
RD	Regular diet
RHO	RAS homologue
RT	Reverse transcription
Sca-1	Stem cell antigen-1
SDF	Stromal cell derived factor
SDS-PAGE	Sodiumdocecylsulfate-polyacrylamide-gelelectrophoresis
SHG	Second harmonic generation
SMC	Smooth muscle cell
SMA	Smooth muscle actin
SPC	Smooth muscle progenitor cell
SR-A	Scavenger receptor A
SRE	Serum response element
SSC	Side scatter
STCAO	Subacute thrombotic coronary artery occlusion
SYK	Spleen tyrosine kinase
TMB	3,3,5,5-tetramethylbenzidine
TNF	Tumour necrosis factor
TPLSM	Two photon laser scanning microscopy
VCAM-1	Vascular cell adhesion molecule-1
vHL	Von Hippel-Lindau tumour suppressor protein
VLA4	Very late antigen 4
VSMC	Vascular smooth muscle cell
vWF	Von Willebrand factor

WPB	Weibel-Palade bodies
1AGP18:1	1-oleyl-2-lyso-*sn*-glycero-3-phosphate

1 Introduction

1.1 Lysophosphatidic acid (LPA)

Lysophosphatidic acid (LPA) is a lipid mediator which is found in different biological samples such as serum and plasma [1]. The structure of LPA consists of a glycerol backbone, a fatty acid chain and a phosphate group. Depending on variability in the fatty acid chain length, the saturation, and the type of linkage to the glycerol backbone, it has various biological functions [1, 2]. LPA is produced following platelet activation and exerts many functions such as SMC contraction, platelet aggregation, wound healing, induces changes in blood pressure, Ca^{2+} mobilisation, chemotaxis, neurite regeneration and differentiation [1].

Two pathways have been described for LPA synthesis [1]. In the first pathway, lysophospholipids (LPL) such as lysophosphatidylcholine (LPC), lysophosphatidylethanolamine (LPE) and lysophosphatidylserine (LPS) are produced via the enzymes secretory-type phospholipase (PL)-A_2 and phosphatidylserine (PS)-specific PLA_1 (Fig. 1) [1]. LPC can also be produced in the plasma from lipoprotein-derived phosphatidylcholine by the action of the enzymes lecithin-cholesterol acyltransferase (LCAT) and PLA1-like enzymes (Fig. 1) [1]. The LPLs which are produced by these various mechanisms are then converted to LPA by the lysophospholipase D (PLD) activity of the enzyme autotaxin (ATX) (Fig. 1). High levels of ATX are present in the blood [1]. The depletion of ATX in serum or plasma leads to the complete absence of LPA. ATX is considered to be the major LPA producing enzyme in the blood [1].

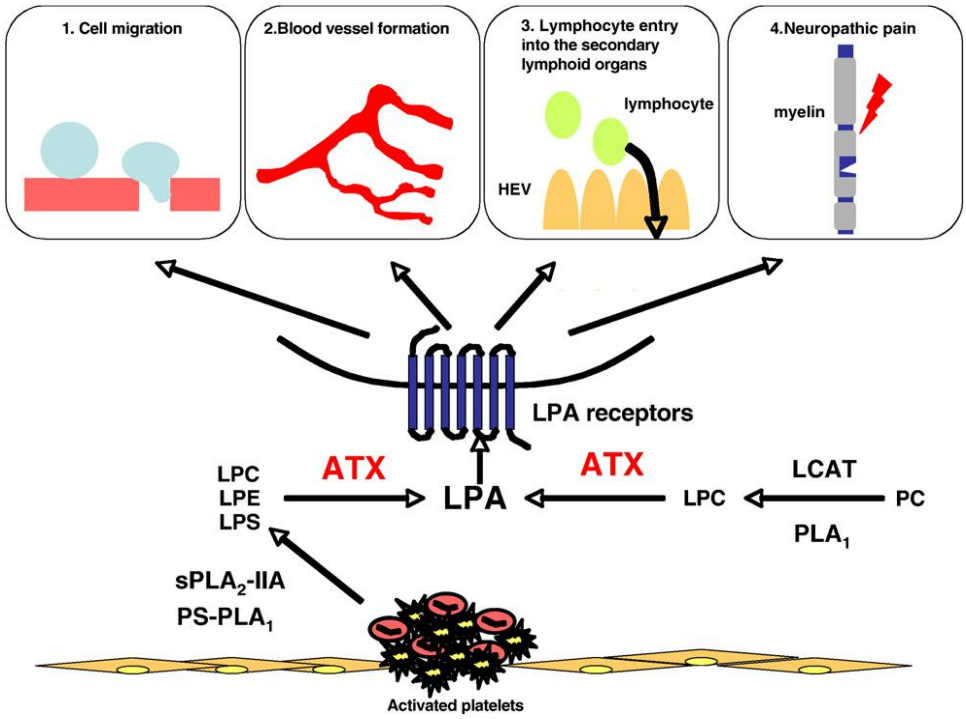

Figure 1: LPA synthesis by ATX

LPL such as LPC, LPE and LPS are produced from activated platelets and from lipoproteins by the action of various enzymes. These LPLs are then converted to LPA via the enzyme ATX [1].

In the second pathway of LPA synthesis, phosphatidic acid (PA) is produced from phospholipids or diacylglycerol (DAG) by the action of the enzymes PLD or diacylglycerol kinase (DGK) (Fig. 2). PA is further converted to LPA by PLA_1- or PLA_2-type enzymes (Fig. 2) [1]. Since the occurrence of PA can be found in the cell membrane, this reaction mostly occurs in the cell or in the plasma membrane.

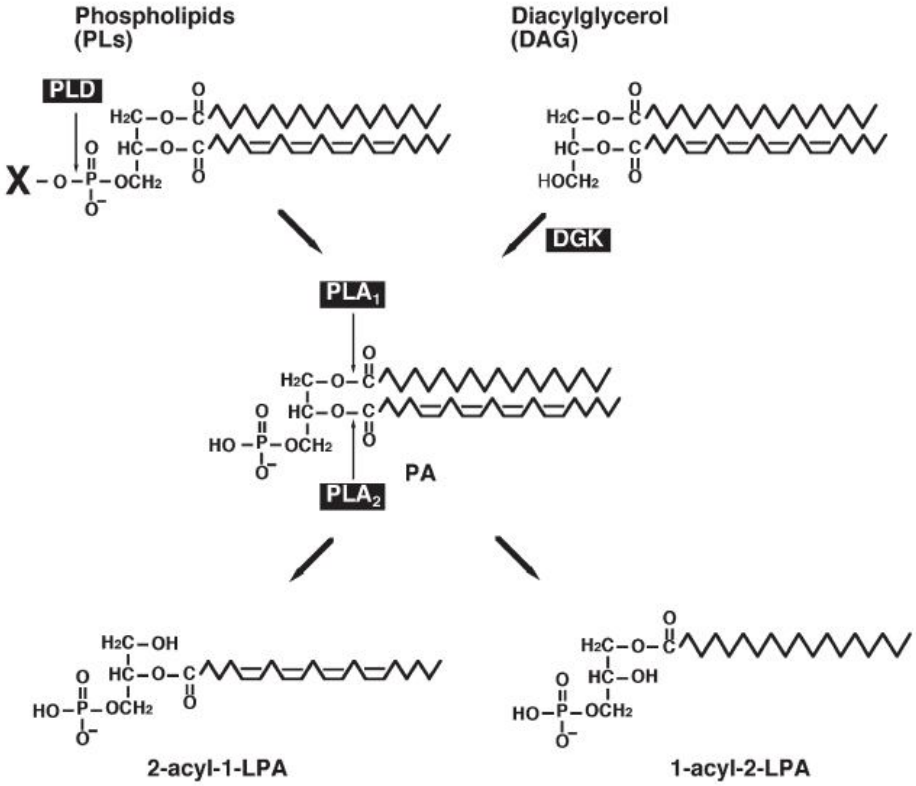

Figure 2: LPA synthesis from PA
PA is produced from phospholipids and DAG by the enzymes PLD and DGK. Then, PA is converted to LPA by the action of PLA1 and PLA2 [1].

LPA elicits its functions via seven G-protein coupled receptors namely LPA_1/EDG2, LPA_2/EDG4, LPA_3/EDG7, LPA_4/GPR23/P2Y9, LPA_5/GPR92, GPR87, and P2Y5/P2RY5 [1, 3, 4]. In addition, LPA also activates the nuclear receptor, peroxisome proliferator activated receptor (PPAR)-γ [5, 6]. Out of these receptors, LPA receptor 1 (LPA_1), LPA_2, and LPA_3 belong to the endothelial differentiation gene (EDG) family [7] and show 50% similarity at the amino acid level [1]. LPA_1, LPA_2, and LPA_3 play a role in physiological and pathological conditions as revealed by genetically null mice [1, 4, 8]. LPA_4, LPA_5, GPR87, and P2Y5 belong to the group of purinergic receptors and are approximately 35% homologous at amino acid level [1]. The pathological importance of these receptors are unknown [1]. Another orphan receptor named P2Y10 has also been identified that can be activated by LPA [9].

The first receptor identified for LPA was LPA_1 [8]. In adult mice LPA_1 is expressed in the brain, heart, lung, stomach, small intestine, spleen, thymus, testis and skeletal muscle [8]. Activation of LPA_1 leads to cell proliferation, MAP kinase activation, activation of serum response element (SRE), AKT activation, adenylyl cyclase (AC) inhibition, protein kinase (PK) C activation, and Rho activation through three types of G proteins namely $G_{i/o}$, G_q, $G_{12/13}$ [8]. LPA_2 expression in mice can be seen in the embryonic brain, testis, kidney, lung, thymus, spleen, and

stomach [8]. Similar to LPA_1, the signalling events induced by LPA_2 also occur via the three G proteins, $G_{i/o}$, G_q, and $G_{12/13}$. LPA_3 expression is present in the testis, kidney, lung, small intestine, heart, thymus, brain, oviduct, placenta, and uterus in adult mice [8]. Following activation of LPA_3 the downstream signalling events occur only via two G proteins, $G_{i/o}$ and G_q [8].

LPA has been demonstrated to be involved in many biological processes associated with atherosclerosis. LPA is generated during mild oxidation of LDL [10]. It is the active component of mildly oxidised LDL (moxLDL) which induces platelet activation, endothelial stress fibre formation and endothelial gap junction formation [10]. LPA accumulation in human carotid atherosclerotic lesions has been identified, with the highest amounts present in the lipid rich core of the plaque [10, 11]. LPA has also been shown to be the major platelet activating lipid in the plaque [10]. *In vitro*, LPA stimulates endothelial-monocyte adhesion by increasing the endothelial expression of adhesion molecules and chemokines such as inter-cellular adhesion molecule-1 (ICAM-1), IL-1β, IL-8, MCP-1, E-selectin, and vascular cell adhesion molecule-1 (VCAM-1) [12, 13]. In addition, increased levels of serum LPA has been detected in hypercholesterolemic rabbits due to increased ATX activity [14]. Although there are many studies which show that LPA is involved in atherosclerosis, there is no direct evidence for this association.

Short term intraluminal incubation of uninjured carotid arteries with unsaturated LPAs but not saturated LPAs induces the formation of neointimal hyperplasia containing mostly SMCs [5]. Out of these unsaturated LPAs, LPA20:4 (1-arachidonoyl-2-lyso-*sn*-glycero-3-phosphate) and the LPA analogue, 1-AGP18:1 (1-oleyl-2-lyso-*sn*-glycero-3-phosphate) were the most efficient in inducing neointima formation in rats [5].

LPA has been shown to up-regulate the chemokine CXCL12 in human adipose tissue derived mesenchymal stem cells which can be inhibited by blocking LPA_1 and LPA_3 using the antagonist Ki16425 [15]. Although LPA induces *in vitro* the proliferation of rat VSMC [16], the exact mechanism by which LPA induces neointima formation is unknown.

1.2 Chemokines

Chemokines are a family of heparin binding proteins that direct leukocyte migration [17-19]. They can be presented on the cell surface by binding to glycosaminoglycans (GAGs), hence producing an immobilised chemokine gradient under flow conditions [20]. Approximately 50 human chemokines and 20 chemokine receptors have been discovered (Table.1) [18, 19, 21].

Most of the chemokines have four cysteine residues and based on the amino acid sequence which is present between the first two cysteine residues they are further classified into chemokine

subfamilies [17, 18, 22]. Chemokines with one amino acid present in between the first two cysteine residues are known as CXC or α-chemokines [17, 19, 22]. These CXC chemokines can be further divided into ELR+ and ELR- chemokines [17]. The ELR+ chemokines, such as CXCL1, have a glutamate-leucine-arginine (ELR) residue preceding the first cysteine residue of the CXC motif. The ELR+ chemokines are chemotactic for neutrophils and have angiogenic properties, whereas the ELR- chemokines are chemotactic for lymphocytes and are mostly angiostatic in nature except for CXCL12 [18, 23]. Inflammatory mediators such as interleukin-1, tumour necrosis factor (TNF)-α or bacterial antigens such as lipopolysaccharide induce the synthesis of ELR+ chemokines [17].

If the first two cysteines are adjacent to each other, chemokines are classified as CC- or β-chemokines (examples- CCL1, CCL2, CCL3, and CCL4) which are the largest family of chemokines. The third subfamily includes only one member (CX_3CL1) and is characterised by three amino acid molecules in between the first two cysteine residues (CX_3C or the γ-chemokine) [19]. The fourth chemokine subtype, called C or δ-chemokines (examples- XCL1, XCL2), contain only two of the four cysteine residues [17, 19, 22].

Initially, chemokines were broadly classified based on their function as homeostatic and inflammatory chemokines [19, 22]. The homeostatic chemokines are continuously produced and secreted and they have many functions, such as immune surveillance and localisation of lymphocytes with the antigens in the lymphatic system [19, 22]. The inflammatory chemokines are induced only during infection or by non-infectious pro-inflammatory stimuli. Here, they guide the migration of leukocytes to the area of infection and inflammation. Later it became clear that some chemokines cannot be designated to either of these functional groups and are therefore referred to as dual function chemokines [24].

Chemokines act via G protein-coupled chemokine receptors [17, 19, 23, 25], which are named according to their chemokine ligands (e.g., chemokine receptors that bind to CXC chemokines are called CXC receptors) (Table.1) [18]. Notably, many chemokines can bind the same chemokine receptor and a single chemokine can bind multiple receptors [23].

Upon binding to the receptor, the N-terminal domain of the chemokine is of crucial importance for receptor activation [18, 22, 26]. Following activation of the chemokine receptor, the guanosine diphosphate (GDP) bound to the α subunit of the G proteins is replaced by guanosine triphosphate (GTP). Then the G proteins disassociate from the receptor and activate downstream molecules resulting in a cascade of signalling events which can lead for example to actin re-arrangement, shape change and cell movement [27].

Receptor	Ligands
CCR1	CCL3,CCL5,CCL7,CCL13,CCL14,CCL15,CCL16,CCL23
CCR2	CCL2,CCL7,CCL8,CCL13,CCL16
CCR3	CCL5,CCL7,CCL8,CCL11,CCL13,CCL15,CCL16,CCL24,CCL26,CCL28
CCR4	CCL17,CCL22
CCR5	CCL3,CCL4,CCL5,CCL8,CCL11,CCL14,CCL16
CCR6	CCL20
CCR7	CCL19,CCL21
CCR8	CCL1
CCR9	CCL25
CCR10	CCL27,CCL28
CXCR1	CXCL6,CXCL7,CXCL8
CXCR2	CXCL1,CXCL2,CXCL3,CXCL5,CXCL6,CXCL7,CXCL8
CXCR3-A	CXCL9,CXCL10,CXCL11
CXCR3-B	CXCL4,CXCL9,CXCL10,CXCL11
CXCR4	CXCL12
CXCR5	CXCL13
CXCR6	CXCL16
CXCR7	CXCL12
XCR1	XCL1,XCL2
CX_3CR1	CX_3CL1
CCX-CKR	CCL19,CCL21,CCL25
D6	CCL2,CCL3L1,CCL4,CCL5,CCL7,CCL8,CCL11,CCL13,CCL14,CCL17, CCL22
DARC/Duffy	CCL2,CCL7,CCL8,CCL11,CCL13,CCL14,CCL16,CCL17,CXCL1,CXCL5, CXCL6,CXCL7,CXCL8,CXCL9,CXCL11,CXCL13

Table 1: Chemokines and chemokine receptors [18]

1.3 Atherosclerosis

Cardiovascular diseases are the main cause of mortality worldwide [28, 29]. One of the most common type of cardiovascular disease is coronary artery disease (CAD) which is mainly caused by atherosclerosis [28, 30]. Atherosclerosis is a chronic inflammatory disease of large- and medium-sized vessels which forms lesions in the vessel wall [28, 31-34]. These lesions are known as atherosclerotic plaques. Over time these plaques gradually increase in size and may cause complications such as a reduction in the lumen size making the vessel stenotic [31, 35, 36]. This stenosis may impair blood flow and thus limit the oxygen supply to tissues like the myocardium. Moreover, plaque rupture may occur resulting in acute obliteration of the vascular lumen due to thrombus formation when pro-thrombotic components of the plaque come into contact with the blood [34-37]. This acute vascular occlusion may cause ischemia and tissue necrosis with devastating clinical consequences, such as myocardial infarction or stroke [32, 34-37].

The development of atherosclerosis is initiated by pro-atherogenic factors such as diabetes or smoking leading to the activation and dysfunction of endothelial cells [32, 35, 37-39]. This results in increased adhesion of circulating leukocytes to the endothelium and increases the permeability of the vessel wall for plasma components, such as low density lipoprotein (LDL) [35, 37-39].

Although LDL is protected from oxidation in the plasma, it is susceptible to enzymatic and non-enzymatic modifications while present within the vessel wall [28, 40, 41]. Within the intima, the LDL particles are oxidised by myeloperoxidase and lipoxygenases or by reactive oxygen species such as HOCL, phenoxyl radical intermediates, or peroxynitrite which are generated in the intima during inflammation [28, 42]. The modified LDL particles further activate the endothelial cells to express various adhesion molecules resulting in the adhesion and transmigration of circulating monocytes to the sub-endothelial space [32, 34, 35] (Fig. 3). Following transmigration, these monocytes differentiate into macrophages which engulf excess of modified LDL particles and become foam cells, characteristic for fatty streaks (Fig. 3). This is due to the unrestricted uptake of modified LDL by macrophages via the scavenger receptors because these receptors do not have a negative feedback regulation system like the LDL receptor. Although many scavenger receptors are involved in this process, the scavenger receptor A (SR-A) and CD36 have been shown to play a significant role [34]. The formation of fatty streaks is the first stage in the development of atherosclerosis [32, 34-36].

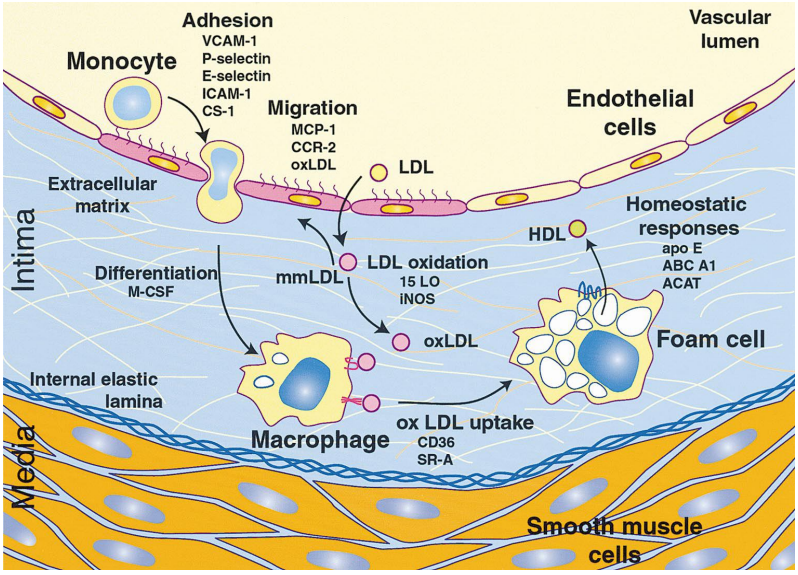

Figure 3: Initiation of atherosclerosis
Activated endothelial cells express various cell surface adhesion molecules leading to monocyte recruitment. The monocytes differentiate into macrophages and take up modified LDL particles to become foam cells [34].

The progression of fatty streaks to atherosclerotic plaque is caused by secretion of cytokines and growth factors by the plaque cells and involves the further accumulation of other inflammatory cell types, smooth muscle cells (SMC), and the deposition of extracellular matrix proteins [34, 37, 38] (Fig. 4).

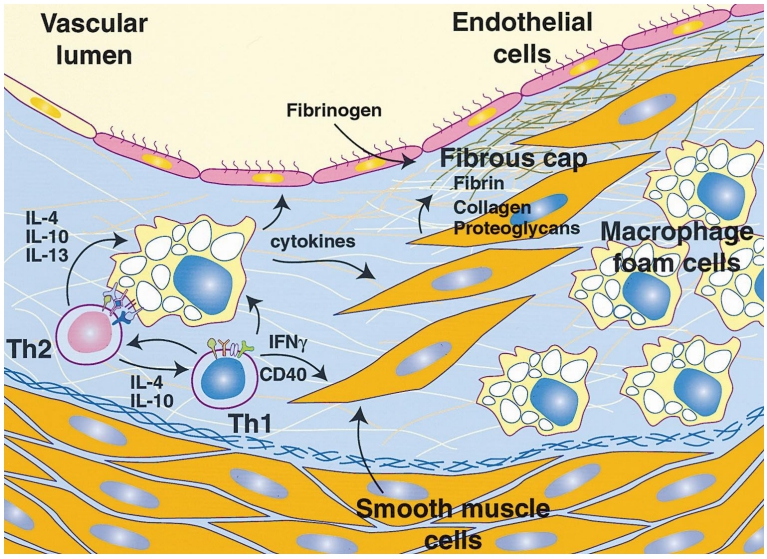

Figure 4: Atherosclerotic lesion progression
Further accumulation of immune cells, secretion of growth factors and formation of fibrous cap leads to plaque progression [34].

Necrosis of the lipid-laden foam cells results in the accumulation of extracellular cholesterol and the formation of a necrotic core which is surrounded by a fibrous cap (Fig. 5). Matrix degrading proteases released from the cells within the plaque can cause thinning of the fibrous cap and promote plaque rupture [32, 34-36] (Fig. 5). This releases the plaque lipids and tissue factor into the blood causing thrombus formation (Fig. 5) [32, 34-36].

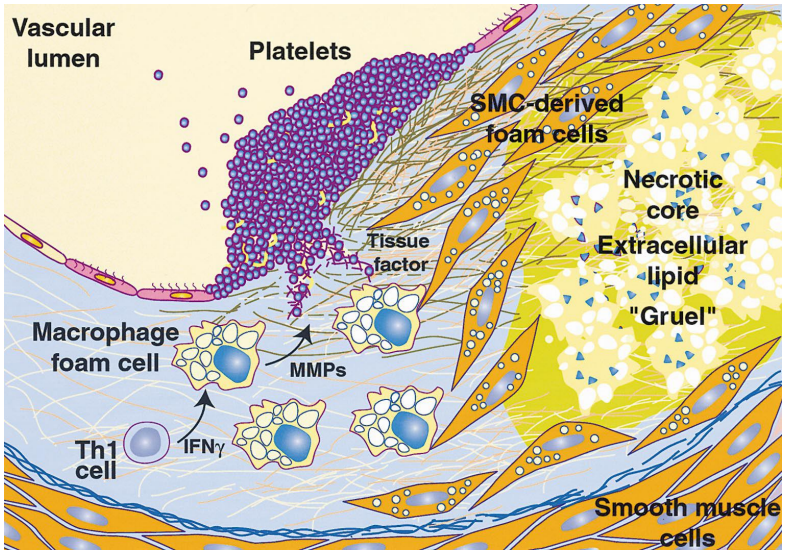

Figure 5: Plaque rupture and thrombosis
Proteases and cytokines produced from the plaque cells degrade the fibrous cap resulting in plaque rupture and thrombus formation [34].

1.3.1 Leukocyte adhesion cascade

The leukocyte adhesion cascade includes the following steps: tethering, rolling, slow rolling, arrest, adhesion strengthening, intravascular crawling, and paracellular or transcellular transmigration [43]. Leukocyte rolling and tethering is mediated by a family of three-carbohydrate recognising molecules named selectins [43-45]. P-selectin and E-selectin are expressed by inflamed ECs whereas L-selectin is expressed by leukocytes. P-selectin is also expressed by platelets [43, 45]. The ligands for selectins are highly glycosylated-glycoproteins, such as P-selectin glycoprotein ligand 1 (PSGL1), which is the primary ligand for all three selectins [43, 46]. PSGL1 is expressed on almost all leukocyte-subtypes. Binding of PSGL1 to L-selectin mediates leukocyte-leukocyte interactions which lead to secondary leukocyte tethering [43]. L-selectin and P-selectin require shear stress to support adhesion of leukocytes which is due to the catch bond character of selectins [47-49]. Binding of selectin to its ligand activates signalling pathways in the selectin-expressing and ligand-expressing cells [43].

Integrins are heterodimeric cell surface cell surface receptors that participate in inducing leukocyte rolling and firm adhesion [43, 44, 46]. Rolling by lymphocytes is due to interactions between very late antigen 4 (VLA4; also called $\alpha_4\beta_1$-integrin) present on lymphocytes and its ligand VCAM1 present on ECs. VLA4-induced rolling is mostly seen in monocytes and T-cells [43, 46]. The leukocyte functional antigen 1 (LFA1; also called $\alpha_L\beta_2$-integrin) is a β_2 integrin that supports rolling by binding to its ligand ICAM1 [43].

Endothelial-leukocyte arrest is triggered by chemokines and is mediated by the binding of leukocyte-specific integrins to their endothelial ligands [43, 46]. The ligand binding capacity of the

integrins, also known as avidity, mainly depends on the integrin affinity and valency. Integrin affinity is increased by inducing a conformational change in each of the integrin heterodimers which increases ligand-binding energy and reduces the rate of ligand-dissociation [43]. Integrin valency corresponds to the density of integrin heterodimers per area of the plasma membrane and is dependent on the mobility and the expression level of the integrin on the cell-surface [43].

During inflammation, inflammatory cytokines induce the expression of chemokines in ECs [43, 45]. Chemokines are immobilised on the endothelial surface through GAGs [43, 45], which facilitates the chemokine binding to their GPCR expressed on leukocytes under flow conditions and activates integrin-mediated adhesion [43, 45]. Chemokines can rapidly regulate the avidity of integrins by increasing both the affinity and valency, also known as inside-out signalling [45, 50, 51]. In contrast, outside-in signalling occurs following binding of the activated integrins to its ligand and regulates many cellular functions such as proliferation, apoptosis and motility [52, 53].

Following firm adhesion, leukocytes transmigrate through the vascular endothelium via either a transcellular or paracellular route [45]. Leukocytes crawl on the endothelial surface in a MAC1- and ICAM1-dependent manner promotes transmigration, indicating that leukocyte crawling assists in the identification of a suitable site for transmigration [43]. In paracellular transmigration, interaction between the endothelial cell-specific adhesion molecules and the leukocytes can reduce the inter-endothelial contacts and induce leukocyte migration through the endothelial-cell junctions [43]. An increased intracellular level of calcium results in contraction of ECs via activation of the myosin light chain kinase and opens up the endothelial-cell contacts [43]. Some endothelial junctional molecules such as platelet/EC adhesion molecule 1 (PECAM1), junctional adhesion molecule A (JAM-A), JAM-B, JAM-C ICAM1, ICAM2, and EC-selective adhesion molecule (ESAM) mediate leukocyte trans-endothelial migration [43].

The rather infrequent transcellular leukocyte migration occurs at thin regions of the endothelium and has been described in the central nervous system and at various sites of inflammation [54]. Leukocyte binding to ICAM1 translocates ICAM1 to actin- and caveolae-dense regions of the plasma membrane, which results in the formation of channels within the ECs through which leukocytes can migrate [43].

1.3.2 Keratinocyte-derived chemokine (KC)/CXCL1

CXCL1/KC is a 73 amino acid peptide that was initially isolated and characterised from malignant melanoma cells for its growth stimulatory activity [55, 56]. CXCL1 is a CXC chemokine containing the N-terminal ELR motif [18]. It has a human ortholog known as GRO

(growth-regulated oncogene)-α [57]. CXCL1 functions via its receptor, CXCR2 [57]. CXCL1 induces the chemotaxis of neutrophils and T lymphocytes [58, 59].

Arterial CXCL1 is important for macrophage accumulation during atherosclerosis via its receptor CXCR2 present on leukocytes [60]. Only CXCL1 but not the other CXCR2 ligand, macrophage inflammatory protein-2 (MIP-2) has been shown to induce monocyte arrest on isolated carotid arteries of atherosclerotic Apolipoprotein (Apo)$E^{-/-}$ mice [61]. In addition, mice with $CXCR2^{-/-}$ BM cells developed significantly less plaque with reduced macrophage accumulation indicating the importance of this receptor in macrophage localisation during atherosclerosis. The loss of CXCR2 does not affect the fatty streak formation but inhibits the development of plaque at later stages of atherosclerosis [60]. Moreover, it has been shown *in vitro* that minimally modified (MM) LDL induces the binding of monocytes to endothelial cells by up-regulating the chemokine CXCL1 on the endothelial surface [62]. In an activated endothelium, CXCL1 is immobilised on the cell surface by binding to heparin sulphate proteoglycans and induces rolling and firm arrest of monocytes to the endothelium via CXCR2 [63]. In contrast, CCL2/monocyte chemotactic protein (MCP)-1 is secreted following endothelial activation [63]. CCL2 via its receptor CCR2 induces monocyte shape change and transmigration when present as a gradient across the endothelial monolayer [63, 64].

1.4 Restenosis

Percutaneous interventions (PI) such as balloon angioplasty and stent implantation are most commonly used techniques to treat CAD [65-67]. Initially when bare metal stents were used, subacute thrombotic coronary artery occlusion (STCAO) occurred in 18% of the patients within 2 weeks of stent implantation [68]. To reduce the occurrence of STCAO following stent implantation, anti-coagulation therapy was used [68]. But this lead to increased bleeding and lengthened hospitalization time of the patients [68]. Following studies showed that stenting was safe when anti-platelet therapy was used instead of anti-coagulant therapy [69-71]. The use of stents became widely accepted following these studies. But another problem that was encountered following stent implantation was the development of in-stent neointimal hyperplasia. The mechanical injury to the vessel wall by PI induces the formation of neointimal thickening which is clinically known as restenosis [65, 72, 73] (Fig. 6). The neointimal tissue primarily consists of SMCs and leukocytes [74, 75]. Following implantation of bare metal stents, a restenosis rate of 10-30% was observed [65, 68]. The development of drug eluting stents reduced the risk for restenosis after PI [66, 76, 77]. These stents slowly release a drug, such as sirolimus or paclitaxel, which

inhibits cell proliferation and migration. In 2003, the approval for the use of drug eluting stents (Cordis's sirolimus-eluting cypher stent) was given by the Food and Drug Administration (FDA) and by the end of 2004, these stents were used in almost 80% of the PI in the United States [78].

Drug eluting stents have reduced the need for revascularisation of the target vessel following stent implantation substantially [66, 76, 77], however, a significant constrain is the requirement of long term treatment with drugs that inhibit platelet aggregation to avoid late stent thrombosis [79]. Drug eluting stents cause impaired endothelial recovery due to non-specific anti-migratory and anti-proliferative activities of the drugs such as rapamycin and paclitaxel. This is a major risk factor for late stent thrombosis [80-82]. Therefore, development of drugs that specifically inhibit the neointimal SMC accumulation without affecting the re-endothelialisation would be desirable.

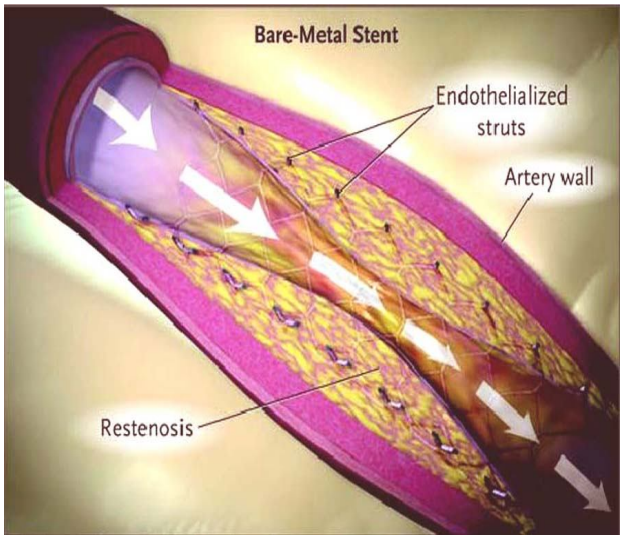

Figure 6: Restenosis
PI such as stent implantation injures the vessel wall leading to neointima formation also known as restenosis [83].

1.4.1 Stromal cell derived factor (SDF)-1α/CXCL12

SDF-1/CXCL12 also known as pre B-cell stimulatory factor belongs to the non-ELR CXC family of chemokines and was initially cloned from supernatant of BM-derived stromal cells [84-86]. CXCL12 is an exception in the CXC chemokine family because even though it is an ELR negative chemokine, it still has angiogenic activity [18]. CXCL12 induces the chemotaxis of $CD34^+$ cells, pre B-cells and hematopoietic progenitor cells [85, 87]. It was thought that CXCL12 induces its biological functions exclusively by binding to CXCR4. until the orphan receptor RDC1, designated now as CXCR7, has been characterised as an alternative CXCL12 receptor [88].

In mice, two CXCL12 isoforms, CXCL12α and CXCL12β, exist which are splicing variants encoded by the same gene [89, 90]. Both have identical amino acid sequences except for the four additional amino acids at the carboxy terminal of CXCL12β [86, 90]. The importance of the existence of two variants is unknown [90]. Four additional human CXCL12 isoforms have also been identified, namely CXCL12γ, CXCL12δ, CXCL12ε and CXCL12Φ, but their physiological and pathological relevance is unknown [91]. CXCL12α is chemotactic for hematopoietic progenitor cells [85]. CXCL12α is highly conserved between different species, for example, the human and murine CXCL12α differ only in one amino acid [85]. Hereafter, CXCL12 will refer to CXCL12α.

The gene encoding CXCL12 is located in chromosome 10 whereas all the other human α and β chemokines are encoded in chromosomes 4 and 17, respectively [92]. All other chemokines are usually expressed during inflammation, whereas CXCL12 mRNA is constitutively present in different organs [86]. The knock down of *CXCR4* or *CXCL12* genes in mice causes embryonic death due to deficiency in B-lymphopoiesis, myelopoiesis, vasculogenesis, and defective heart development [93, 94]. The retention of hematopoietic stem cells in the bone marrow (BM) requires high concentration of CXCL12 in the BM compared to the circulation [95]. Overexpression of CXCL12 in the circulation by an adenoviral vector resulted in the mobilisation of hematopoietic progenitor cells to the peripheral circulation [95]. CXCR4 antagonists such as plerixafor are used as drugs to mobilise stem cells from the BM to the circulation, so that these stem cells can be collected for transplantation to patients suffering from non-Hodgkin's lymphoma or multiple myeloma [96].

1.4.2 CXCL12-induced stem cell mediated vascular repair

The CXCL12/CXCR4 axis plays a crucial role in neointima formation following vascular injury in mice by inducing the stem cell-mediated vascular repair [97, 98]. Immediately after vascular injury, approximately 70% of the medial SMCs are apoptotic [99]. The repair of the vessel wall by resident SMCs is not adequate resulting in the recruitment of smooth muscle progenitor cells (SPCs) from the BM [99]. High concentration of CXCL12 in the circulation mobilises progenitor cells from the BM to the circulation. Therefore it is assumed that progenitor cells are retained within the BM due to the high CXCL12 concentration in the BM compared to the circulation [95]. As early as 1 day following wire-induced vascular injury in mice, CXCL12 protein is up-regulated in the vascular smooth muscle cells (VSMC) and in the circulation [98]. It is assumed that there is a change in the CXCL12 concentration gradient between the circulation and the BM, which

triggers the mobilisation of the SPCs (these SPCs express the stem cell antigen-1 (Sca-1), PDGFR-β and CXCR4 but not hematopoietic lineage markers) to the circulation (Fig. 7). Blocking the CXCL12 receptor, CXCR4 following injury inhibited the mobilisation of SPCs and neointima formation [100]. This indicates that, the SPCs which are mobilised following injury are further recruited to the site of injury via CXCR4 resulting in the formation of neointimal hyperplasia (Fig. 7). But the molecule produced following injury which induces this stem cell-mediated vascular repair is unknown. Following vascular injury, a majority of the medial SMCs are apoptotic [97]. When cultured SMCs were exposed to apoptotic bodies generated from injured SMCs, it induced the expression of CXCL12 [97]. Following injury, apoptosis could be the signal which induces the expression of CXCL12 in the vessel wall.

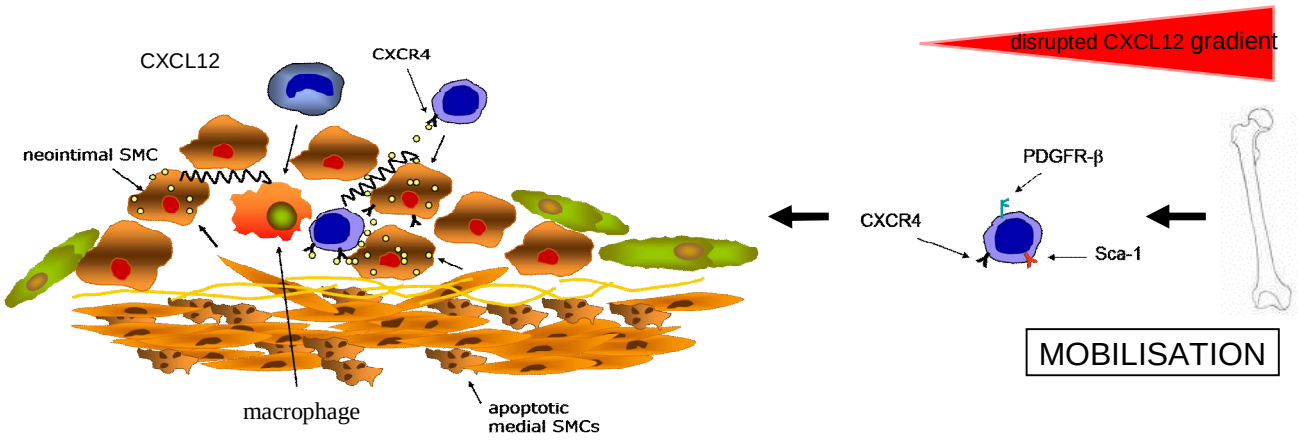

Figure 7: Model of CXCL12 mediated vascular repair
Following vascular injury, the concentration of CXCL12 is upregulated in the circulation disrupting the CXCL12 gradient between the BM and the circulation. This induces the mobilisation of SPCs to the circulation which are then recruited to the site of injury resulting in neointima formation. (Modified according to Schober 2008)

Hypoxia inducible factor (HIF)-1 is a transcription factor which regulates oxygen and energy haemostasis [101]. It is a multi-subunit protein which is made of two basic helix loop helix proteins namely, HIF-1α and HIF-1β or aryl hydrocarbon receptor nuclear translocator (ARNT) [102]. HIF-1 is a constitutively produced transcription factor. Under normoxia, HIF-1α is unstable and is targeted to proteosomal degradation, whereas HIF-1β is stably expressed in the nucleus irrespective of the oxygen level [103].

Under normoxia, the HIF-1α subunit is hydroxylated in the proline and asparaginyl residues by the enzymes proline hydroxylase and factor inhibiting HIF-1α (FIH), respectively (Fig. 8A). Following hydroxylation, the von Hippel-Lindau tumour suppressor protein (vHL) binds to HIF-1α, and ubiquitinylates it, thereby targeting HIF-1α for proteosomal degradation (Fig. 8A) [102].

Under hypoxia, the oxygen dependent hydroxylation of HIF-1α is downregulated; hence HIF-1α is protected from poly-ubiquitinylation and degradation by the proteosomal complex (Fig. 8B). Then, HIF-1α is transferred to the nucleus where it binds to HIF-1β and the transcriptional co-activator proteins such as p300/CBP; and regulates gene transcription at the HIF response elements (HRE) of the target gene (Fig. 8B).

HIF-1α plays an important role in neointima formation following vascular injury [104]. In mice, transcriptional upregulation of HIF-1α is evident following carotid injury. This in turn induces the expression of CXCL12 in the neointimal tissue [104]. CXCL12 has been shown to induce neointima formation following vascular injury by the recruitment of BM-derived SPCs [97, 98]. Following carotid injury, HIF-1α regulates the stem cell based repair of arteries by upregulating CXCL12 expression. But the upstream molecule produced following vascular injury which activates this HIF-1α-dependent stem cell repair mechanism remains to be determined.

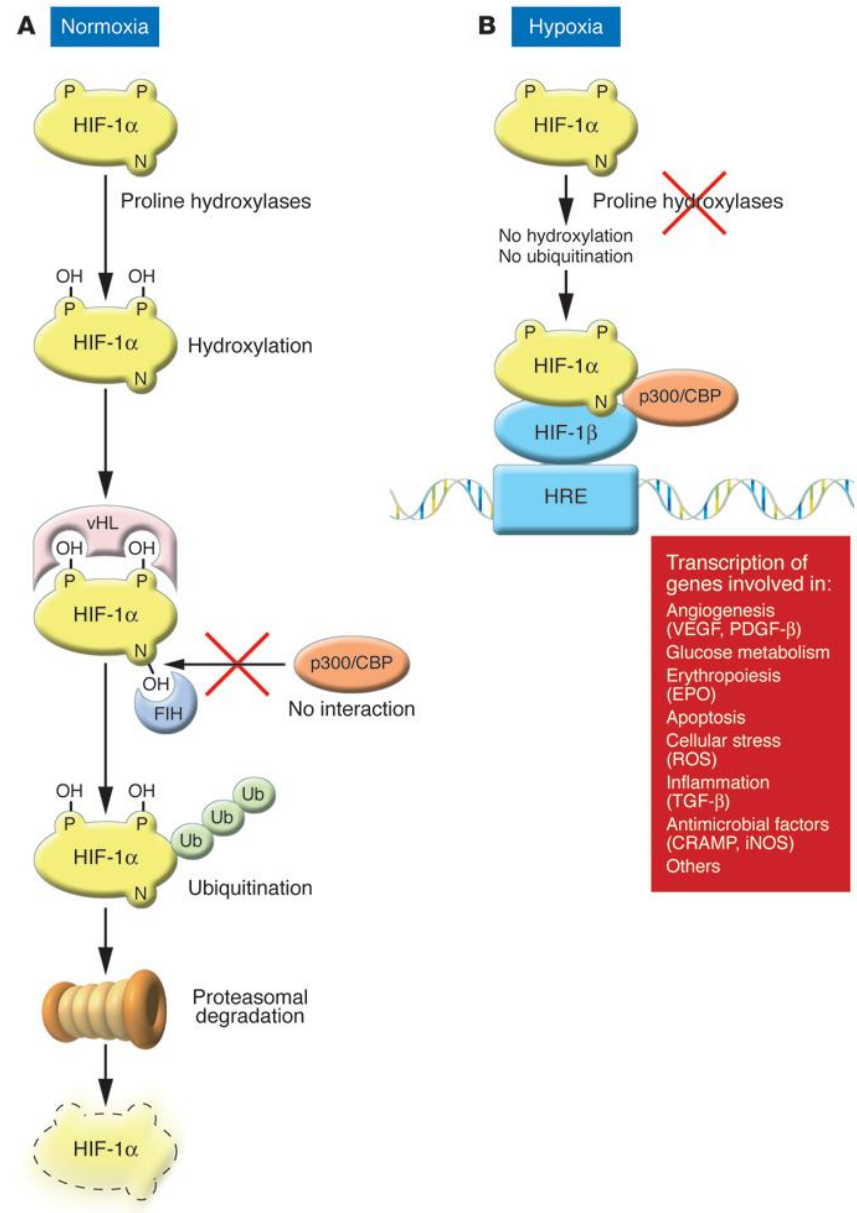

Figure 8: Regulation of HIF-1α subunit under hypoxia and normoxia

a) Under normoxia, HIF-1α protein is hydroxylated by proline hydroxylase at the proline residues and by FIH at the asparaginyl residues. FIH also inhibits the interaction of HIF-1α with P300/CBP transcriptional co-activator proteins. Then, HIF-1α is bound and ubiquitinylated by vHL, and finally degraded by the proteosomal complex. b) Oxygen, the co-factor for proline hydroxylase is absent during hypoxia. HIF-1α is protected from hydroxylation and degradation by the proteosomal complex under hypoxia. So, it binds to HIF-1β and regulates gene expression at the HRE sites of the target gene [102].

1.5 Aim of the study

The CXCL12/CXCR4 axis has been shown to play an important role in neointima formation following vascular injury by inducing the mobilisation and recruitment of SPCs from the BM [97-99]. Unsaturated LPAs which can upregulate CXCL12 *in vitro*, can induce neointimal hyperplasia containing mainly SMCs even in the absence of injury [15, 105]. Following vascular injury, HIF-1α is upregulated and regulates the neointimal expression of CXCL12 [104]. MmLDL induces monocyte adhesion to the endothelium by upregulating the endothelial expression of CXCL1 [62]. Furthermore, LPA which can be produced during mild oxidation of LDL induces monocyte adhesion to the endothelium by upregulating various adhesion molecules and chemokines [10, 12, 13].

The hypothesis of this study is that LPA induces different chemokine axes depending on the vascular cell type and this in turn triggers different types of atherosclerotic diseases. LPA acts on SMCs to induce the CXCL12-mediated SPC recruitment during neointima formation and it acts on endothelial cells to induce CXCL1-mediated monocyte adhesion during hyperlipidemia-induced atherosclerosis. Following are the objectives of this study:

- To identify the molecular mechanism of LPA-induced neointima formation and the role of the individual LPA receptors, LPA_1 and LPA_3 in mediating this effect.
- To determine if LPA can recruit BM-derived SPCs to the neointima and to define the role of LPA receptors in this process.
- To find out if LPA is the active component of moxLDL that induces monocyte adhesion to the endothelium and to identify the role of CXCL1 in mediating this effect. In addition, to determine the role of the individual LPA receptors, LPA_1 and LPA_3 in mediating LPA-induced monocyte recruitment.
- To find out the role of different LPA species in promoting atherogenesis and the role of the LPA receptors in mediating atherosclerotic plaque development.

2 Materials and methods

All solutions were prepared with Millipore water (Milli-Q Plus ultrapure purification, Millipore, Billerica, USA). The reagents were purchased from Sigma-Aldrich (Steinheim, Germany), Carl Roth (Karlsruhe, Germany), Merck (Darmstadt, Germany) and Fluka (Buchs, Switzerland) unless stated otherwise in the text.

2.1 General equipment

Balance -	Sartorius CPA64 (Sartorius mechatronics, Germany)
Centrifuge -	Heraeus multifuge 3S-R (Heraeus, Osterode, Germany) Hettich mikro 200R (Hettich laborapparate, Germany)
Flow cytometer -	FACSCantoII (BD Biosciences, San Jose, CA, USA)
Microscopes -	Leica DMLB (Leica, Wetzlar, Germany) and Olympus SZX10 (Olympus optical, Germany)
Laminar flow hood -	Herasafe (Heraeus, Osterode, Germany)
pH-meter -	SCHOTT Instruments Lab 850 (SI Analytics GmbH, Mainz, Germany)
Spectrophotometer -	nanoVue plus (GE Healthcare, Uppsala, Sweden) and nanodrop 1000 (PeqLab, Erlangen, Germany)
PCR thermocyclers -	MyCycler (Bio-Rad, Hercules, USA) and 7900HT fast real-time PCR system (Applied Biosystems, Darmstadt, Germany)
Tissue homogenizer -	TissueLyserLT (Qiagen, Hilden, Germany)
Autoclave -	systec 2540EL (systec, Wettenberg, Germany)
Microtome -	Cut 6062 (SLEE medical GmBH, Mainz, Germany)
Plate reader -	microplate reader SpectraFluor Plus (Tecan, Crailsheim, Germany)
Image reader -	LAS 3000 (Fujifilm, Dusseldorf, Germany)

2.2 Antibodies

2.2.1 Primary antibodies

Antigen	Details	Supplier
α-SMA	monoclonal mouse anti-human alpha smooth muscle actin antibody (clone 1A4)	Dako
Mac-2	anti-mouse monoclonal Mac-2 antibody (clone M3/38)	Cedarlane
CXCL12	human/mouse CXCL12/SDF-1 antibody (clone 79018)	R&D systems
HIF-1α	rabbit polyclonal hypoxia inducible factor-1 alpha antibody	Santa cruz biotechnology
SM22 alpha	rabbit polyclonal SM22 alpha antibody	Abcam
Calponin	rabbit monoclonal calponin antibody (clone EP798Y)	Abcam
von Willebrand factor (vWF)	rabbit polyclonal von Willebrand Factor antibody	Abcam
CD3	rabbit polyclonal CD3 antibody	Dako
CXCR4	rat polyclonal CXCR4 antibody	Santa Cruz biotechnology
Sca-1	goat polyclonal stem cell antigen-1 antibody	R&D systems
LPA_1 receptor	rabbit polyclonal lysophosphatidic acid receptor 1 antibody	Imgenex
LPA_3 receptor	rabbit polyclonal lysophosphatidic acid receptor 3 antibody	Imgenex
β-galactosidase	rabbit polyclonal β-galactosidase antibody	Abcam
CXCL1	rabbit polyclonal CXCL1 antibody	peprotech
CXCL1	monoclonal rat anti-mouse CXCL1/KC antibody (clone 124014)	R&D systems
IgG	monoclonal rat anti-rat IgG antibody (clone 54447)	R&D systems

2.2.2 Fluorescent antibody and streptavidin conjugates

goat-anti-rabbit IgG	Dylight549-conjugated (KPL)
anti-rabbit IgG	biotinylated (Serotec)
streptavidin	Dylight549-conjugated (KPL)
donkey-anti-mouse IgG	FITC-conjugated (Jackson immunoResearch)
donkey-anti-rat IgG	FITC-conjugated (Jackson immunoResearch)
goat-anti-mouse IgG	Dylight488-conjugated (KPL)
donkey-anti-rabbit IgG	FITC-conjugated (Jackson immunoResearch)
donkey-anti-goat IgG	FITC-conjugated (Jackson immunoResearch)
donkey-anti-mouse IgG	cy3-conjugated (Jackson immunoResearch)

2.3 Buffers

Hanks´ complete solution:

1 x HBSS, 0.1% BSA and 5 mM EDTA

FACS staining buffer:

Phosphate buffered saline (PBS), 2% BSA, 2% mouse serum, 2% rabbit serum, 2% human serum

Flow cytometry lysis buffer:

150mM NH_4Cl, 10mM $KHCO_3$, 0.1mM EDTA, pH 7.4

MOPS buffer:

145 mmol/L NaCl, 4.7 mmol/L KCL, 2.0 mmol/L $CaCl_2$ $2H_2O$, 1.2 mmol/L $MgSO_4$ $7H_2O$, 5.0 mmol/ glucose, 2.0 mmol/L sodium pyruvate, 1.2 mmol/L NaH_2PO_4 H2O and 2.0 mmol/L MOPS, pH 7.4

ELISA lysis buffer:

100mM NaCl, 0.1mM EDTA, 20mM Tris (pH-7.4), 10% glycerol, 0.2% NP-40 and 0.1% Triton-100 containing protease inhibitors (1 tablet in 10 ml of lysis buffer, Roche).

Blotting buffer (1X)):

25mM Tris base, 192mM Glycine, 10% methanol, 0.005% SDS

TBS (1X):

25mM Tris-HCL, pH 7.4, 2.7 mM KCl, 137 mM NaCl

Hanks Balanced Salt Solution (HBSS):

144mM NaCl, 14.9mM HEPES, 5.5mM glucose, 4.7mM KCl, 2.5mM $CaCl_2$, 1.2mM KH_2PO_4 and 1.2mM $MgSO_4$, pH 7.4

Citrate buffer:

630ml millipore water, 12.6ml solution A (2.101g citric acid in 100ml millipore water), 57.4ml solution B(14.70g nitrium citrate in 500ml of millipore water), 320µl Tween 20, pH 6.

Western blot lysis buffers:

Lysis buffer A: 100mM NaCl, 20mM KCL, 0.5mM Na2HPO4, 20mM Tris (pH-7.4) with protease inhibitors (1 tablet in 10 ml of lysis buffer, Roche).
Lysis buffer B: 100mM NaCl, 0.1mM EDTA, 20mM Tris (pH-7.4), 10% glycerol, 0.2% NP-40 and 0.1% Triton-100 with protease inhibitors (1 tablet in 10 ml of lysis buffer, Roche).

Movat's staining solutions:

a) Alcian blue solution (1%): 1g Alcian blue 8 GX (Sigma A5268) was dissolved in 100ml of millipore water, filtered and 1ml of acetic acid was added.
b) *Alkaline ethanol:* 5ml ammonium hydroxide was mixed with 95ml of 96% ethanol.
c) *Orcein-Verhoeffschem Hematoxylin solution (stock solution):*
Solution A- 1g Orcein (Merck, 1071000025), 98ml 70% ethanol, 1ml 25% HCL
Solution B- 8g Hematoxylin (Sigma, H3136), 160ml 100% ethanol
Solution C- 9.6g Iron(III)-Chloride (Merck, 8039450500), 90ml Millipore water
Solution D- 1g Iodine, 2g Potassium iodide, 97ml Millipore water

d) *Orcein-Verhoeffschem Hematoxylin solution (working solution):* freshly prepared.

Solution A- 25ml

Solution B- 20ml

Solution C- 8ml

Solution D- 8ml

e) *Acidic alcohol:*

1ml of 25% HCL was added to 100ml of 95% ethanol.

f) *Brilliant Crocein Scarlet MOO (Stock solution):*

Solution A- 0.1g Brilliant Crocein Scarlet, 0.5ml Acetic acid, 99.5ml Millipore water

Solution B- 0.1g Acid fuchsin (Merck, 105231), 0.5ml Acetic acid, 99.5ml Millipore water

g) *Brilliant Crocein Scarlet MOO (working solution):*

Solution A- 40ml

Solution B- 10ml

h) *0.5% acetic acid:*

1ml of acetic acid was added to 200ml of millipore water.

i) *6% alcoholic saffron:*

6g of saffron was dissolved in 94ml of absolute ethanol and stored at 56ºC for 48 hours before use.

Elastica van Gieson (EVG) staining solutions:

Solution A:

10g of hematoxylin was dissolved in 100ml of 96% ethanol

Solution B:

29% Iron(III)-Chloride solution (145g of Iron(III)-Chloride was dissolved in 500ml of millipore water) and 7.5ml of 37% HCL was added to 950ml of millipore water.

4% paraformaldehyde (PFA):

16g of PFA was added to 184ml of millipore water and dissolved by adding 5ml of 10M NaOH in addition to heating at 100°C. The pH was increased to 7.4-8 by adding 25% HCL. This was followed by adding equal volume of 2X PBS and filtering the solution with a filter paper.

Immunofluorescence staining:

Blocking solution A:

5.4ml PBS, 600µl 10%BSA, 3 drops horse serum

LPA18:0 (50µM) stock solution:

11.5mg of LPA18:0 was added to 500ml of PBS and was continuously stirred overnight.

Ki16425 stock solution:

10mg of Ki16425 was dissolved in 1ml of dimethyl sulfoxide (DMSO).

Ki16425 working solution:

10µl of the stock solution was dissolved in 90µl of PBS.

2.4 Animal experiments

Mice were housed 4 per cage, had free access to water and mouse chow and were maintained on a 12 hour light-dark schedule. The animal experiments were reviewed and approved by local authorities (LANUV NRW) in accordance with the German animal protection law.

2.4.1 Endoluminal injury to the carotid artery

Female ApoE$^{-/-}$ mice (Jackson Laboratory, female, 8-12 weeks old, n=11) on high fat diet (HFD, 21% crude fat, 0.15% cholesterol and 19.5% casein, Altromin, Germany) were subjected to wire-induced endothelial denudation of the left carotid artery using an angioplasty guide wire (0.36 mm diameter). The mice were anesthetised with ketamine hydrochloride (80 mg/kg, IP) and xylazine (5 mg/kg, IP) and the left carotid artery was exposed. The common, external, and internal carotid arteries were temporarily ligated to interrupt the blood flow. The angioplasty guide wire was inserted into the common carotid artery (CCA) via a transverse arteriotomy made in the external carotid artery (ECA). The wire was moved 3 times back and forth in the artery in rotations resulting in endothelial denudation of the CCA. After removal of the wire, the ECA was ligated and the blood flow restored through the common and the internal carotid arteries (ICA) [98]. The mice were injected (IP) with Ki16425 (5 mg/kg/day, Sigma, filter sterilised using a syringe filter, pore size of 0.20 µm, Corning) [106] or control buffer (10% DMSO made in PBS, daily, filter sterilised using a syringe filter, pore size of 0.20 µm, Corning) every day for 3 weeks following injury. Ki16425 selectively inhibits LPA_1 and LPA_3 with a Ki value of 0.34 µM and 0.93 µM respectively. The first injection was given to the anesthetised mice before injury. Perfusion fixation with 4% PFA was performed 28 days after injury. The mice were anesthetised with ketamine hydrochloride (80 mg/kg, IP) and xylazine (5 mg/kg, IP), a cut was made in the right atrium and an incision was made in the left ventricle through which a catheter was inserted. 4% PFA was perfused using a syringe pump (Aladdin-1000, World Precision Instruments, Inc, 336 µl/min) for

10 minutes through the left ventricle and the solution was allowed to flow out through the right atrium. The carotid arteries were harvested and kept in formalin over night at 4ºC and the next day the samples were dehydrated and paraffin embedded (see also section 2.5.4). Blood was taken intracardially for serum cholesterol measurements.

2.4.2 LPA-incubation of the carotid artery

C57BL/6 mice (Charles River, Sulzfeld, female, 8-12 weeks old, n=13-17) were used to perform endoluminal incubation of the carotid artery with LPA.

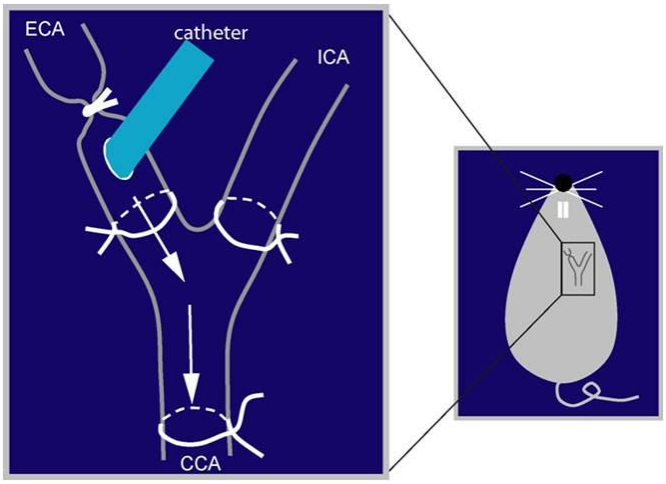

Figure 9: Schematic representation of intraluminal treatment of mouse carotid arteries
The CCA, the ECA and the ICA were ligated to temporarily interrupt the blood flow. Then, a transverse arteriotomy was made in the ECA through which a catheter was advanced into the ECA without touching the bifurcation. The treatment solution was injected into the CCA via the catheter. Following incubation, the catheter and the treatment solution were removed. The second caudal ligature of the ECA was closed and the blood flow was restored through the CCA and the ICA.

The mice were anesthetised with ketamine hydrochloride (80 mg/kg, IP) and xylazine (5 mg/kg, IP) and the left carotid artery was exposed. The blood flow was temporarily interrupted by ligation of the common and the internal carotid arteries (Fig. 9). A transverse arteriotomy was made in the ECA through which a catheter (Rat intrathecal catheter, Alzet Inc) was inserted without touching the bifurcation (Fig. 9). The treatment solution (Table.2) was administered via the catheter to the lumen of the CCA and incubated for 30 minutes. After removal of the treatment solution and the catheter, the ECA was ligated and the blood flow through the CCA and ICA was re-established. All treatment solutions were filter sterilised using a syringe filter (pore size 0.20 µm, Corning). Perfusion fixation with 4% PFA was performed after 28 days as stated in section 2.4.1. The carotid

arteries were harvested and kept in formalin over night at 4ºC and the next day the samples were dehydrated and paraffin embedded (see also section 2.5.4). For protein isolation, the mice were perfused with ice cold PBS at 1, 9 or 28 days following LPA20:4-incubation and the carotid arteries were harvested and stored at -80ºC until protein isolation. The mobilisation of SPCs into the circulation was measured before, 1 day and 9 days following incubation by flow cytometry (see also section 2.5.1). The mice were anesthetised using isoflurane and the blood was taken at different time points by retro-orbital bleeding.

Treatment solution	Concentration	Ki16425 (100 μm)	Supplier
LPA20:4, D(+)-sn-O-arachidonoyl-glyceryl-3-phosphate	40 μM	without	Avanti Polar Lipids
LPA20:4, D(+)-sn-O-arachidonoyl-glyceryl-3-phosphate	40 μM	with	Avanti Polar Lipids
1-APG18:1 L-sn-1-O-oleyl-glyceryl-3-phosphate	40 μM	without	Echelon Biosciences
1-APG18:1 L-sn-1-O-oleyl-glyceryl-3-phosphate	40 μM	with	Echelon Biosciences
PBS	-	without	Dulbecco

Table 2: Treatment solutions used for intraluminal incubation of carotid artery

2.4.3 Diet-induced atherosclerosis

ApoE$^{-/-}$ mice (female, 6 weeks old, n=8) were fed a HFD for 12 weeks. During these 12 weeks they were injected (IP) everyday with Ki16425 (5 mg/kg/day) or control buffer (10% DMSO made in PBS, daily). All the treatment solutions were filter sterilised using a syringe filter (pore size 0.20 μm, Corning). At the end of 12 weeks, perfusion fixation with 4% PFA was performed as stated in section 2.4.1. The aortic roots were harvested and kept in formalin over night at 4ºC and the next day the samples were dehydrated and paraffin embedded (see also section 2.5.4). Blood was taken

intracardially for serum cholesterol measurements. The aortas were taken for quantification of lipid deposition in the aortic wall by Oil red O staining (see also section 2.5.4).

2.4.4 LPA injection

ApoE$^{-/-}$ mice (female and 6-7 weeks old, n=18) were fed a HFD for 4 weeks prior to and throughout the duration of treatment. They were treated (IP) with LPA20:4, LPA18:0 (1-stearoyl-2-lyso-sn-glycero-3-phosphate, Avanti Polar Lipids, 2 nmol each injection), or PBS for 4 weeks (twice weekly). All the treatment solutions were filter sterilised using a syringe filter (pore size 0.20 µm, Corning). Following treatment, perfusion fixation with 4% PFA was performed as stated in section 2.4.1. The aortic roots were harvested and kept in formalin over night at 4ºC and the next day the samples were dehydrated and paraffin embedded (see also section 2.5.4). The aorta was harvested for Oil red O staining (see also section 2.5.4). Blood was taken intracardially for serum lipid measurements.

2.4.5 Partial ligation of the carotid artery

ApoE$^{-/-}$ mice (female, 7-10 weeks old, n=7) on HFD were anesthetised by ketamine hydrochloride (80 mg/kg, IP) and xylazine (5 mg/kg, IP), and then the left carotid artery was exposed. The external carotid, internal carotid, and occipital arteries were ligated; thus outflow of blood was only possible via the superior thyroid artery (Fig. 10). This procedure acutely reduced the blood flow velocity and in turn, the shear stress in the CCA. This reduced blood flow in addition to diet-induced hyperlipidemia forms atherosclerotic plaques in the CCA [107]. Following ligation, the left carotid artery was perivascularly treated with LPA20:4 (2 nmol, once weekly for 4 weeks) or PBS (once weekly for 4 weeks) dissolved in pluronic gel (37%, Sigma). All the treatment solutions were filter sterilised using a syringe filter (pore size 0.20 µm, Corning). 4 weeks after ligation, perfusion fixation with 4% PFA was performed as stated in section 2.4.1. The carotid arteries were harvested and kept in formalin over night at 4ºC and the next day the samples were dehydrated and paraffin embedded (see also section 2.5.4).

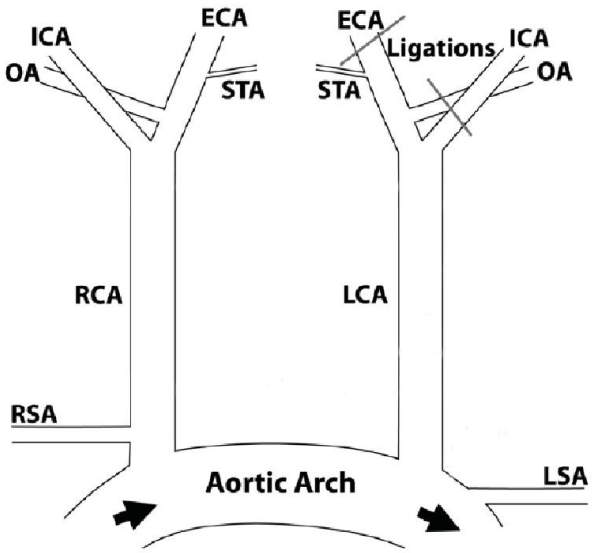

Figure 10: Schematic representation of partial ligation of the left carotid artery
ICA – internal carotid artery, ECA – external carotid artery, OA – occipital artery, STA – superior thyroid artery, RCA – right carotid artery, LCA – left carotid artery, RSA – right subclavian artery, LSA – left subclavian artery [107].

2.4.6 Bone marrow transplantation

To study the role of BM-derived SPCs in LPA-induced neointima formation, BM cells from SM22-LacZ mice which express LacZ under the SM22 promoter [108], were transplanted into C57BL/6 mice (female 6-8 weeks, n=6). C57BL/6 mice were subjected to whole body irradiation (2x6.5 Gy, 4h apart, Faxitron CP-160). The next day, femurs and tibias were removed aseptically from donor SM22-LacZ mice, the marrow cavities were flushed with sterile PBS and a single cell suspension was prepared by pipetting the cells up and down repeatedly followed by passing the cells through a cell strainer (40 µm, BD Falcon) to remove any large pieces of tissue or bone which may be present. 24 hours following irradiation, 2 to 3 million BM cells from the donor were injected via the tail vein into the recipient mouse which was held in a mouse strainer. 4 weeks following BM transplantation, endoluminal incubation of the carotid artery with LPA20:4 (40 µM) and Ki16425 (100 µM) or sterile PBS was performed (see also section 2.4.2). All the treatment solutions were filter sterilised using a syringe filter (pore size 0.20 µm, Corning). 4 weeks following incubation, the carotid arteries were imaged with two photon laser scanning microscopy (see also section 2.5.6). Successful repopulation of the BM was studied by quantifying the peripheral blood cells for the SM22-LacZ genotype (see also section 2.6.2).

2.4.7 SiRNA treatment

To study the role of LPA_1, LPA_3, and CXCL12 in LPA-induced neointima formation, carotid arteries from C57BL/6 (female, 10-12 weeks n=17) mice were treated perivascularly with the respective siRNAs dissolved in pluronic gel. The slow and continuous release of siRNA into the tissue is mediated by Pluronic gel. Pluronic F-127 also known as poloxamer 407 is a hydrophilic non-ionic surfactant [109]. It consists of a hydrophobic block of polypropylene glycol in the centre flanked by two hydrophilic blocks of polyethylene glycol. Due to the presence of both hydrophilic and hydrophobic molecules, at low concentrations they form monomolecular micelles and at high concentrations they form multimolecular aggregates [109]. Pluronic F-127 is a thermo-reversible gel that is liquid at low temperatures (4-5ºC) and becomes a gel upon warming to room temperature [109]. At low temperatures in an aqueous solution, the pluronic F-127 molecules are surrounded by a hydration layer. But when the temperature is increased, the hydrogen bonds between the solvent and the hydrophilic chains of the pluronic F-127 molecules are broken which results in hydrophobic interactions between the polypropylene domains leading to gel formation [109].

50% pluronic gel (Sigma Aldrich) was made by dissolving 10 g of pluronic F-127 powder in 20 ml of millipore water with continuous stirring on ice and filter sterilised with a sterile syringe filter (pore size of 0.20 µm, Corning). The transfection reagent (DharmaFECT4, Thermo scientific) was diluted 50 times with PBS (Dulbecco) and kept on ice until use. The siRNA (Accell SMART pool, Dharmacon) was dissolved in PBS (Dulbecco). 4 nmol of LPA_1-specific siRNA, 3 nmol of LPA_3-specific siRNA, 4 nmol of CXCL12-specific siRNA or 4 nmol of non-targeting siRNA was taken in a volume of 5 µl and mixed with 0.5 µl of the diluted transfection reagent and kept on ice for 10 min. Then 14.5 µl of the 50% pluronic gel was mixed with the 5.5 µl of the siRNA solution containing transfection reagent to get a final gel concentration of 35%. This was used to treat the carotid artery perivascularly. After four days, arteries were intraluminally incubated with LPA20:4 as described previously (see also section 2.4.2). Following 28 days, perfusion fixation with 4% PFA was performed as stated in section 2.4.1. The carotid arteries were harvested and kept in formalin over night at 4ºC and the next day the samples were dehydrated and paraffin embedded (see also section 2.5.4). The mobilisation of $Sca1^+/lin^-$ cells was analysed one day before and one day following LPA20:4-incubation (see also section 2.5.1). The mice were anesthetized using isoflurane and the blood was taken at different time points by retro-orbital bleeding.

In a separate study, $ApoE^{-/-}$ mice (female, 8-10 weeks, n=10) were put on a HFD for 4 weeks. Then non-targeting siRNA, LPA_1-, LPA_2-, or LPA_3-specific siRNA (4 nmol of LPA_1, 3 nmol of LPA_3, 4 nmol of LPA_2 and 4 nmol of non-targeting siRNA, Accell SMART pool, Dharmacon)

dissolved in 35% pluronic gel was applied around the carotid artery. Intravital microscopy (see also section 2.4.8) was performed 4 days or 14 days after siRNA treatment.

2.4.8 Intravital microscopy (IVM)

The role of LPA receptors in hyperlipidemia-induced endothelial-leukocyte interaction was studied by IVM. $ApoE^{-/-}$ (female, age, n=10) mice were fed a HFD for 4 weeks before the carotid arteries were treated perivascularly with non-targeting siRNA, LPA_1-, LPA_2- or LPA_3-specific siRNA dissolved in pluronic gel (see also section 2.4.7). All the treatment solutions were filter sterilised using a syringe filter (pore size 0.20 µm, Corning). IVM was performed 4 days or 14 days after siRNA treatment. The mice were anaesthetised (ketamine, 80 mg/kg and xylazine 0.3 mg/kg, IP) and the left carotid artery was exposed. The circulating leukocytes were labelled with Rhodamine6G (0.03 mg/kg) by intravenous injection (IV). Leukocyte-endothelial adhesion at the carotid bifurcation area was recorded with a microscope (BX51, saline-immersion 10x objective, Olympus) equipped with a CCD camera (EM-CCD camera C9100, Hamamatsu). Quantification of leukocyte adhesion was performed by digital image analysis (ImageJ) [110]. Cells adherent to the endothelium for 30 seconds were counted as adherent cells.

2.4.9 *Ex vivo* perfusion of carotid artery

Ex vivo perfusion of carotid arteries can be used as a model to study the mononuclear cell adhesion to the vessel wall [111]. Human Mono Mac 6 (MM6) cells were used in the study. MM6 cells belong to a monocytic cell line that was established from the peripheral blood of a monoblastic leukemia patient [112]. These cells react with a panel of monoclonal antibodies that are specific for mature monocytes such as M42, 63D3, LeuM3, Mo2, and UCHMI [112]. They exhibit functional and phenotypic characters of mature monocytes [112]. To label the MM6 cells with calcein AM (Invitrogen), the cells were incubated with 1 µM calcein at 37°C for 30 minutes. This was followed by washing with PBS 2 times.

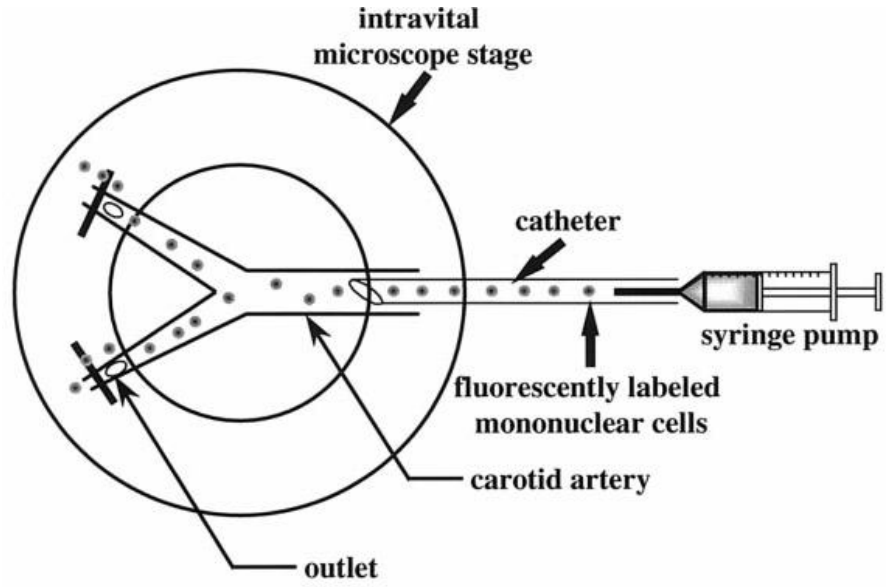

Figure 11: Schematic representation of *Ex vivo* perfusion of carotid artery
The figure depicts an excised carotid artery placed in an intravital microscope stage. The catheter is inserted into the CCA and using a syringe pump the CCA is perfused with the perfusion solution. There is a puncture hole at the end of the external and internal carotid arteries which serves as an outlet [111].

Mice were anaesthetised (ketamine, 80 mg/kg and xylazine 0.3 mg/kg, IP) and the LCA was exposed. The ICA and ECA were cleaned thoroughly such that the connective tissue, vagus nerve, bone, and fat tissue surrounding the artery were removed. This was followed by ligation of the ICA, ECA, and the CCA. A puncture was made in the ICA and ECA using a 30-gauge needle such that the puncture site was not too close to the bifurcation. An incision was made in the CCA through which a catheter was inserted and the artery was perfused with MOPS buffer solution (see also section 2.3) using a syringe pump (Aladdin-1000, World Precision Instruments, Inc.). The solution was allowed to flow out through the puncture holes made in the ICA and the ECA. The artery was then transferred to an intravital microscopic stage [111] (Fig. 11) and perfused with the treatment solutions (Table.3) for 1 or 3 hours at 37°C. This was immediately followed by perfusion with calcein-AM labeled monocytic MonoMac6 (10^6/ml) cells at a speed of 4 µl/min. The adhesive interactions between the MM6 cells and the vessel wall were recorded using stroboscopic epifluorescence illumination (Drelloscop 255-01; Drello, Monchengladbach, Germany) and an intensified camera system (DAGE-MTI SIT-68). The firm adhesion (>30 seconds) and rolling (<1 second) of monocytes at the bifurcation area were quantified visually during a time interval of 5 minutes. All the treatment solutions were filter sterilised using a syringe filter (pore size 0.20 µm, Corning).

Genotype and number of mice/experiment	Age/sex	Carotid artery treatment solution	Duration of treatment	MM6 cell treatment
C57BL/6 mice, n=3	8-10 weeks, female	MOPS buffer solution	3 h	none
C57BL/6 mice, n=3	8-10 weeks, female	LPA20:4, Echelon Biosciences Inc, 40 µM	3 h	isotype control IgG, 10 µg/ml, clone 20102, R&D systems, 20 min
C57BL/6 mice, n=3	8-10 weeks, female	LPA20:4, Echelon Biosciences Inc, 40 µM	3 h	CXCR4 Ab, 10 µg/ml, clone 12G5, R&D systems, 20 min
C57BL/6 mice, n=3	8-10 weeks, female	LPA20:4, Echelon Biosciences Inc, 40 µM	3 h	CXCR2 Ab, 10 µg/ml, clone 48311, R&D systems, 20 min
C57BL/6 mice, n=11	8-10 weeks, female	MOPS buffer solution	1 h	none
C57BL/6 mice, n=3	8-10 weeks, female	nLDL, Calbiochem, 200 µg/ml	1 h	none
C57BL/6 mice, n=5	8-10 weeks, female	moxLDL, 200 µg/ml	1 h	none
C57BL/6 mice, n=5	8-10 weeks, female	moxLDL, 200 µg/ml	1 h	CXCR2 Ab, 10 µg/ml, clone 48311, 20 min
C57BL/6 mice, n=5	8-10 weeks, female	Pre-treatment by perfusion with CXCL1 Ab (20 min, 50 µg/ml, clone 48415, R&D systems) followed by perfusion with moxLDL, 200 µg/ml	1 h	none

C57BL/6 mice, n=3	8-10 weeks, female	moxLDL, 200 µg/ml and Ki16425, 100 µM, Sigma	1 h	none
C57BL/6 mice, n=5	8-10 weeks, female	moxLDL, 200 µg/ml	1 h	isotype control IgG, 10 µg/ml, clone 20102, R&D systems, 20 min
C57BL/6 mice, n=3	8-10 weeks, female	moxLDL, 200 µg/ml and S32826, 5 µM, Cayman Chemicals	1 h	none
C57BL/6 mice, n=3	8-10 weeks, female	LPA20:4, 10 µM, Echelon Biosciences Inc	1 h	none
C57BL/6 mice, n=3	8-10 weeks, female	LPA20:4, 10 µM, Echelon Biosciences Inc	1 h	CXCR2, 10 µg/ml, clone 48311, 20 min
C57BL/6 mice, n=3	8-10 weeks, female	Pre-treatment by perfusion with CXCL1 Ab (20 min, 50 µg/ml, clone 48415, R&D systems) followed by perfusion with LPA20:4, 10 µM, Echelon Biosciences Inc	1 h	none
C57BL/6 mice, n=3	8-10 weeks, female	LPA20:4, 10 µM, Echelon Biosciences Inc	1 h	isotype control IgG, 10 µg/ml, clone 20102, R&D systems, 20 min

Table 3: Various treatment conditions used for *ex vivo* perfusion of the carotid artery

2.5 Cell characterisation and protein assays

2.5.1 Flow cytometry

Flow cytometry is a technique used to analyse many characteristics of cells as they pass through a fluid stream. These characters include size, granularity, and fluorescence intensity (e.g. by fluorescently conjugated antibody detection). Individual cells are passed through a laser beam during which the scattering of laser light and fluorescence emission are measured. The mobilisation of $Sca1^+/lin^-$ SPC population in the circulation was measured using antibodies against Sca-1 and for the hematopoietic lineage markers. The $Sca1^+/lin^-$ cell population was measured in a mononuclear gate [104].

To stain the cells, first 8-10 drops of venous blood was taken by retro-orbital bleeding and anticoagulated with EDTA. The blood was incubated with 3 ml of lysis buffer (see also section 2.3) for 10 minutes at room temperature to lyse the red blood cells. It was then washed with 2ml of Hanks' complete solution (see also section 2.3) and approximately 10^6 cells were taken for the staining. 1 µl of the phycoerythrin (PE)-conjugated Sca-1 antibody (E-Bioscience, clone-Ly-6A/E) and 2 µl of each biotinylated lineage antibody (E-Bioscience, CD3 clone- 145-2C11, CD45R clone- RA3-6B2, CD11b clone- M1/70, erythroid marker clone- TER-119, LY-6G clone- RB6-8C5) were resuspended in 50 µl of a 1:1 solution of FACS staining buffer (see also section 2.3) and Hanks' complete solution (see also section 2.3). The antibody solution was added and incubated in the dark on ice for 30 minutes. The cells were then washed with Hanks' complete solution (see also section 2.3). 0.75 µl of biotinylated FITC (Vector labs) was resuspended in 50 µl of a 1:1 solution of FACS staining buffer (see also section 2.3) and Hanks' complete solution (see also section 2.3) and added to the tubes which were then incubated on ice in the dark for 30 min. The samples were measured using a FACSCantoII (BD Bioscience) flow cytometer. In the control tubes, the primary antibodies were omitted and only the biotinylated FITC was added. To determine the CXCR4 expression on $Sca\text{-}1^+/lin^-$ cells, a FITC conjugated rat anti-CXCR4 antibody was used. Raw data were analysed with FlowJo software (Tree star, Inc, Ashland, OR, USA). To determine the $Sca\text{-}1^+/lin^-$ cell population, first the dot plot containing the forward scatter (FSC) and side scatter (SSC) was taken. The FSC value is proportional to the diameter of the cell and the SSC value is proportional to the granularity of the cell. The mononuclear cells were identified based on their size and granularity and a mononuclear cell gate was made (Fig. 12A). The fluorescence intensities of these cells for PE (expressed on the Y axis) and FITC (expressed on the X axis) (Fig. 12B) was analysed. The quadrants were set based on the negative control such that more than 95% of the events from the negative control lie in the $Sca\text{-}1^-/lin^-$ quadrant. For each quadrant, the

percentage of cells was derived from the quadrant statistics determined by the FlowJo software. The percentage of Sca-1$^+$/lin$^-$ cells was calculated by subtracting the percentage of Sca-1$^+$/lin$^-$ cells in the sample from the percentage of Sca-1$^+$/lin$^-$ cells in the negative control.

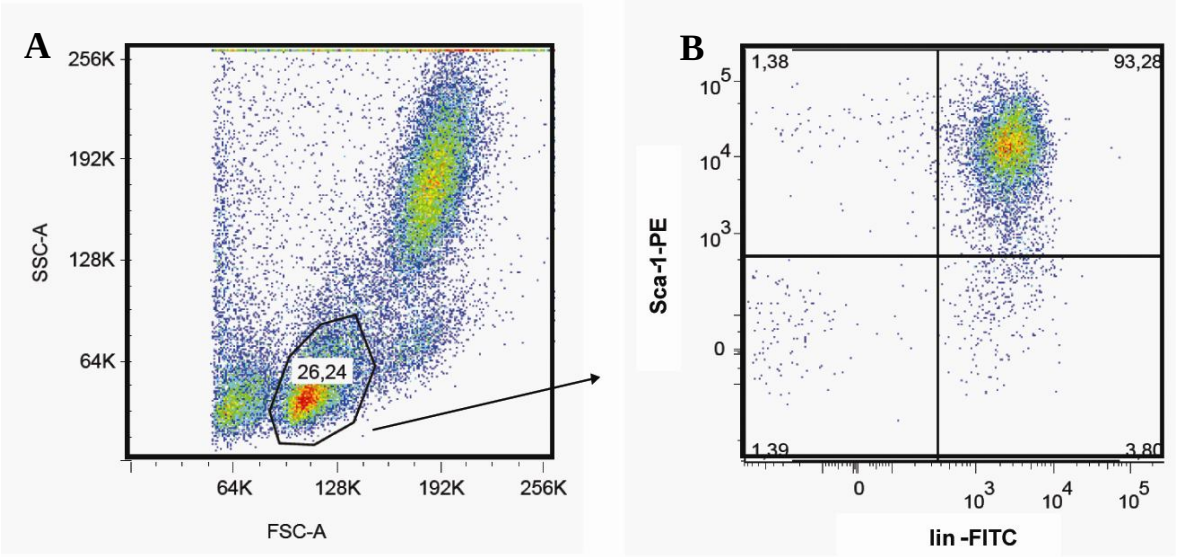

Figure 12: Quantification of Sca-1$^+$/lin$^-$ cell population using flow cytometry

(A) The measured cells are shown in the dot plot and the gate discerns the mononuclear cell population. (B) The fluorescence intensities of the mononuclear cells for PE and FITC are shown. The FITC fluorescence is in the X axis (lineage, hematopoietic marker) and PE fluorescence (Sca-1, stem cell marker) on the Y axis. The percentage of Sca-1$^+$/lin$^-$ cells is shown in the upper left quadrant.

2.5.2 Enzyme-linked immunosorbant assay (ELISA)

a) Following LPA20:4-incubation, the CXCL12 protein in the carotid artery was measured after 1 day, 9 days and 28 days by ELISA. Untreated carotid arteries were used as controls. The carotid arteries were harvested after perfusion with ice cold PBS and were mechanically disrupted (Tissue lyser LT, Qiagen) in ice cold ELISA lysis buffer (see also section 2.3). The lysate was then incubated on ice for 10 minutes and centrifuged at 3500 g for 10 minutes at 4ºC. The CXCL12 protein concentration was determined in the supernatant using 96-well plates pre-coated with a CXCL12 capture Ab (Ray Biotech, INC). Standard and carotid artery samples (100 µl each) were added to the appropriate wells and incubated for 2.5 h at room temperature. Then, the wells were washed four times with the wash solution followed by the addition of an anti-mouse biotinylated CXCL12 detection Ab for 1 h under shaking conditions. After a further washing step, horseradish peroxidase (HRP)-conjugated streptavidin (100 µl per well) was added and incubated for 45 minutes at room temperature. 100 µl of TMB one-step substrate solution (3,3,5,5-tetramethylbenzidine) was then added, following a washing step, and the reaction was stopped after 30 minutes (room temperature, in the dark) by the addition of 50 µl of stop solution (2 M

sulphuric acid). The addition of TMB substrate solution results in one electron oxidation of TMB by HRP. This one electron oxidation product is a cation free radical which is blue in colour and has an absorption maximum of 653 nm. Further acidification of this radical with sulphuric acid yields the completely oxidised product (diimine) which is formed by two electron oxidation. This product yields a yellow colour and has an absorption of 450 nm. The absorbance was measured at 450 nm with a microplate reader (see also section 2.1). A graph was plotted for the values obtained from the standards and this was used to determine the concentration of CXCL12 protein in the samples.

b) The concentration of CXCL1 protein in the medium of cultured ECs was determined using ELISA. Following treatment of ECs with LPA20:4, native LDL (nLDL) or moxLDL with or without the different inhibitors (see also section 2.7), the secreted CXCL1 protein in the medium was determined using a mouse CXCL1 ELISA kit (R&D System).

Cell surface ELISA for CXCL1 was performed on cultured ECs to identify the CXCL1 protein immobilised on the cell surface. ECs were cultured in a 96-well plate (see also section 2.7) and treated with LPA20:4, moxLDL or nLDL in the presence or absence of the various inhibitors for 1 hour. Then, the cells were fixed with 4% PFA followed by incubation with a CXCL1 Ab (clone 48415, R&D system; 1 µg/ml in PBS/1% skim milk) [113]. Then, the secondary Ab (HRP conjugated goat anti-rat IgG, Santa Cruz Biotechnology) was added. This was followed by the addition of the substrate for HRP, 3,3,5,5-tetramethylbenzidine (TMB, 1-step ultra TMB-ELISA solution, Thermo Fisher Scientific Inc., Rockford, IL) which results in colour development. The reaction was stopped by adding 2 M H_2SO_4. The absorbance of the coloured solution was measured at 450nm with a microplate reader (see also section 2.1).

2.5.3 Western Blot analysis

HIF-1α protein in the carotid arteries was studied following LPA20:4 incubation by western blot analysis. Following LPA20:4-incubation, carotid arteries were harvested after 1 day, 9 days and 28 days. Untreated right carotid arteries were used as controls. The carotid arteries were harvested after perfusion with ice cold PBS. The arteries were mechanically disrupted (Tissue lyser LT, Qiagen) in ice cold lysis buffer A (80 µl per sample) (see also section 2.3). Then the whole lysate was transferred to a new tube and centrifuged at 3000 g for 10 minutes at 4ºC. The supernatant was then removed and the pellet was dissolved in 80 µl of lysis buffer B (see also section 2.3) and incubated on ice for 10 minutes. Then it was centrifuged at 3000 g for 10 minutes at 4ºC. The supernatant containing the nuclear protein was taken and stored in -80ºC till use. 30 µg of protein was taken from each sample and separated by SDS-PAGE (Sodiumdocecylsulfate-

polyacrylamide-gelelectrophoresis). A 7.5% gel was used for the separation. SDS binds to the polypeptides resulting in a negative charge and seperates the protein by size. Electrophoresis was carried out in a Mini-PROTEAN® 3 cell system (Bio-Rad, Hercules, USA) at 120 V. The separated proteins were transferred onto a nitrocellulose membrane (Amersham/GE Healthcare, Uppsala, Sweden) at 100V for 1 h in ice cold blotting buffer (see also section 2.3). The non-specific binding regions in the membrane were blocked by incubating it with 5% milk in TBS for 1.5 h at room temperature. Then, the membrane was incubated with the primary antibodies, HIF-1α (1:500 dilution, for 1 h at room temperature, Santa Cruz Biotechnologies) and GAPDH (1:3000 dilution, at 4°C overnight, Bethyl Laboratories). Following incubation, the membrane was washed with TBS/0.05% tween (see also section 2.3) three times. To detect the primary antibodies the membrane was incubated with a HRP-conjugated, anti-rabbit secondary Ab for 1 h at room temperature. In the presence of hydrogen peroxide (H_2O_2) the protein-bound HRP converts luminol to an excited intermediate dianion, which emits light on return to its ground state. This light can be captured by an image reader (see also section 2.1).

2.5.4 Histochemistry

The samples (carotid arteries, aortic root) for histological staining were harvested from the mice after fixation with 4% PFA. Then the tissue was kept in formalin over night at 4ºC. The next day the tissue was dehydrated (SLEE MAIN2, Table.4). This was followed by embedding the tissue in liquid paraffin (approximate temperature 60ºC) and the blocks were allowed to harden (Leica EG1160). The carotids were embedded such that the bifurcation was facing downwards and care was taken that it was embedded vertical and straight. A microtome (see also section 2.1) was used to section the paraffin blocks at 5 μm thickness. For carotid arteries the sections were collected starting from the bifurcation and for the aortic roots the sections were collected starting from the first valve that was visible. After sectioning, the slides were kept at 37ºC in an incubator for 5-6 h or at room temperature overnight to prevent the detachment of tissue while staining.

Reagent	Duration	Temperature
Ethanol 70%	30 min	20ºC
Ethanol 70%	30 min	20ºC
Ethanol 96%	30 min	20ºC
Ethanol 96%	30 min	20ºC
Ethanol 100%	30 min	20ºC
Ethanol 100%	30 min	20ºC
Ethanol 100%	30 min	20ºC
Xylol	30min	45ºC
Xylol	30 min	45ºC
Xylol	30 min	45ºC
Paraffin I	30min	62ºC
Paraffin II	30min	62ºC
Paraffin III	overnight	62ºC

Table 4: Different steps of paraffin embedding

To determine the neointimal area in the carotid arteries of mice following wire injury or LPA incubation, Movat's pentachrome staining was performed. Cross sections of the carotid artery (5 µm thickness, 4 sections per mouse) were obtained at a standard distance (50 to 300 µm) starting from the bifurcation and stained with Movat's pentachrome.

1) For Movat's staining the sections were first subjected to deparaffinisation and rehydration by the following procedure:
   Incubate in Xylol for 30 minutes.
   Incubate in 100% isopropanol for 5 minutes.
   Incubate in 100% isopropanol for 5 minutes.
   Incubate in 96% isopropanol for 5 minutes.
   Incubate in 70% isopropanol for 5 minutes.
   Incubate in millipore water for 5 minutes
   Incubate in PBS for 5 minutes.
2) Stained for 20 minutes in alcian blue solution (1%) (see also section 2.3) followed by 5 minute wash in tap water.
3) Incubated in alkaline ethanol for 10 minutes at 56ºC (see also section 2.3).
4) Washed in running tap water for 2 minutes.
5) Dipped in millipore water and stained in Orcein-Verhoeffschem Hematoxylin solution for 30 minutes at 37ºC (see also section 2.3) followed by washing in running tap water for 3 minutes.
7) Differentiated in 2% Iron (III)-Chloride for 2 minutes.
8) Incubated in acidic alcohol for 2 minutes (see also section 2.3) and then dipped in tap water for 5 minutes.
9) Stained in Brilliant Crocein Scarlet MOO solution for 10 minutes (see also section 2.3).
10) Washed in 0.5% acetic acid for 30 seconds (see also section 2.3) and differentiated in 5% phosphor-tungstic acid for maximum 4 minutes.
11) Dipped in 0.5% acetic acid for 30 seconds.
12) Washed in 100% ethanol three times for 1 minute each.
13) Stained in 6% alcoholic saffron for 8-15 minutes (see also section 2.3) in a closed container.
14) Dehydrated in absolute ethanol two times for 3 minutes each. Finally the tissue was dipped in xylol and a cover slip was placed using vitrocloud (langenbrinck).

The neointimal area in the carotid artery was quantified by computerized image analysis (Diskus software, Hilgers, Bonn). First the lumen area was marked and then the internal elastic

lamina (IEL) and the external elastic lamina (EEL) were marked. The area of lumen, IEL and EEL was automatically calculated by the software (Diskus). The neointimal area was calculated by subtracting the area of IEL from the lumen area. The medial area was calculated by subtracting the area of EEL from the area of IEL (Fig. 13).

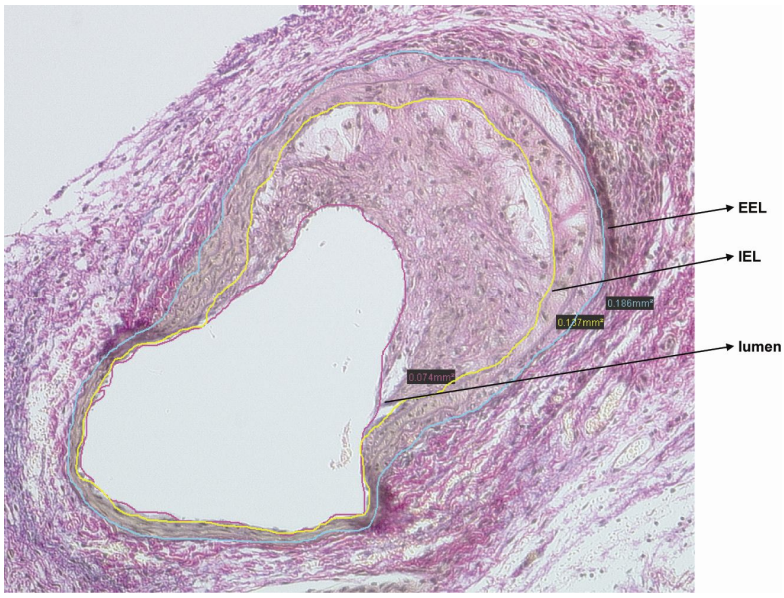

Figure 13: Morphometric analysis of the CCA
EEL- external elastic lamina, IEL- internal elastic lamina.

The atherosclerotic plaques in the aortic root or carotid arteries of mice were analysed in Movat's pentachrome stained or EVG stained sections (4 sections per mouse, 5 µm thick). The plaque area was quantified by computerized image analysis (Diskus software, Hilgers, Bonn). The circumference of the plaque was marked in each valve and the area of plaque in each valve was calculated by the software. The plaque area per valve was calculated by taking the average of the plaque area in all three valves.

EVG staining was performed using the following protocol:

1) The sections were deparaffinised and rehydrated by the following procedure:
   Incubate in Xylol for 30 minutes.
   Incubate in 100% isopropanol for 5 minutes.
   Incubate in 100% isopropanol for 5 minutes.
   Incubate in 96% isopropanol for 5 minutes.
   Incubate in 70% isopropanol for 5 minutes.
   Incubate in millipore water for 5 minutes
   Incubate in PBS for 5 minutes

2) Stained in resorcein-fuchsin solution (Roth, X877.1) for 15 minutes at 56ºC followed by slowly dipping in tap water 1-2 times.
3) Differentiated in 80% ethanol followed by dipping in tap water and millipore water.
4) Incubated in solution A+ B (100ml solution A and 100 ml solution B, freshly prepared, see also section 2.3) for 5 minutes.
5) Differentiated with 0.5% HCL-alcohol by dipping in the solution a few times.
6) Washed in tap water till the colour of the nucleus turned blue.
7) Incubated in pikrofuchsin (Merck, 1.15974/4) for 1 minute and washed in tap water shortly.
8) Dipped shortly in 70% ethanol followed by 96% ethanol.
9) Incubated in 100% ethanol for 3 minutes followed by 5 minutes in xylol and then the cover slip was placed using vitrocloud.

The lipid area in the aorta was studied by Oil red O staining. The thoracic and abdominal aortas were cut longitudinally and prepared *en face.* The aorta was dipped in 60% isopropanol for 15 to 20 seconds followed by incubation in 0.3% Oil red solution for 15 minutes. The aorta was then washed in 60% isopropanol for 10 to 15 seconds. Finally, the aorta was washed in water and mounted on the slide. The stained lipid depositions in the aortic wall were quantified in digitized images using ImageJ software. The circumference of the aorta was marked and percentage of positively stained area was quantified out of the total area of aorta in each image.

2.5.5 Immunofluorescence

To determine the composition of the neointimal area following wire injury and LPA incubation, quantitative immunostaining was performed in carotid artery sections (5 µm thick) using antibodies against α-smooth muscle actin (SMA), Mac-2, SM22, calponin, vWF, β-galactosidase, and CD3 (Table.5, see also section 2.2.1). Appropriate isotype matched IgG antibodies were used as negative controls (Santa Cruz biotechnology). For detection of the primary Ab, a FITC-, Dylight549-, Dylight488 or cy3-conjugated secondary Ab was used (see also section 2.2.2). The nuclei were counterstained with 4',6-Diamidino-2-phenylindol (DAPI). The percentage of positively stained area was quantified per neointimal area using image analysis software (ImageJ). The analysis was performed by setting the threshold according to the background of the negative control stainings. The CD3 staining, however, was analysed by counting the number of CD3+ cells. Briefly, the CD3+ cells were identified by the co-localisation of the CD3 and the DAPI staining and expressed as the percentage of CD3+ cells out of the total number of DAPI+ nuclei in the neointima. In sections stained for α-SMA and Sca-1, the double positive cells were counted

and expressed as the percentage of α-SMA$^+$/Sca-1$^+$ cells out of the total number of cells in the neointima (Table.6). In addition, double immunostaining was performed for HIF-1α and CXCL12 (Table.6, see also section 2.2.1). LPA_1 and LPA_3 stainings were performed with the appropriate primary antibodies (see also section 2.2.1). The bound primary antibodies were visualized by a biotinylated secondary Ab followed by a streptavidin-Dylight549 conjugate (Table.5, see also section 2.2.1 and 2.2.2). The images were recorded with a fluorescence microscope (see also section 2.1) connected to a CCD camera (JVC). The analysis was performed by setting the threshold according to the background of the negative control stainings. The specificity of the LPA_1 and LPA_3 antibodies were checked using sections from $LPA_1^{-/-}$ and $LPA_3^{-/-}$ mouse carotid arteries respectively (obtained from Jerold Chun, Department of Molecular Biology, Dorris Neuroscience Center, The Scripps Research Institute, La Jolla, CA, USA).

Antigen	**Antigen retrieval**	**Blocking**	**Primary Ab**	**Detection system**
α-SMA	none	Blocking solution A (see section 2.3), 30 min	mouse monoclonal (MC) α-SMA Ab, 1:200, 4ºC, overnight (ON)	donkey-anti-mouse IgG-FITC-conjugated Ab, 1:100, 30 min
Mac-2	none	Blocking solution A (see section 2.3), 30 min	rat MC Mac-2 Ab, 1:400, 4ºC, ON	donkey-anti-rat IgG-FITC-conjugated Ab, 1:100, 30 min
CD3	Citrate buffer, 20 min (100ºC)	10% goat serum, 30 min	rabbit polyclonal (PC) CD3 Ab, 1:100, 4ºC, ON	goat-anti-rabbit IgG-Dylight549-conjugated Ab, 1:400, 30 min
CXCL1	Citrate buffer, 20 min (100ºC)	Blocking solution A (see section 2.3), 30 min	rabbit PC CXCL1 Ab, 1:50, 4ºC, ON	goat-anti-rabbit IgG-Dylight549-conjugated Ab, 1:200, 30 min
LPA_1	Citrate buffer, 20 min (100ºC)	Blocking solution A (see section 2.3), 30 min followed by blocking with avidin/biotin solution (avidin 15 min and subsequently biotin 15 min)	rabbit PC LPA_1 Ab, 1:500, 4ºC, ON	anti-rabbit IgG-biotinylated Ab, 1:100, 30 min followed by Streptavidin-Dylight549-conjugated, 1:500, 30 min

LPA_3	Citrate buffer, 20 min (100ºC)	Blocking solution A (see section 2.3), 30 min followed by blocking with avidin/biotin solution (avidin 15 min and subsequently biotin 15 min)	rabbit PC LPA_3 Ab, 1:250, 4ºC, ON	anti-rabbit IgG-biotinylated Ab, 1:100, 30 min followed by Streptavidin-Dylight549-conjugated, 1:500, 30 min
β-galactosidase	Citrate buffer, 20 min (100ºC)	Blocking solution A (see section 2.3), 30 min	rabbit PC β-galactosidase Ab, 1:1000, 4ºC, ON	goat-anti-rabbit IgG-Dylight549-conjugated Ab, 1:200, 30 min
vWF	Citrate buffer, 20 min (100ºC)	Blocking solution A (see section 2.3), 30 min	rabbit PC vWF Ab, 1:1000, 4ºC, ON	goat-anti-rabbit IgG-Dylight549-conjugated Ab, 1:200, 30 min
SM22 alpha	none	10% goat serum, 30 min	rabbit PC SM22 alpha Ab, 1:200, 4ºC, ON	goat-anti-rabbit IgG-Dylight549-conjugated Ab, 1:200, 30 min
calponin	none	10% goat serum, 30 min	rabbit MC calponin Ab, 1:100, 4ºC, ON	goat-anti-rabbit IgG-Dylight549-conjugated Ab, 1:200, 30 min

Table 5: Immunostaining protocols
Ab details are given in sections 2.2.1 – 2.2.2

The composition of the atherosclerotic lesions in the aortic root was analysed by immunostaining (2-3 sections per mouse) using antibodies against α-SMA, Mac-2, and CXCL1 (Table.5, see also section 2.2.1). The atherosclerotic lesions in the carotid arteries were stained for the macrophage-specific marker Mac-2 (Table.5, see also section 2.2.1). The primary antibodies were detected using appropriate secondary antibodies (see also section 2.2.2). The percentage of the positively stained area out of the total plaque area was calculated from the measurements made using image analysis software (ImageJ). In addition, the Mac-2+ cell number in the plaques was determined by counting the Mac-2 and DAPI positive cells and expressed as the percentage of Mac-2+ cells out of the total number of plaque cells. Double immunostaining was performed using antibodies against LPA_1, LPA_3, or CXCL1 with a Mac-2 or vWF Ab (Table.6, see also section 2.2.1).

Formalin-fixed and paraffin-embedded human carotid plaque sections were obtained from atherectomy specimens. They were used for double immunostaining for LPA_1 or LPA_3 with Mac-2 or vWF (Table.6, see also section 2.2.1). Appropriate unspecific primary antibodies were used as negative controls.

Antigen retrieval	**Blocking**	**1st primary Ab**	**1st secondary Ab**	**2nd primary Ab**	**2nd secondary Ab**
Citrate buffer, 20 min (100ºC)	10% goat serum, 30 min	mouse MC CXCL12 Ab, 1:50, 4ºC, ON	goat-anti-mouse IgG-Dylight488-conjugated, 1:400, 30 min	rabbit PC HIF-1α alpha Ab, 1:50, 1 h at room temperature	goat-anti-rabbit IgG-Dylight549-conjugated, 1:400, 30 min
Citrate buffer, 20 min (100ºC)	Blocking solution A (see section 2.3), 30 min	rabbit PC CXCL1 Ab, 1:50, 4ºC, ON	goat-anti-rabbit IgG-Dylight549-conjugated, 1:200, 30 min	rabbit PC vWF Ab, 1:1000, 4ºC, ON	donkey-anti-rabbit IgG-FITC-conjugated, 1:100, 30 min
Citrate buffer, 20 min (100ºC)	Blocking solution A (see section 2.3), 30 min followed by blocking with avidin/biotin solution (avidin 15 min and subsequently biotin 15 min)	rabbit PC LPA_1 Ab, 1:500, 4ºC, ON	anti-rabbit IgG-biotinylated Ab, 1:100, 30 min, followed by Streptavidin-Dylight549-conjugated, 1:500, 30 min	rabbit PC vWF Ab, 1:1000, 4ºC, ON	donkey-anti-rabbit IgG-FITC-conjugated, 1:100, 30 min
Citrate buffer, 20 min (100ºC)	Blocking solution A (see section 2.3), 30 min followed by blocking with avidin/biotin solution (avidin 15 min and subsequently biotin 15 min)	rabbit PC LPA_1 Ab, 1:500, 4ºC, ON	anti-rabbit IgG-biotinylated Ab, 1:100, 30 min, followed by Streptavidin-Dylight549-conjugated, 1:500, 30 min	rat MC Mac-2 Ab, 1:400, 1 h at room temperature	donkey-anti-rat IgG-FITC-conjugated Ab, 1:100, 30 min

Citrate buffer, 20 min (100ºC)	Blocking solution A (see section 2.3), 30 min followed by blocking with avidin/biotin solution (avidin 15 min and subsequently biotin 15 min)	rabbit PC LPA_3 Ab, 1:250, 4ºC, ON	anti-rabbit IgG-biotinylated Ab, 1:100, 30 min followed by Streptavidin-Dylight549-conjugated, 1:500, 30 min	rabbit PC vWF Ab, 1:1000, 4ºC, ON	donkey-anti-rabbit IgG-FITC-conjugated, 1:100, 30 min
Citrate buffer, 20 min (100ºC)	Blocking solution A (see section 2.3), 30 min followed by blocking with avidin/biotin solution (avidin 15 min and subsequently biotin 15 min)	rabbit polyclonal LPA_3 Ab, 1:250, 4ºC, ON	anti-rabbit IgG-biotinylated Ab, 1:100, 30 min followed by Streptavidin-Dylight549-conjugated, 1:500, 30 min	rat MC Mac-2 Ab, 1:400, 1 h at room temperature	donkey-anti-rat IgG-FITC-conjugated Ab, 1:100, 30 min
-	Blocking solution A (see section 2.3), 30 min	goat PC Sca-1 Ab, 1:10, 4ºC, ON	donkey-anti-goat IgG-FITC-conjugated, 1:100, 1 h	mouse MC α-SMA Ab, 1:200, 4ºC, ON	donkey-anti-mouse IgG-cy3-conjugated, 1:300, 1 h

Table 6: Double-immunostaining protocols
Ab details are given in sections 2.2.1 – 2.2.2

2.5.6 Two-photon laser scanning microscopy (TPLSM)

To determine, whether LPA20:4-induced neointima formation is due to the recruitment of BM-derived SPCs, BM cells from mice which express β-galactosidase under a SMC-specific promoter (SM22-LacZ) were transplanted into C57BL/6 mice (18-20 weeks, female, n=6) (see also section 2.4.6). Then, the carotid arteries were incubated with LPA20:4 and the neointimal β-galactosidase expressing cells were studied using TPLSM (see also section 2.5.6).

In contrast to the conventional single-photon microscopy methods which use UV or visible light to excite fluorescent molecules, TPLSM uses two photons of the infrared light to excite the fluorophore [114]. Due to two-photon excitation, out of focus absorption and background fluorescence are strongly suppressed. The use of infrared light reduces the scattering in the tissue which enhances penetration depth. Other advantages of TPLSM are enhanced resolution and optical sectioning [115].

28 days following LPA20:4-incubation, carotid arteries were excised (including the bifurcation) and incubated in chloroquine (300 µm in HBSS, see also section 2.3), ImaGene Green C_{12} FDG lacZ Gene Expression Kit, Invitrogen, Karlsruhe, Germany) for 30 minutes to block the endogenous lysosomal β-D-galactosidase activity. Then, the arteries were mounted in a perfusion chamber (Fig. 14a) which was filled with HBSS (see also section 2.3) and the temperature was maintained at 37°C. To study the activity of the β-galactosidase, C_{12} fluorescein di-β-d-galactopyranoside (FDG) substrate (ImaGene Green, Invitrogen, 33 µM in HBSS) was perfused through the artery at a rate of 12 µl/min for 30 minutes. Phenylethyl β-D-thiogalactopyranoside (PETG) reagent (ImaGene Green, 1 mM in HBSS) was used to stop the β-galactosidase reaction. SYTO41 and propidium were used to perform a live-dead-cell staining, which identified that the lacZ signal was derived only from live cells. The intraluminal pressure was restored prior to imaging. A multiphoton system (TriM Scope, LaVision Biotec GMBH, Bielefeld, Germany) in single beam mode coupled to a motorised up-right microscope (Olympus BX61WI with a 20X NA 0.95 water immersion objective; Olympus GMBH, Hamburg, Germany) was used to image the arteries. For two-photon excitation, the pulsed Ti-Sapphire laser (MaiTai HP, Spectra Physics, Mountain View, US) was tuned to 830 nm. This was used to visualise the second harmonic generation (SHG) signal of collagen, C_{12} FDG (ImaGene Green), and the autofluorescent signal originating from the elastic laminae. Detection of the emitted fluorescent signals was achieved with two photomultiplier tubes (PTMs) tuned to corresponding parts of the emission spectra: SHG, 453-497 nm (PMT 1); C_{12} FDG, 500-550 nm (PMT 2); autofluorescence signal of elastin was detected in both PMT 1 and PMT 2. ImSpector Pro 4.0.43 acquisition software (LaVision Biotec GMBH) was used to obtain series of xy images at successive depth (z-stack) (Fig. 14b). Further image processing was performed with Image-Pro 3D analyser 7.0 software (Media Cybernetics, Silver Spring, USA).

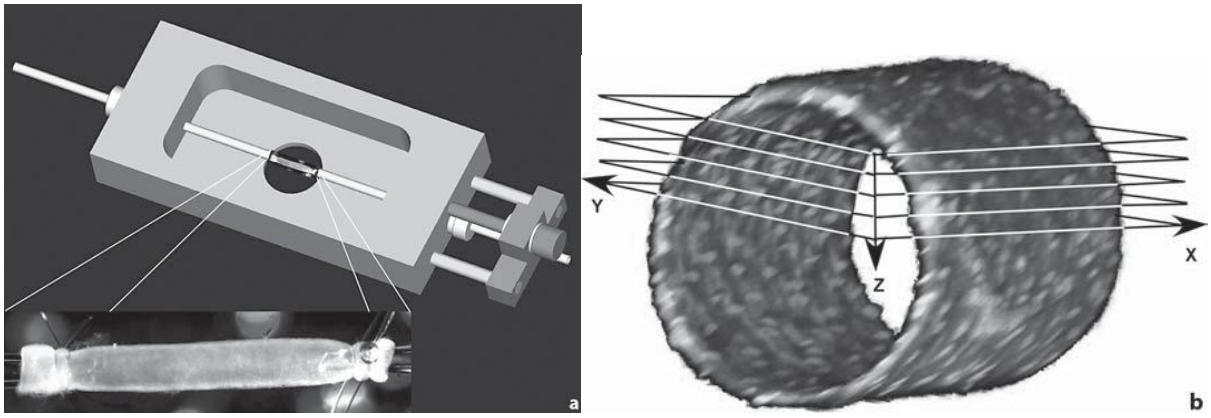

Figure 14: TPLSM-perfusion chamber and 3D reconstruction of an artery
a) The image shows a mouse uterine artery mounted on two glass pipettes. The distance between the two pipettes is adjustable. b) The image shows the 3D re-construction of a uterine artery and the z-stack of optical xy-slices [115].

LPA20:4-induced endothelial-surface deposition of CXCL1 was studied using TPLSM. Carotid arteries from C57BL/6 mice were isolated and mounted in a perfusion chamber (Fig. 14a). The arteries were then perfused *ex vivo* with LPA20:4 (10 µM, Echelon Biosciences Inc.) or a control buffer for 1 hour at 37°C. This was immediately followed by perfusion with a Cy3-labelled CXCL1 Ab (50 µg/ml, clone 48415, R&D Systems) for 15 minutes at a rate of 2 µl/min and by washing with HBSS (see also section 2.3) for 15 minutes. The endothelial surface deposition of CXCL1 was imaged by detecting the Cy3-derived fluorescence. Imaging was performed using an Olympus FV1000MPE multi-photon system that was coupled to an upright microscope (Olympus BX61WI) with a 25X NA 1.05 water immersion objective (Olympus GMBH, Hamburg, Germany). For two-photon excitation, the pulsed Ti-sapphire laser (MaiTai DeepSee, Spectra Physics, Mountain View, US) was set to 800 nm. The detection of the fluorescent signal was achieved with three PMTs, which were each set to detect a separate range of the emission spectrum: intrinsic fluorescent signals of SHG, 400-490 nm (PMT 1); calcein labeled MM6 cells, 510-525 nm (PMT 2); autofluorescent signal from elastin, 505-560 nm (PMT 2); anti PE-labeled CD31, 560-660 nm (PMT 3); and Cy3-labeled CXCL1, 560-660 nm (PMT 3). The Fluoview FV10-ASW 2.0 acquisition software (Olympus GMBH, Hamburg, Germany) was used to obtain a series of xy-images (Fig. 14b) at varying depths (z-stack) and Image-Pro 3D analyser 7.0 (Media Cybernetics, Silver Spring, USA) was used for further image processing.

The CXCL1 Ab was conjugated with Cy-3 using a Cy-3 mAb labelling kit (GE Healthcare). The CXCL1 Ab was first dissolved such that the concentration was 1mg/ml and 100 µl of this diluted Ab solution was taken and added to 5 ml of coupling buffer from the kit (1 M Sodium Carbonate buffer). Then the entire volume was transferred to a vial containing the Cy3 dye and

mixed thoroughly. This was incubated at room temperature for 30 minutes with additional mixing every 10 minutes. The gel filtration column for the separation of labeled protein from non-conjugated dye was mounted on a ring stand and 3 ml of fresh elution buffer (Phosphate buffered saline containing 0.1% Sodium azide as preservative) was allowed to flow through it. Then the Ab labeling mixture was transferred to the top of the column. 1.1 ml of elution buffer was added which moves through the column during which a fast moving pink band of labeled Ab will separate from the un-conjugated dye. Additional 1.1 ml of elution buffer was added to the column and the fast moving pink band of labeled Ab was collected in a clean tube as it elutes from the column.

2.5.7 Serum analysis

At the end of the experiment, approximately 500-700 µl of blood was taken in serum tubes (Sarstedt) and allowed to stand at room temperature for 2 hours. The tubes were centrifuged at 2000 g for 20 minutes and the serum present in the supernatant was collected to measure the serum lipids and proteins. Serum cholesterol, C-reactive protein (CRP), alanine transaminase (ALT), triglycerides and creatinine levels were measured with an automatic analyser (Vitros 250, Johnson and Johnson).

2.6 Molecular biology methods

2.6.1 Quantification of RNA

The RNA concentration was determined by measuring the absorbance at 260 nm (A_{260}) in a spectrophotometer (see also section 2.1). The absorbance at 280 nm was also measured to determine the RNA purity. RNA with an A_{260}/A_{280} ratio of 1.8-2.0 was used.

2.6.2 Quantitative real-time polymerase chain reaction (PCR)

The differential regulation of the LPA receptors by vascular injury and hyperlipidemia was studied by quantitative real-time PCR. The PCR was performed using Quantitect SYBR green PCR kit (Qiagen) and commercially available primers for the LPA receptors (Quantitect primer assay, Qiagen). In order to quantify gene expression from small amounts of RNA, it is necessary to amplify the gene transcript. The RNA sample is first reverse-transcribed to cDNA with the enzyme reverse transcriptase and the cDNA is subjected to PCR amplification. SYBR green is a DNA

binding dye that binds to all double stranded DNA during PCR and results in fluorescence which can be measured. In this technique, the amplified cDNA is measured as the reaction progresses. During PCR, an increase in the DNA product leads to an increase in fluorescence intensity which can be measured at each cycle and hence the DNA concentration is quantified. This in turn can be used to calculate the expression of a target gene.

RNA was isolated from carotid arteries, aorta or cultured macrophages using RNeasy micro kit (Qiagen, Hilden, Germany). In this procedure RNA was isolated by inducing the selective binding of RNA to the silica membrane of the RNeasy MinElute spin column. The binding of the RNA to the membrane is promoted by guanidine-thiocyanate which is present in the lysis buffer and ethanol which is added before transferring the sample to spin column. Traces of DNA that may be present were removed by treatment with DNaseI. The RNA concentration was determined (see also section 2.6.1) and up to 600 ng of total RNA was reverse transcribed using Quantitect reverse transcription kit (Qiagen). First the RNA was incubated with genomic DNA wipe out buffer at 42° C for 2 minutes to effectively remove any genomic DNA that may be present. Then, the RNA was incubated with the reverse transcription master mix at 42° C for 15 minutes and the reaction was stopped by incubation at 95° C for 3 minutes (refer to table 7 for more details). The cDNA was subjected to PCR amplification with primer sets specific for LPA_1, LPA_2 and LPA_3 (Quantitect primer assay, Qiagen) in a real time cycler (Opticon, MJ Research) (refer to tables 8 and 9 for more details). GAPDH, β-actin and rpl13a were used as the reference genes. The relative expression levels were calculated using multiple internal control genes [116], adjusted for differences in PCR efficiency (Qbase, Biogazelle) and logarithmically transformed. Expression of the housekeeping gene which is used to normalize the target gene expression should not vary among different samples used in the study. However, previous studies show that housekeeping gene expression can vary in different tissues, therefore the use of one housekeeping gene to normalize gene expression may lead to errors [116]. In order to obtain accurate measurement of gene expression, multiple internal control genes were used and the analysis was performed using the Qbase software. This software calculates the expression stability of the housekeeping genes in different samples. This is based on the principle that the ratio of two housekeeping gene expression is identical among all the samples [116]. An increasing variation in the ratio corresponds to decreasing expression stability of the housekeeping genes. In addition, the PCR efficiency was also determined for each primer and was included in the analysis. Determination of PCR efficiency is important for accurate quantification. The PCR efficiency was determined for the different primers (LPA_1, LPA_2, LPA_3, RPL, GAPDH and β-actin) used in the study by a serial dilution series. CDNA obtained from aorta of C57/BL6 mice were diluted to 40 ng, 20 ng, 10 ng, 5 ng and 1 ng.

PCR was performed for each primer with the different dilutions of cDNA. The Qbase software calculates the PCR efficiency E for each primer based on the formula $E=10^{(-1/slope)}$ and includes it in the analysis. The Q base software has the option of analysing the q-RT PCR results by including the PCR efficiency for each primer and taking into account multiple reference genes.

Reverse transcription (RT,) table 7:

SOLUTION	VOLUME
gDNA wipe out buffer, 7x	2µl
quantiscript reverse transcriptase	1µl
quantiscript RT buffer, 5x	4µl
RT primer mix	1µl
template RNA	up to 600 ng
RNase free water	to make up to 20 µl

Real time PCR, table 8:

SOLUTION	VOLUME
cDNA or water	2 µl
Quantitect SYBR Green PCR master mix, 2x	12.5 µl
Quantitect primer assay (containing both forward and reverse primers), 10x	2.5 µl
water	8 µl

Real time PCR program, table 9:

STEPS	TEMPERATURE AND DURATION	
Initial activation	95° C, 15 min	
Denaturation	94° C, 15 sec	40
Annealing	55° C, 30 sec	
Extension	72° C, 30 sec	

The gene expression of CXCL1, CCL2, CCL5 or CX_3CL1 was studied using quantitative real-time PCR. The PCR was performed in a 7900HT fast real-time PCR system (Applied Biosystems,

Darmstadt, Germany). The taqman probe contains a reporter dye at the 5' end and a nonfluorescent quencher at the 3' end. During the PCR reaction, the probe is cleaved separating the reporter dye and the quencher dye. This increases the fluorescence of the reporter. The accumulation of the PCR products is detected by monitoring the increase in fluorescence of the reporter dye.

Total RNA was isolated from PFA-fixed, paraffin embedded aortic root sections or from cultured endothelial cells (Recover all total nucleic acid isolation, Ambion and RNeasy micro kit, Qiagen, Hilden, Germany) and reverse transcribed (High capacity cDNA reverse transcription kit, Applied Biosystems, Foster city, CA) according to the manufacturer's protocol (refer to table 10 for more details). The RT reaction consists of the following four steps: 25°C for 10 min, 37°C for 120 min, 85°C for 5 min and 4°C. Taqman Gene expression assays (Applied Biosystems) were performed to quantify CXCL1, CX_3CL1, CCL5, or CCL2 expression. GAPDH was used as the reference gene (refer to tables 11 and 12 for more details). The relative expression levels were normalized to the reference gene and logarithmically transformed (Qbase, Biogazelle).

Reverse transcription, table 10:

SOLUTION	VOLUME
RT buffer, 10x	2 µl
dNTP mix (100 mM), 25x	0.8 µl
RT random primers, 10x	2 µl
multiscribe reverse transcriptase	1 µl
RNase inhibitor	1 µl
nuclease free water	3.2 µl
RNA (up to 500 ng)	10 µl

Real time PCR, table 11:

SOLUTION	VOLUME
taqman universal PCR master mix	5 µl
taqman gene expression assay mix, 20x	0.5 µl
cDNA diluted in RNase-free water	4.5 µl

Real time PCR program, table 12:

STEPS	TEMPERATURE AND DURATION	
UNG activation	50° C, 2 min 95° C, 10 min	
Denaturation	95° C, 15 sec	40
Annealing/extension	60° C, 1 min	

Following transplantation of mice with BM cells expressing LacZ under a SMC-specific promoter, successful repopulation was confirmed after 4 weeks. This was performed by quantifying the peripheral blood cells for the SM22-LacZ genotype. DNA was isolated from the whole blood of the mice which were subjected to BM transplantation, a SM22-LacZ mouse and from a C57BL/6 mouse (BioSprint, Qiagen). A standard curve was made using DNA from the LacZ and C57BL/6 mice. The percentage of repopulation was quantified using the standard curve. The standards were made using LacZ and C57BL/6 mice DNA such that the total concentration of DNA used for the PCR was 40 ng.

The standards were the following:

1) 40 ng of LacZ DNA
2) 20 ng of LacZ DNA + 20 ng of C57BL/6 DNA
3) 10 ng of LacZ DNA + 30 ng of C57BL/6 DNA
4) 5 ng of LacZ DNA + 35 ng of C57BL/6 DNA
5) 2.5 ng of LacZ DNA + 37.5 ng of C57BL/6 DNA
6) 1 ng of LacZ DNA + 39 ng of C57BL/6 DNA

Quantitative real-time PCR was performed using SYBR Green (Maxima SYBR Green qPCR master mix, Fermentas) in a real time cycler (Opticon, MJ Research) (refer to tables 13 and 14 for more details). The LacZ primers were purchased from Sigma-Aldrich. The percentage of LacZ genotype in the mice subjected to BM transplantation was calculated using the standard curve (Prism, GraphPad).

Real time PCR, table 13:

SOLUTION	VOLUME
SYBR Green master mix	12.5 µl
nuclease free water	9.5 µl
each forward and reverse primer	0.5 µl
cDNA	2 µl

Real time PCR program, table 14:

STEPS	TEMPERATURE AND DURATION
Initial denaturation	95° C, 10 min
Denaturation	95° C, 15 sec
Annealing	63° C, 30 sec
Extension	72° C, 30 sec

40

LacZ forward primer - ACGGCAAGCCGTTGCTGATTCG

LacZ reverse primer – AGCAGGATATCCTGCACCATCG

2.7 Cell culture

To culture Mono Mac 6 cells, the frozen cells were thawed and 1 ml of cell suspension was diluted to 10 ml with culture medium (RPMI 1640, Gibco, L-Glutamine 2 mM, Gibco Penicillin 200 U/ml and Streptomycin 200 µg/ml, Gibco, non essential amino acids, Gibco, OPI supplement containing oxalacetic acid, sodium pyruvate and insulin, Sigma, 10% fetal bovine serum). The cells were centrifuged at 300 g for 5 minutes and resuspended in culture medium. Then $10*10^5$ cells were seeded in a 24 well cell culture plate and cultured overnight. Following this initial step, the cells were seeded at a density of $2*10^5$ cells/ml with 2 ml per well in a 24 well plate and cultured at 37°C in an incubator with 5% CO_2 for 3-4 days before they were used for experiments. All the solutions and medium were filter sterilised using a syringe filter (pore size 0.20 µm, Corning).

To isolate endothelial cells (EC), aortas were harvested from C57BL/6 mice and the periadventitial fat and connective tissue removed under sterile conditions. The tissue was cut into 1-2 mm^2 sections and cultured in endothelial growth medium (Promocell, Heidelberg, Germany)

for 7 days (37°C, 5% CO_2) to allow the outgrowth of ECs [117]. Following outgrowth, the tissue was removed and the ECs were cultured in endothelial growth medium till the cells were 90% confluent. Then the cells were digested using accutase and passaged to new flasks. The medium was changed every 2 days. All the solutions and medium were filter sterilised using a syringe filter (pore size 0.20 µm, Corning). Lectin (*Lycopersicon esculentum*; Sigma, Munich, Germany) staining was performed to further confirm the EC phenotype. The staining was done by first dissolving the FITC-labelled lectin in endothelial growth medium such that the concentration was 20 µg/ml and the cells were incubated with this for 20 hours. Following incubation, the cells were washed with PBS three times for three minutes each. Then the cells were fixed with 4% PFA for 10 minutes and finally washed with PBS. Sub-confluent ECs (passages 3-5) were cultured in low serum medium (2%) and treated with LPA20:4 (10 µM), nLDL (200 µg/ml), or moxLDL (200 µg/ml) for 1 h with or without Ki16425 (100 µM).

To isolate BM cells, the femurs and tibias were aseptically removed from donor C57BL/6 mice and flushed with 5 ml of Dulbecco's modified eagle medium (DMEM, PAA). Then the cells were disaggregated by pipetting the cells up and down. The cells were then passed through a cell strainer (BD falcon, 40 µm) and centrifuged at 300 g for 10 minutes. Then, the cells were counted and diluted to 18000 cells/ml in DMEM-F12/10% FCS/10% L929-conditioned medium. The mononuclear phagocytic progenitor cells require macrophage colony stimulating factor (M-CSF) to differentiate into macrophages. This M-CSF is secreted by L929 cells and hence L929 conditioned medium was used to supply M-CSF to these cells. 2 ml of cells were seeded to each well of a 16 well plate and cultured at 37°C in an incubator for 3 days. Following 3 days, 1 ml of the medium was discarded and 1ml of fresh medium was added. On the 7^{th} day the differentiated macrophages were harvested for experiments. To confirm the macrophage phenotype, F4/80 (APC-labelled anti-mouse rat IgG2a, eBiosciences, Frankfurt, Germany) and CD11b (PerCP-Cy™5.5-labelled anti-mouse rat IgG2b, BD Pharmingen, Heidelberg, Germany) expression was determined by flow cytometry (BD FACS Canto II). On the 7^{th} day, the macrophages were digested with accutase (500 µl per well) and the cells were collected by centrifuging for 5 minutes at 300 g. Cells were incubated with the antibodies, F4/80 (1.5 µg) and CD11b (0.4 µg) for 30 minutes in the dark on ice. Then they were washed with 3ml of Hanks complete solution (see also section 2.3) at 300 g for 5 minutes and the measurements were taken. Appropriate isotype matched IgG antibodies were used as negative controls (eBiosciences and BD Pharmingen). The gates were set based on the negative controls.

2.7.1 Quantification of ATX activity

ECs were cultured in 24 well plates for 24 hours followed by incubation with a fluorescent ATX substrate, FS-3 (3 µM/HBSS, Echelon Biosciences, Salt Lake City, UT) for 3 hours at 37°C. FS-3 is a lysophosphatidylcholine analouge that is conjugated with a fluorophor and a quencher [118]. FS-3 incubated (3 µM/HBSS) without ECs was used as a control. The fluorescence intensity in the medium was detected with a microplate reader (see also section 2.1). All the treatment solutions were filter sterilised using a syringe filter (pore size 0.20 µm, Corning).

2.7.2 Preparation of moxLDL

Human nLDL (1 mg/ml, Calbiochem, Darmstadt, Germany) was mildly oxidised in the presence of 5 µM $CuSO_4$ at 37°C for 4 hours. Oxidative modification of LDL was monitored by determining the formation of conjugated dienes. This was performed at an optical density of 234 nm in semi continuous measurements (Nanodrop, see also section 2.1). Further oxidation of the moxLDL samples was stopped at the beginning of the propagation phase by the addition of 10 µM EDTA (final concentration) [119]. This was followed by washing the LDL with endothelial growth medium (serum free) or MOPS buffer (see also section 2.3) over a PD-10 desalting column (GE Healthcare, Uppsala, Sweden) [120]. The protein concentration was measured using DC protein assay kit (Bio-Rad, Munich, Germany) and the LDL was filtered (0.45 µm). This was stored at 4°C for no longer than 14 days.

2.8 Data illustration and statistical analysis

The data represent means ± SEMs. The data were compared with either an unpaired Student's t-test or 1- or 2- way ANOVA, followed by a Newman-Keuls or linear trend post-test when appropriate (Prism, GraphPad). The SAS 8.0 software (SAS Institute Inc., Cary, NC) was used to perform the ANOVA analysis for the randomized block design. A p-value <0.05 was considered significant.

3 Results

3.1 LPA and vascular injury

3.1.1 LPA receptor expression following vascular injury

Short-term incubation of the carotid artery with unsaturated LPA induces neointima formation even in the absence of vascular injury [5, 105]. To further study the mechanism of LPA-induced neointima formation, the expression of the LPA receptors, LPA_1 and LPA_3 was analysed in uninjured and injured carotid arteries.

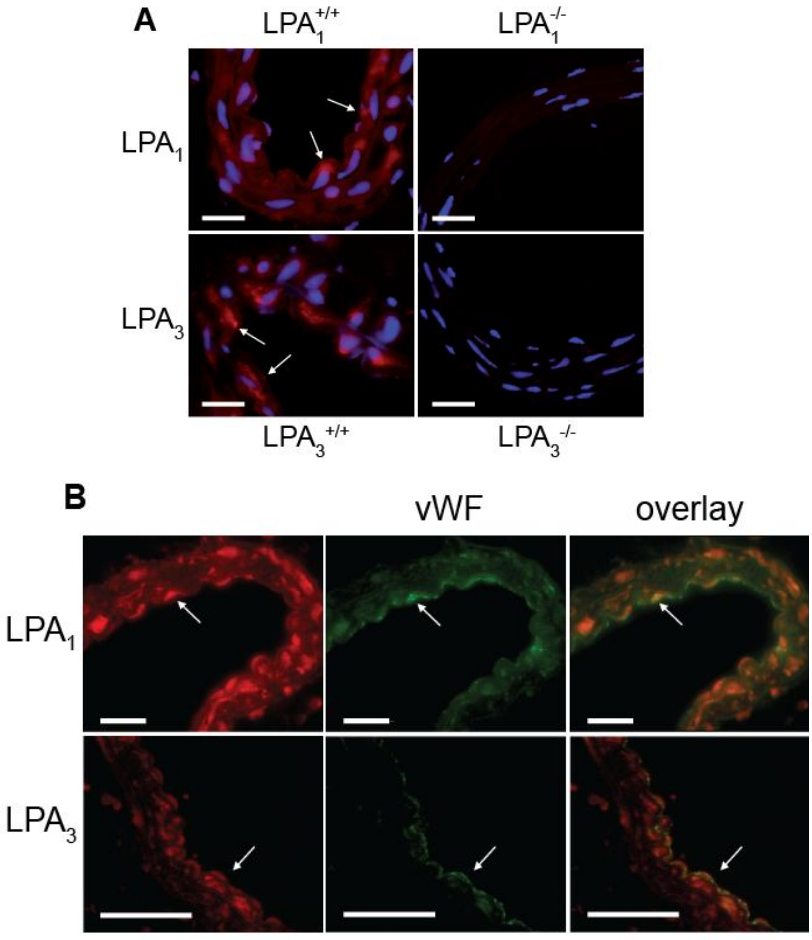

Figure 15: Mouse vascular ECs express LPA_1 and LPA_3
(A) To determine the specificity of the immunostaining for LPA_1 or LPA_3, carotid arteries of $LPA_1^{-/-}$ and $LPA_3^{-/-}$ mice were used as negative controls. (see chapter 2.5.5 for details). Scale bar: 20 µm. Nuclei were counterstained with DAPI. The arrows indicate the positive staining. (B) Double immunostaining for LPA_1 (red) or LPA_3 (red) with vWF (green) was performed in C57BL/6 mouse carotid arteries (see 2.5.5 for details). Scale bars: 20 µm (LPA_1) and 50 µm (LPA_3). The arrows indicate co-localisation of LPA_1 or LPA_3 with vWF.

LPA_1 and LPA_3 immunopositive staining was evident in wild-type mice, whereas no positive staining was seen in $LPA_1^{-/-}$ and $LPA_3^{-/-}$ mice respectively (Fig. 15A). This demonstrates the specificity of the LPA_1 and LPA_3 antibodies. Moreover, LPA_1 and LPA_3 protein is expressed in ECs of uninjured carotid arteries from C57BL/6 mice (Fig. 15A-B).

Immunostaining revealed that LPA_1 and LPA_3 are expressed in the media of uninjured carotid arteries in $ApoE^{-/-}$ mice (Fig. 16A-C). In contrast, expression of LPA_1 and LPA_3 1 week and 2 weeks following vascular injury was predominantly detectable in the neointima (Fig. 16D-I).

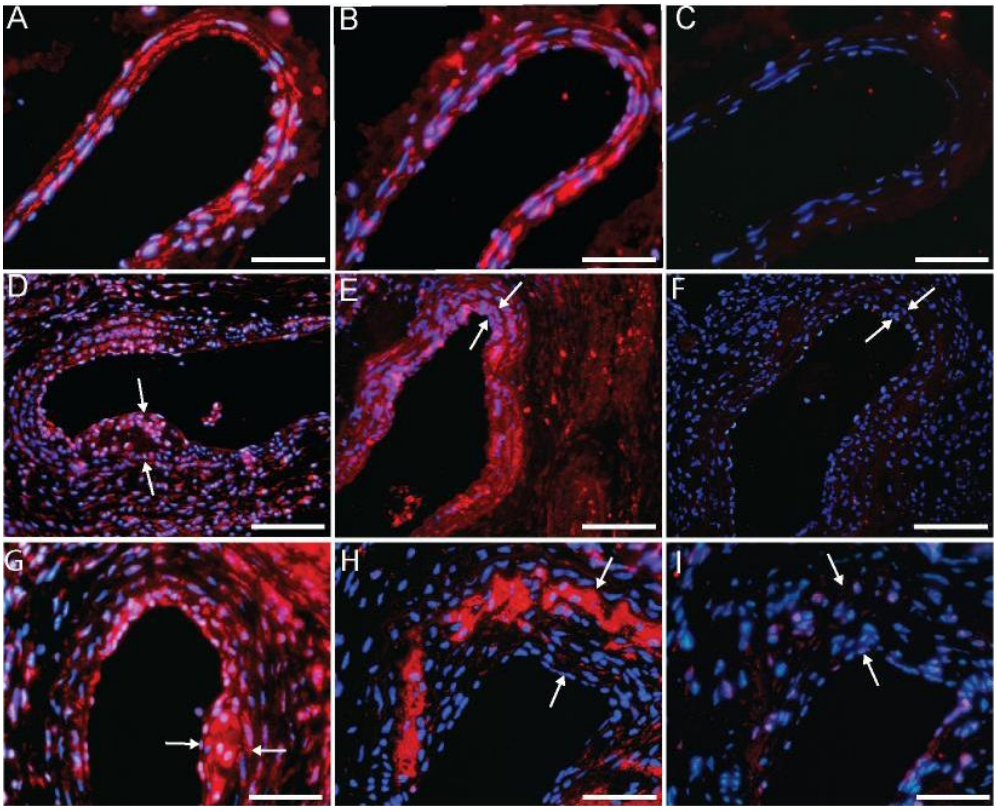

Figure 16: LPA receptor expression in uninjured and injured carotid arteries

The expression of LPA_1 (A) and LPA_3 (B) was detected in the media of uninjured carotid arteries. Neointimal expression of LPA_1 (D) and LPA_3 (E) 1 week following injury was demonstrated by immunostaining (see chapter 2.5.5 for details). Neointimal expression of LPA_1 (G) and LPA_3 (H) 2 weeks following vascular injury was demonstrated by immunostaining (see chapter 2.5.5 for details). The negative control shows negligible background staining (C, F, I). The nuclei are stained with DAPI in blue. Scale bars 100 μm (A-F) and 50 μm (G-I).

The cells which express LPA_1 and LPA_3 in the neointima 2 weeks after injury were further analysed by double immunostaining for macrophage-specific (Mac-2) or EC (vWF)-specific markers and for the LPA receptors. LPA_1 was evident in ECs (Fig. 17A), whereas LPA_3 was primarily expressed in macrophage-derived foam cells (Fig. 17B).

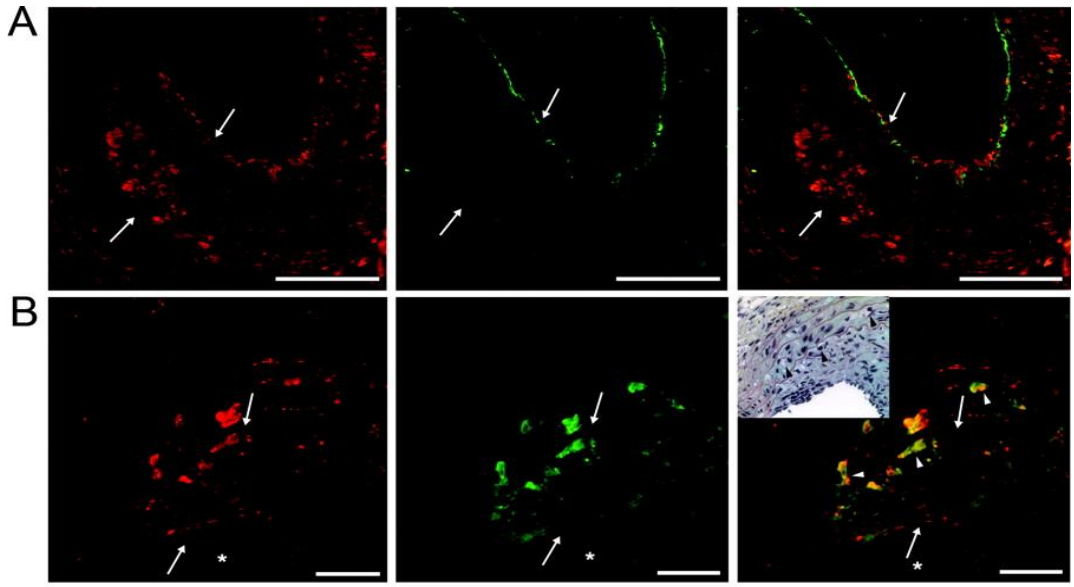

Figure 17: Cell-type specific expression of LPA receptors in the neointima
(A) At 2 weeks following vascular injury, LPA_1 (left) is predominantly co-localised with vWF (middle)-positive ECs as demonstrated by double immunostaining for vWF and LPA_1 (right, overlay) (see chapter 2.5.5 for details). (B) LPA_3 (left) is primarily co-localised with Mac-2 positive (middle) macrophages as shown by double immunostaining for LPA_3 and Mac-2 (overlay, right) (see chapter 2.5.5 for details). The inset shows an adjacent pentachrome-stained section (see chapter 2.5.4 for details). Arrowheads indicate the foam cells. Arrows indicate the neointima and stars delineate the lumen. Scale bars 100 μm (A) and 50 μm (B).

To study the regulation of LPA receptor expression by vascular injury and hyperlipidemia, the mRNA expression of the different LPA receptors was quantified 1 and 2 weeks following vascular injury. In uninjured $ApoE^{+/+}$ mice on regular diet (RD), the LPA_1 mRNA expression is higher compared to both LPA_2 and LPA_3. The expression of LPA_1 is 1.8-times and 2.4-times higher than the expression of LPA_2 or LPA_3, respectively (Fig. 18). Hyperlipidemia reduced the expression of LPA_2 mRNA, whereas LPA_1 and LPA_3 mRNA expression was unaltered compared to mice fed a RD (Fig. 18). 1 week and 2 weeks following vascular injury, LPA_1 mRNA was downregulated. In contrast, mRNA expression of LPA_2 and LPA_3 was up-regulated 1 week following injury (Fig. 18). These results show that LPA receptors are differentially regulated by vascular injury and hyperlipidemia. The LPA receptors LPA_1 and LPA_3 are both expressed in the arterial vessel walls after wire injury and during hyperlipidemia.

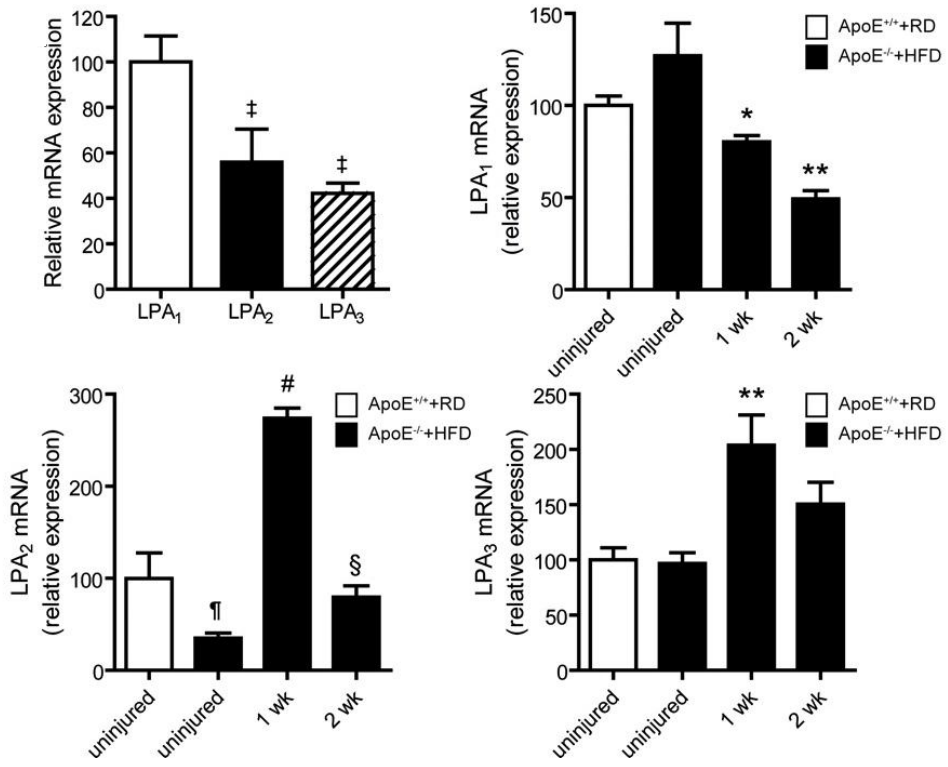

Figure 18: Regulation of LPA receptor expression by vascular injury and hyperlipidemia
The mRNA expression of LPA_1, LPA_2 and LPA_3 in uninjured carotid arteries of $ApoE^{+/+}$ mice on RD is shown in the upper left panel. The effect of HFD and vascular injury on mRNA expression of LPA_1 (upper right), LPA_2 (lower left) and LPA_3 (lower right) was studied by quantitative real time RT-PCR (see 2.6.2 for details). ‡P<0.05 versus LPA_1; *P<0.05 versus $ApoE^{-/-}$ uninjured group; **P<0.05 versus both uninjured groups; ¶P<0.05 versus $ApoE^{+/+}$ uninjured; #P<0.001 versus both uninjured and 2 week groups; §P<0.001 versus 1 week group. n=3-4 mice.

3.1.2 Blocking LPA_1 and LPA_3 inhibits the neointimal accumulation of SMCs and macrophages

It has previously been shown that blocking of LPA_1 and LPA_3 using Ki16425 significantly reduces neointima formation following vascular injury in $ApoE^{-/-}$ mice [121]. We further studied the effect of Ki16425 on the cellular composition of the neointima following carotid wire injury. The mice were injected (IP) daily with Ki16425 (5 mg/kg/day) or control buffer (10% DMSO dissolved in PBS) for 3 weeks following injury. The arteries were harvested 1 week after the last injection of Ki16425. Treatment with Ki16425 reduced the SMC content in the neointima compared to vehicle-treated group, as demonstrated by the reduced α-SMA-, SM22- and calponin-immunopositive area in the neointima (Fig. 19A). In addition, Ki16425 diminished the neointimal Mac-2 positive area by 49%, whereas the CD3+ T-cell number was unaltered compared to the vehicle-treated group (Fig. 19B-C).

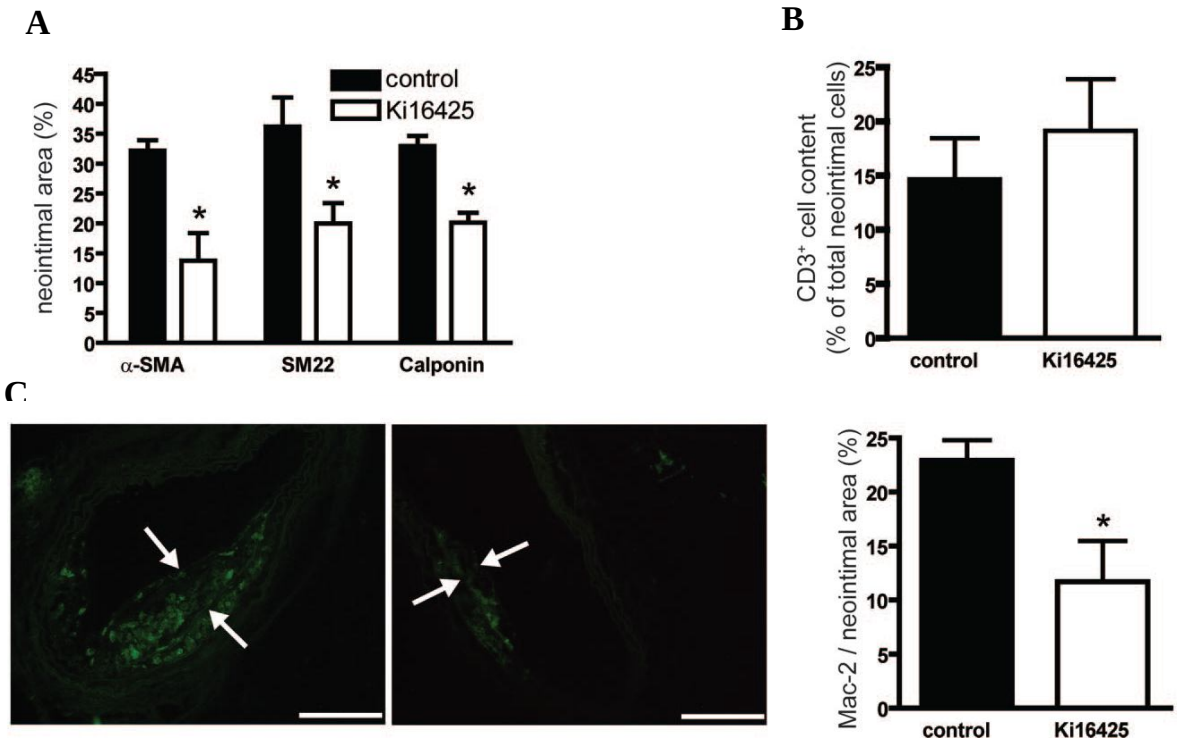

Figure 19: Effect of Ki16425 on the cellular composition of the neointima
(A) Ki16425 reduced the SMC content in the neointima as demonstrated by reduced α-SMA, SM22 and calponin staining (see chapter 2.5.5 for details). n=4-6 mice. (B) The CD3+ T-cell content of the neointima was unaltered by treatment with Ki16425 (see chapter 2.5.5 for details). n=4-5 mice. Immunostaining for Mac-2 in control buffer- (C, left) and Ki16425-treated (C, middle) mice revealed that Ki16425 significantly reduced the Mac-2-positive area in the neointima (C, right) (see chapter 2.5.5 for details). Scale bars: 100 μm. *P<0.05. Arrows delineate the neointima. n=5-6 mice

Almost complete re-endothelialisation of the injured artery was observed in control buffer- and Ki16425-treated mice 28 days following injury as shown by immunostaining for vWF (Fig. 20). Therefore, a role of LPA receptors in endothelial recovery is unlikely. In addition, vWF-positive cells were absent in the neointima (Fig. 20), indicating that lesional neovascularisation is not affected by Ki16425.

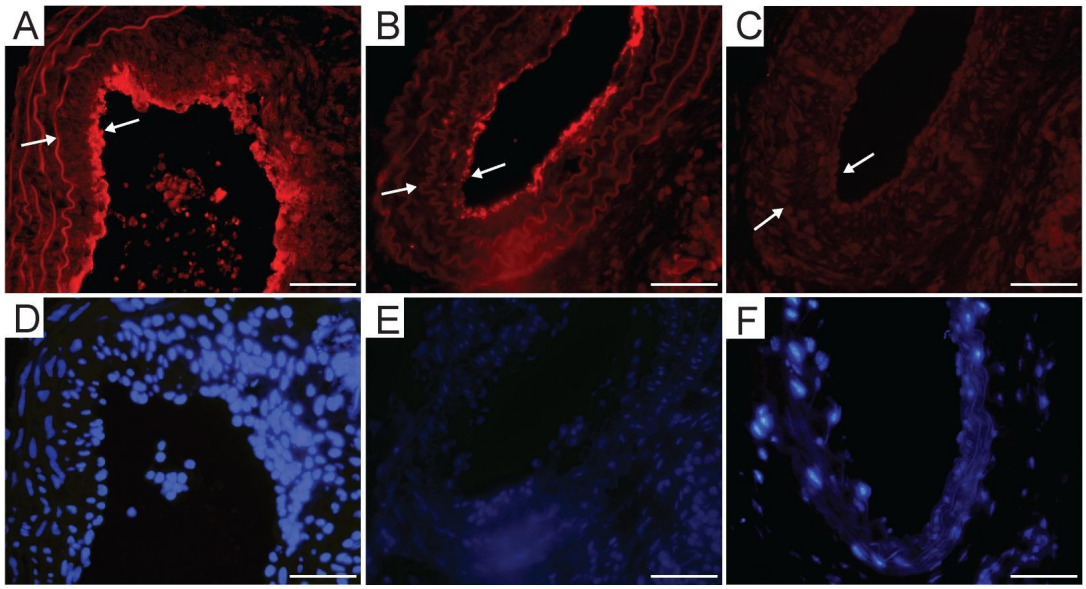

Figure 20: Effect of Ki16425 on endothelial recovery following vascular injury

Almost complete re-endothelialisation was evident in both the control buffer- (A, D) and the Ki16425-treated (B, E) group, as shown by immunostaining for vWF (see chapter 2.5.5 for details). The nuclei were stained with DAPI (D-F) Negligible background fluorescence was seen in the negative controls (C). Scale bars: 50 μm. The arrows delineate the neointima.

Studies have shown that blocking LPA_1 and LPA_3 following vascular injury reduces the neointimal expression of the transcription factor HIF-1α and of the chemokine CXCL12 [121]. HIF-1α is upregulated following injury and regulates the neointimal expression of CXCL12 [104]. Moreover, the CXCL12/CXCR4 axis plays an important role in neointima formation by inducing stem cell-mediated vascular repair following vascular injury [97, 98]. Blocking LPA_1 and LPA_3 by Ki16425 inhibits the injury-induced mobilisation of Sca-1^+/lin^- SPCs into the circulation [121]. To study the role of LPA receptors in neointimal SPC accumulation, we quantified Sca-1/α-SMA immunopositive cells in the neointima following treatment with Ki16425. We found that blocking LPA_1 and LPA_3 reduced the neointimal accumulation of Sca-1^+/α-SMA^+ cells by 46% (Fig. 21).

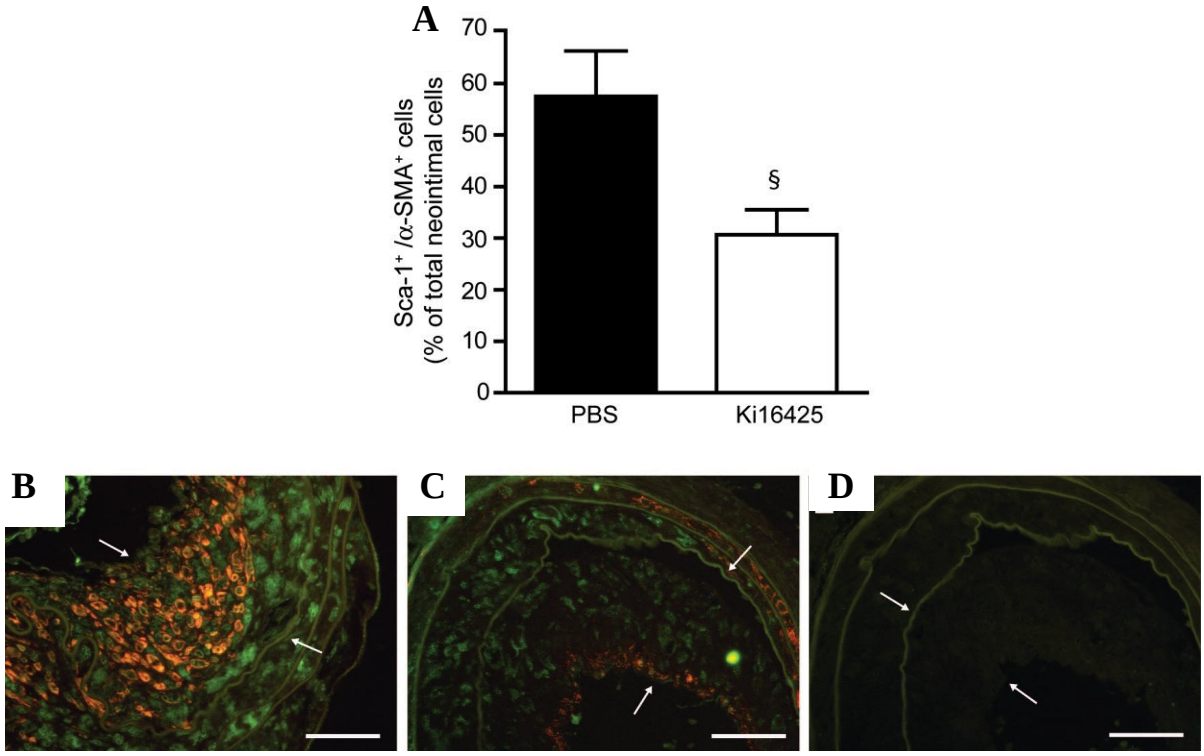

Figure 21: Role of Ki16425 in the neointimal accumulation of Sca-1$^+$/α-SMA$^+$ cells
(A) The neointimal accumulation of Sca-1$^+$/α-SMA$^+$ cells was reduced by treatment with Ki16425 as determined by double immunostaining for Sca-1 and α-SMA (see chapter 2.5.5 for details). Representative merged images for Sca-1 (green) and α-SMA (red) double staining from control buffer (B) and Ki16425 (C) treated mice are shown. The negative control staining shows negligible background staining (D). §P<0.05 versus PBS. Scale bars: 50 μm. The arrows delineate the neointima. n=4-5 mice.

Of note, Ki16425 did not affect serum cholesterol, triglycerides, ALT, and creatinine levels (Table.15).

	PBS	Ki16425	P value
Cholesterol mmol/L	13.6 ± 1.1 N=6	11.6 ± 1.7 N=9	P=0.417
Triglyceride mmol/L	0.89 ± 0.33 N=6	0.82 ± 0.13 N=9	P=0.813
ALT U/L	32.6 ± 8 N=6	33.3 ± 7 N=9	P=0.951
Creatinine μmol/L	25.1 ± 2.5 N=6	22.2 ± 2.4 N=9	P=0.434

Table 15: Serum biochemistry of ApoE$^{-/-}$ mice treated with Ki16425 or vehicle (see chapter 2.5.7 for details).

Since blocking LPA_1 and LPA_3 following vascular injury reduced the neointimal accumulation of macrophages, the role of LPA in arterial monocyte recruitment was further studied in *ex vivo* perfused carotid arteries using monocytic MM6 cells. Pre-perfusion of the carotid arteries with LPA20:4 (40 µM) for 4 h increased the adhesion of monocytes to the endothelium implying a direct role of LPA20:4 in atherogenic monocyte recruitment (Fig. 22). Moreover, pre-treatment of the MM6 cells with either a blocking CXCR2 or CXCR4 antibody diminished the LPA20:4-induced monocyte adhesion (Fig. 22). Taken together, these results indicate that blocking LPA_1 and LPA_3 following vascular injury may reduce the neointimal accumulation of macrophages via impaired monocyte adhesion to the vessel wall.

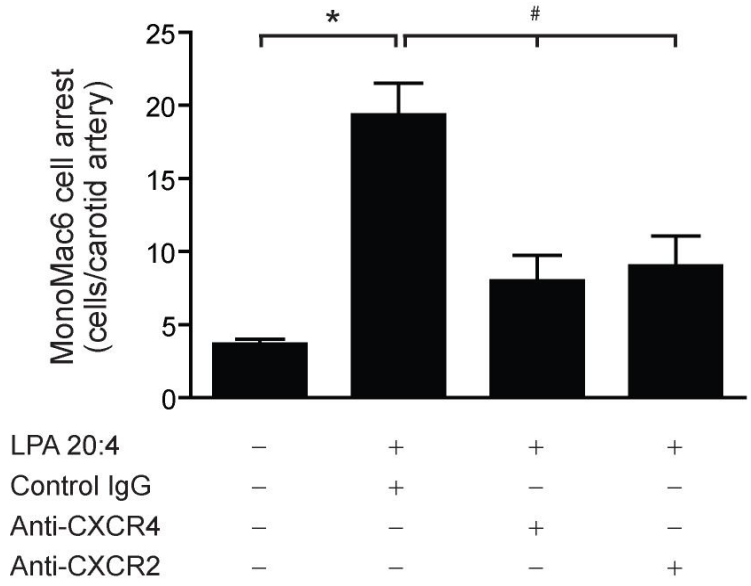

Figure 22: Role of LPA in monocyte adhesion
The carotid arteries were pre-perfused *ex vivo* with LPA20:4 (40 µM, 3 hours) followed by perfusion with MM6 cells. LPA20:4-treatment significantly increased MM6 cell adhesion to the vessel wall compared to untreated arteries. This LPA-induced adhesion was inhibited when the MM6 cells were pre-treated with blocking antibodies against CXCR4 or CXCR2 prior to perfusion (see chapter 2.4.9 for details). *P<0.05, #P<0.05. n=3 mice.

3.1.3 LPA20:4 induces the expression of CXCL12 and HIF-1α

The molecular mechanisms of LPA-induced neointima formation were studied after endoluminal incubation of carotid arteries from C57BL/6 mice with unsaturated LPA20:4. The HIF-1α and CXCL12 protein expression in the vessel wall was quantified by Western analysis or ELISA, respectively. Right carotid arteries without LPA incubation were used as controls. HIF-1α was upregulated as early as 1 day following incubation and remained elevated until day 28 as compared to control (Fig. 23A). In addition, CXCL12 was increased in the vessel wall 1 day, 9

days, and 28 days after LPA20:4-incubation compared with control (Fig. 23B). Taken together, these data suggest that unsaturated LPA20:4 induces prolonged upregulation of HIF-1α and CXCL12 in the vessel wall.

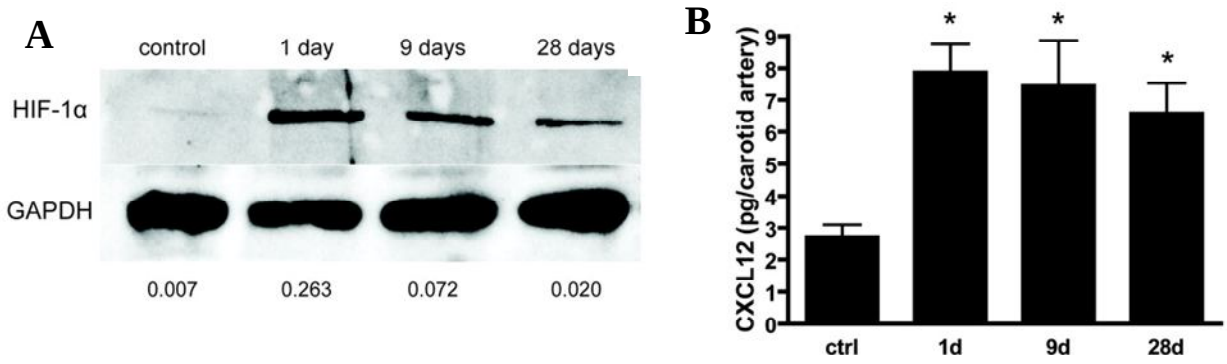

Figure 23: LPA-induced HIF-1α and CXCL12 expression

(A) Western blot was performed to quantify HIF-1α and the band intensity was normalized to the GAPDH signal (representative western blot from 3 independent experiments is shown) (see chapter 2.5.3 for details). The numbers represent the ratio of band intensity for each time point. (B) The CXCL12 protein in the carotid arteries was quantified by ELISA following endoluminal incubation with LPA20:4 (see chapter 2.5.2 for details). *P<0.05 versus control. n=3-5 mice.

To obtain additional evidence for a HIF-1α-dependent regulation of CXCL12 expression following LPA incubation [104], we studied whether HIF-1α and CXCL12 were expressed in the same neointimal cells by double immunostaining. CXCL12 was predominantly expressed in neointimal cells with nuclear localisation of HIF-1α, indicating increased transcriptional activity of HIF-1 in cells that express CXCL12 (Fig. 24).

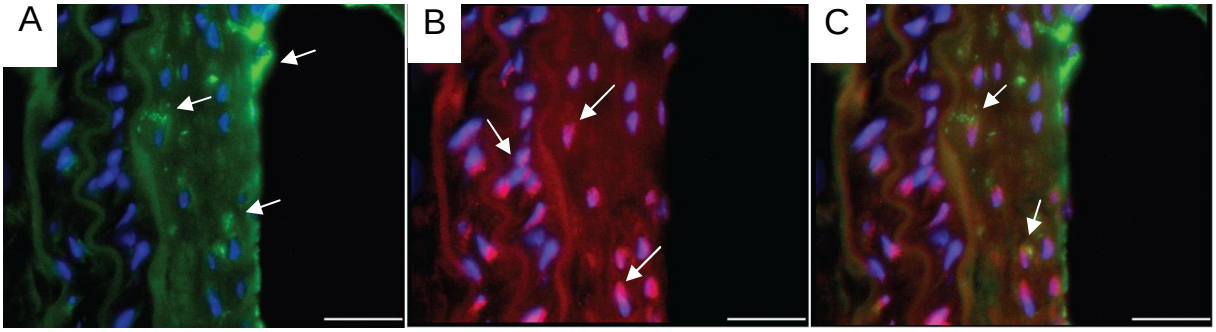

Figure 24: Cellular co-localisation of HIF-1α and CXCL12

(A) CXCL12 immunopositive area was evident primarily in the neointimal cells (green). HIF-1α (B) was detectable in the nucleus of both neointimal and medial cells (red). Overlay shows the cellular co-localisation of nuclear HIF-1α and CXCL12 in the neointimal cells (C) (see chapter 2.5.5 for details). DAPI was used to stain the nuclei. Scale bars: 25 µm. Arrows indicate the positive staining.

To study the role of LPA-induced CXCL12 expression in the vessel wall on SPC mobilisation, CXCL12 was silenced by perivascular application of siRNA during LPA-incubation. Silencing of

CXCL12 blocked the LPA20:4-induced SPC mobilisation after 24 h and the neointima formation after 28 days compared to non-targeting control siRNA (Fig. 25A-B). The arterial expression of CXCL12 is essential for LPA20:4-induced SPC mobilisation and neointima formation.

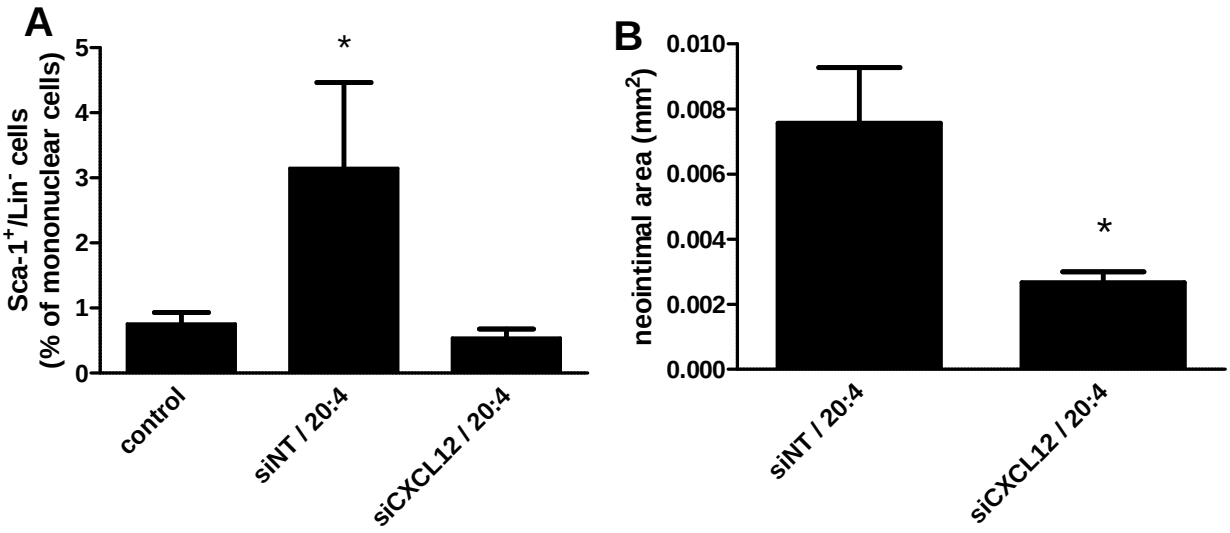

Figure 25: Arterial CXCL12 is important for LPA20:4-induced neointima formation
(A) LPA20:4-induced mobilisation of SPCs 24 hours was blocked by CXCL12-specific siRNA (siCXCL12) but not with the non-targeting siRNA (siNT) as shown by flow cytometry (see chapter 2.5.1 for details). Control = before LPA20:4 incubation. *P<0.05 versus all other groups. n=3-5 mice. (B) Treatment with siCXCL12 reduced the LPA20:4-induced neointima formation as compared to siNT treatment. *P<0.05. n=3 mice.

3.1.4 Unsaturated LPA induces SPC mobilisation via LPA_1 and/or LPA_3

To study whether LPA_1 and LPA_3 are involved in LPA-induced mobilisation of SPCs, circulating Sca-1^+/lin^- cells were quantified by flow cytometry after co-incubation of the carotid artery with LPA and Ki16425. Endoluminal incubation of the carotid artery with LPA20:4 increased the mobilisation of SPCs at 1 day compared to PBS (Fig. 26). Co-incubation with the LPA_1 and LPA_3 antagonist Ki16425 prevented the LPA20:4-induced SPC mobilisation (Fig. 26). Therefore, LPA20:4 acts via LPA_1 and/or LPA_3 to induce the mobilisation of SPCs.

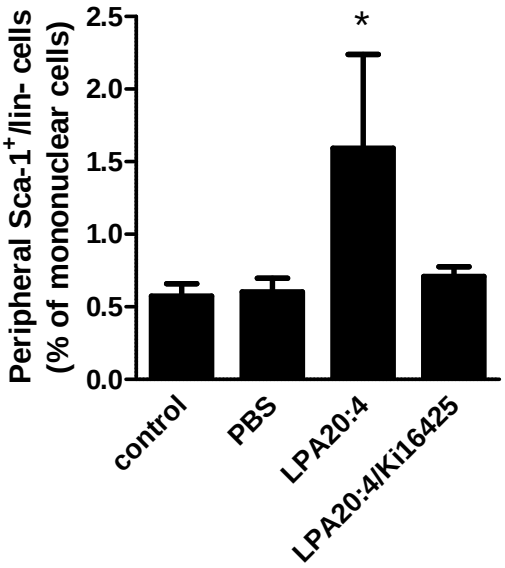

Figure 26: LPA20:4 acts via LPA_1 and LPA_3 to induce SPC mobilisation
Endoluminal incubation of the carotid artery with LPA20:4 induced the mobilisation of Sca-1^+/lin^- cells following 1 day and this was blocked by co-incubation with Ki16425 as shown by flow cytometry (see chapter 2.5.1 for details). Control = before LPA20:4 incubation. *P<0.05 versus all other groups. n=3-5 mice.

In contrast to LPA20:4, 1AGP18:1 is known to mobilise SPCs 9 days after incubation of the carotid artery, suggesting delayed upregulation of HIF-1 and CXCL12. Co-incubation of 1AGP18:1 with Ki16425 also inhibited the increase of SPCs after 1AGP18:1 treatment (Fig. 27). Therefore, the difference between the time courses of the SPC mobilisation following LPA20:4 and 1AGP18:1 treatment is not due to activation of different LPA receptors.

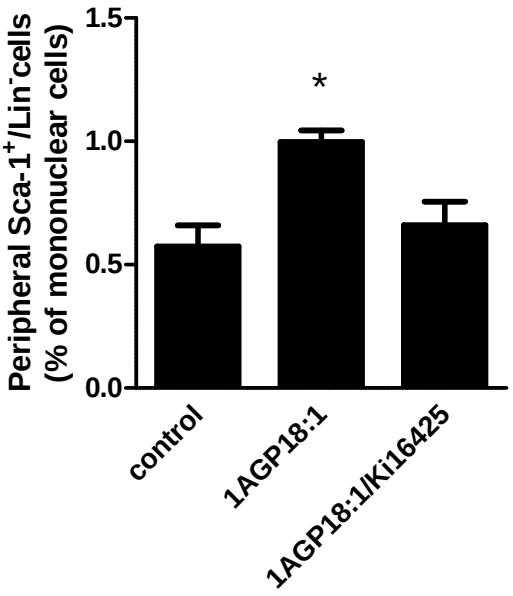

Figure 27: 1AGP18:1 acts via LPA_1 and LPA_3 to induce SPC mobilisation
Endoluminal incubation of the carotid artery with 1AGP18:1 induced mobilisation of Sca-1^+/lin^- cells after 9 days. Co-incubation with Ki16425 blocked the 1AGP18:1-induced SPC mobilisation after 9 days as determined by flow cytometry (see chapter 2.5.1 for details). Control = before 1AGP18:1 incubation. *P<0.05 versus all other groups. n=4-5 mice.

3.1.5 LPA induces neointima formation by the recruitment of SPCs

LPA-induced neointima formation was studied 28 days following incubation. In contrast to PBS, LPA20:4 and 1AGP18:1 induced neointima formation in the carotid artery after short-term incubation (Fig. 28). This LPA-induced neointima formation was blocked by co-incubation with Ki16425 (Fig. 28), indicating that LPA20:4- and 1AGP18:1-induced neointima formation is mediated by LPA_1 and/or LPA_3.

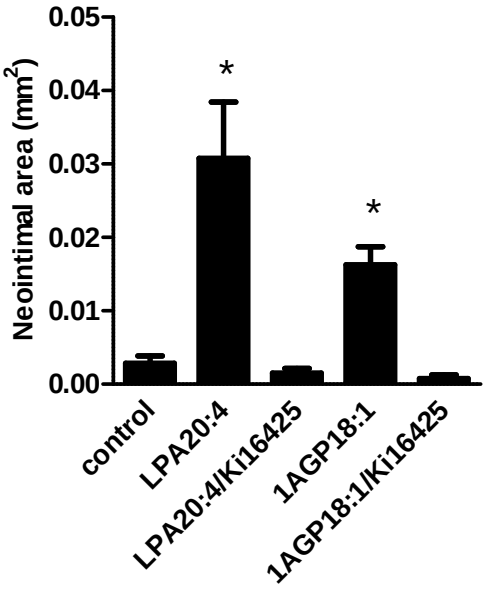

Figure 28: LPA20:4 and 1AGP18:1 induce neointima formation via LPA_1 and LPA_3
Endoluminal incubation of the carotid artery only with 1AGP18:1 and LPA20:4 induced neointima formation following 28 days and this was blocked by co-incubation with Ki16425 (see chapter 2.5.4 for details). Control = PBS incubation. *P<0.05 versus all other groups. n=4-5 mice.

To study whether LPA-induced neointima formation is associated with recruitment of SPCs, whole body irradiated C57BL/6 mice were transplanted with SM22-LacZ+ BM cells. The carotid artery was incubated with LPA20:4 and 4 weeks later, neointimal LacZ+ cells were studied by TPLSM. Following LPA20:4 incubation, BM-derived LacZ+ SPCs were detected in the neointima, whereas co-incubation with Ki16425 greatly reduced neointimal LacZ+ SPCs (Fig. 29A-B). In mice with wild-type BM, only negligible background fluorescence was observed in the carotid artery (Fig. 29C).

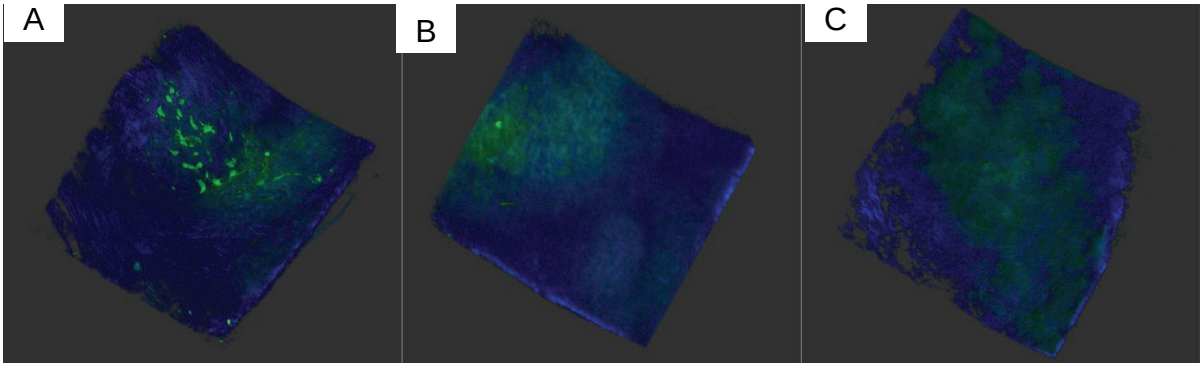

Figure 29: The role of BM-derived SPCs in LPA-induced neointima formation
(A) 3-D reconstruction of the carotid artery imaged by TPLSM shows LacZ+ cells (green) in LPA20:4-induced neointima of mice transplanted with SM22-LacZ BM cells (see chapter 2.5.6 for details). (B) The LacZ+ neointimal cells were greatly reduced following co-incubation of LPA20:4 with Ki16425. (C) Negligible background fluorescence was seen in the untreated carotid artery. Blue, second harmonic generation signal of collagen; aquamarine, auto fluorescence of elastin bands. Control = PBS.

In addition, immunostaining for β-galactosidase was performed in chimeric mice with SM22-LacZ+ BM cells, following LPA20:4-incubation with or without Ki16425. After 4 weeks, β-galactosidase positive cells were detectable in the neointima of LPA20:4-treated arteries (Fig. 30A). In contrast, no β-galactosidase positive cells were detectable in carotid arteries that were incubated with LPA20:4 and Ki16425 (Fig. 30B). Negligible background was observed in carotid artery sections stained with a non-specific control antibody (Fig. 30C). These results suggest that LPA20:4 induces neointima formation by recruiting SPCs from the BM via activation of LPA_1 or/and LPA_3 in the vessel wall.

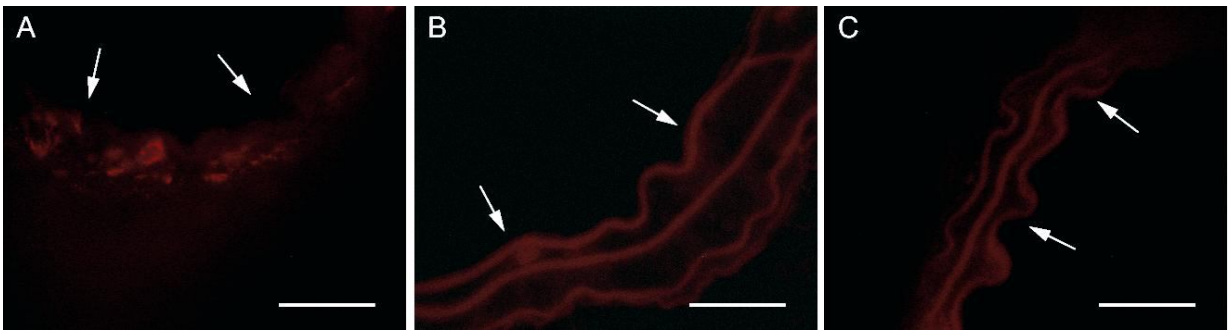

Figure 30: LPA20:4-induced recruitment of BM-derived SPCs
(A) Immunostaining for β-galactosidase showed recruitment of BM-derived SPCs to the neointima 28 days following endoluminal incubation of the carotid artery with LPA20:4. (B) After combined incubation with LPA20:4 and Ki16425, no β-galactosidase positive cells were detectable in the neointima. (C) No specific immunostaining was found using a non-specific control antibody (see chapter 2.5.5 for details). The arrows indicate the luminal side of the artery. Scale bars: 25 µm.

3.1.6 LPA20:4-induced SPC mobilisation and neointima formation requires LPA_1 and LPA_3

To identify which LPA receptor is involved in the LPA-induced SPC mobilisation and neointima formation, LPA_1 and LPA_3 were silenced in the carotid arteries by perivascular application of siRNA. Treatment with 4 nmol of LPA_1- or 3 nmol of LPA_3-specific siRNA reduced the LPA_1 mRNA expression by 83.9% (n=2-3 mice, $P<0.05$) and LPA_3 mRNA expression by 84% (n=2-3 mice, $P<0.05$) respectively compared to treatment with non-targeting siRNA after 4 days. Therefore, 3 nmol of LPA_3-specific and 4 nmol of LPA_1-, LPA_2-specific or of non-targeting siRNA was used. Treatment with LPA_1- or LPA_3-specific siRNA blocked the LPA20:4-induced mobilisation of Sca-1^+/lin^- cells 1 day following incubation compared to non-targeting siRNA treatment (Fig. 31A). Following LPA20:4-incubation, the neointimal area was also reduced in the LPA_1- or LPA_3-siRNA treated compared to non-targeting siRNA-treated mice (Fig. 31B). Taken

together, these results imply that LPA_1 and LPA_3 are independently involved in LPA20:4-induced neointima formation.

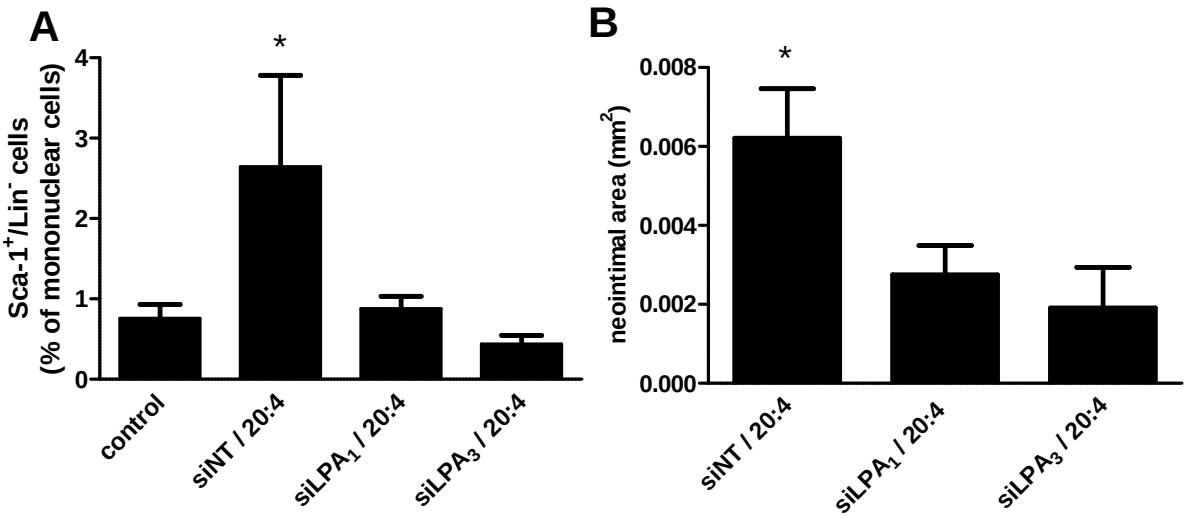

Figure 31: Role of LPA_1 and LPA_3 in LPA20:4-induced neointima formation
(A) Mobilisation of SPCs at 1 day after LPA20:4 incubation was blocked by treatment with LPA_1-($siLPA_1$) or LPA_3 ($siLPA_3$)-specific siRNA but not with the non-targeting siRNA (siNT) as shown by flow cytometry (see chapter 2.5.1 for details). Control = before LPA20:4 incubation. *P<0.05 versus all other groups. n=4-5 mice. (B) Treatment with $siLPA_1$ or $siLPA_3$ reduced the neointima formation 28 d after LPA20:4 incubation as compared to siNT treatment. *P<0.05 versus all other groups. n=4-5 mice.

3.2 LPA and atherosclerosis

3.2.1 MoxLDL-induced monocyte recruitment is mediated by LPA

We studied the role of LPA in moxLDL-induced monocyte adhesion, because LPA is produced following mild oxidation of LDL and triggers monocyte recruitment (section 3.1.2) [10]. In contrast to native LDL, pre-treatment of *ex vivo* perfused carotid arteries with moxLDL increased the rolling and adhesion of monocytic MM6 cells to the vessel wall (Fig. 32A-B). Blocking of CXCR2 on monocytes or CXCL1 in the vessel wall using neutralizing antibodies reduced the moxLDL-induced monocyte rolling and adhesion (Fig. 32A-B). Moreover, blocking the LPA_1 and LPA_3 receptors which are expressed on ECs (as shown in Fig.15) using Ki16425 during moxLDL perfusion completely blocked rolling and adhesion of monocytes (Fig. 32A-B). These results indicate that moxLDL activates LPA receptors in the vessel wall and releases CXCL1, which triggers the rolling and adhesion of monocytes via CXCR2.

LDL oxidation results in the synthesis of LPC [122] which is a physiological substrate for ATX, the enzyme which converts LPC into LPA [1]. To study whether vessel-wall-derived ATX is involved in moxLDL-induced monocyte recruitment, carotid arteries were pre-treated with the

ATX inhibitor S32826 in addition to moxLDL. S32826 significantly reduced moxLDL-induced rolling and adhesion of monocytes (Fig. 32A-B), indicating that ATX generates LPA from moxLDL-derived LPC and is essential in moxLDL-induced monocyte recruitment.

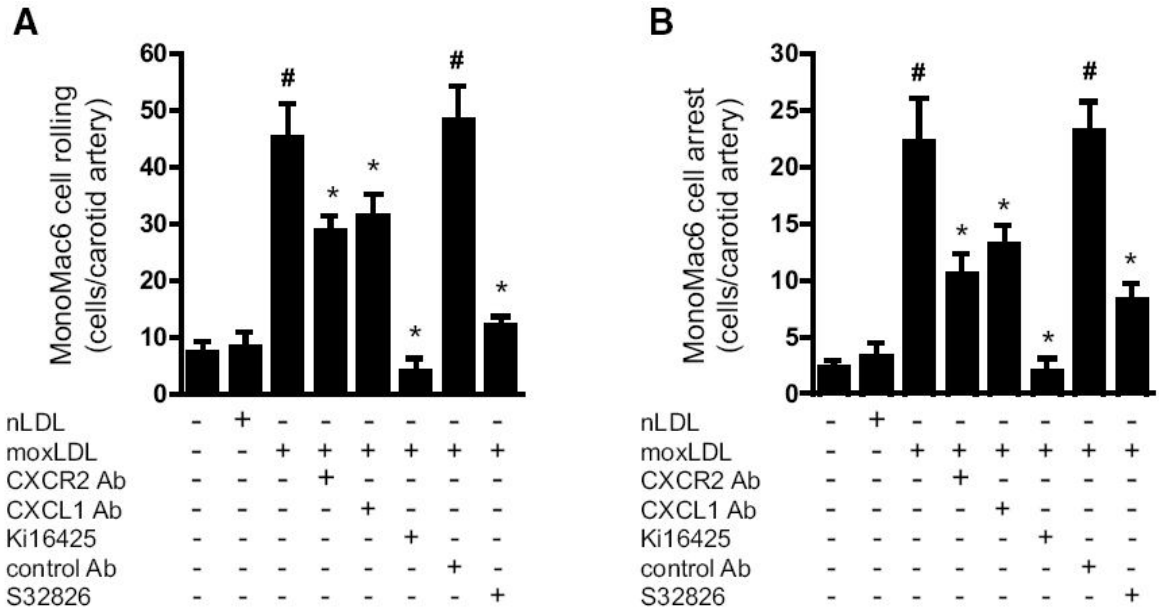

Figure 32: MoxLDL-induced rolling and arrest of monocytic MM6 cell requires CXCL1 and the LPA receptors on.
(A) Mouse carotid arteries were perfused *ex vivo* with nLDL or moxLDL for 1 h followed by perfusion with MM6 cells (see chapter 2.4.9 for details). The rolling of MM6 cells was quantified during 10 min of perfusion. *P<0.05 versus moxLDL with or without control Ab, #P<0.05 versus vehicle and nLDL. n= 3-4 mice. (B) Mouse carotid arteries were perfused *ex vivo* with nLDL or moxLDL for 1 h followed by perfusion with MM6 cells (see chapter 2.4.9 for details). The adhesion of MM6 cells to the vessel wall was quantified during 10 min of perfusion. *P<0.05 versus moxLDL with or without control Ab, #P<0.05 versus vehicle and nLDL. n= 3-4 mice.

To investigate the role of LPA in moxLDL-induced monocyte adhesion via the CXCL1/CXCR2 axis, carotid arteries were perfused with LPA20:4 and the monocyte adhesion and rolling were studied. Similar to previous results which show that treatment with LPA20:4 (40 μM) for 3 h induces monocyte arrest in a CXCR2-dependent manner (Fig. 22), treatment with LPA20:4 (10 μM) for 1 h also significantly increased monocyte rolling and adhesion to the vessel wall (Fig. 33A-B). This reduced concentration of LPA20:4 mimics more closely the LPA levels during atherogenesis, whereas wire injury may result in much higher LPA concentrations in the vessel wall due to the activation of platelets. The LPA20:4-induced rolling and adhesion of MM6 cells was inhibited by blocking either CXCR2 on monocytes or CXCL1 in the vessel wall (Fig. 33A-B). LPA20:4 induces monocyte rolling and adhesion to the endothelium via the CXCL1/CXCR2 axis.

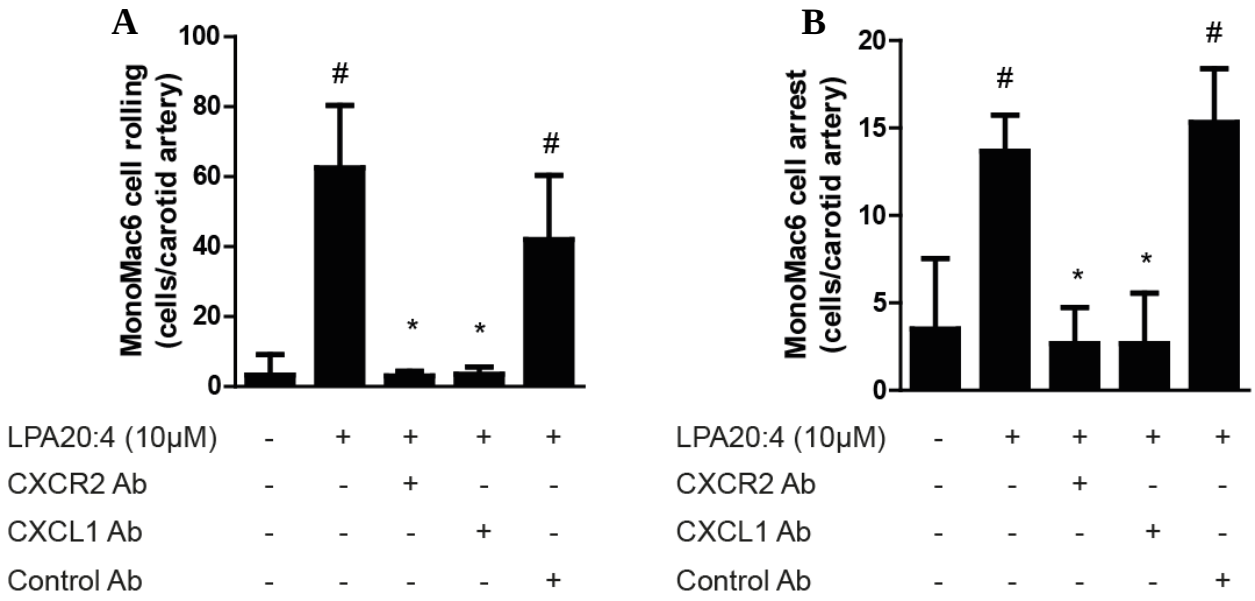

Figure 33: LPA20:4-induced monocyte rolling and adhesion requires CXCL1
(A) Mouse carotid arteries were perfused *ex vivo* with LPA20:4 (10 µm) for 1 h followed by perfusion with MM6 cells (see chapter 2.4.9 for details). The rolling of MM6 cells was quantified. *P<0.05 versus LPA20:4 with or without control Ab, #P<0.05 versus vehicle. n= 2-3 mice. (B) Mouse carotid arteries were perfused *ex vivo* with LPA20:4 (10 µm) for 1 h followed by perfusion with MM6 cells (see chapter 2.4.9 for details). The adhesion of MM6 cells was quantified. *P<0.05 versus LPA20:4 with or without control Ab, #P<0.05 versus vehicle. n=3-4 mice.

Collectively, these results suggest that LPA mediates moxLDL-induced monocyte adhesion and rolling via endothelial LPA receptor-mediated release of CXCL1.

3.2.2 LPA20:4 induces the release of endothelial CXCL1

The mechanism of moxLDL-induced release of CXCL1 from ECs was studied *in vitro*. Blocking the LPA receptors inhibited the secretion and surface immobilisation of CXCL1 triggered by moxLDL as determined by ELISA (Fig. 34A-B). Therefore, LPA is involved in moxLDL-induced secretion and surface deposition of endothelial cell-derived CXCL1.

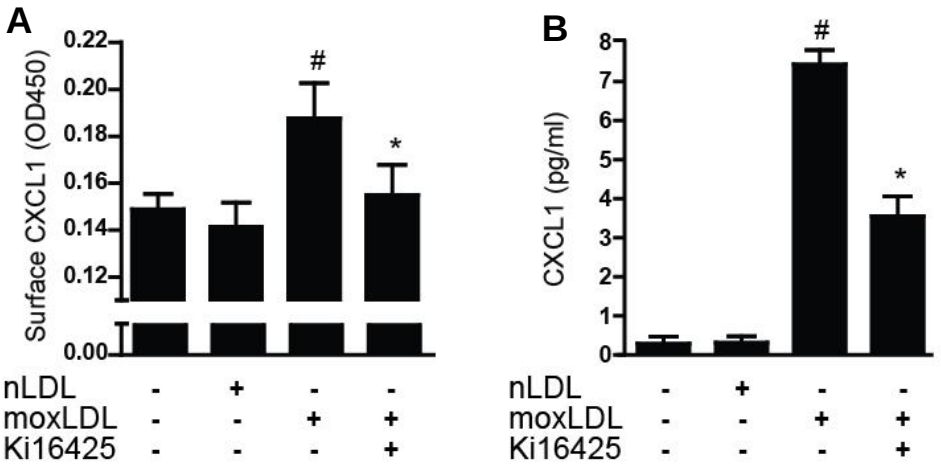

Figure 34: Role of LPA in moxLDL-induced release of CXCL1 from ECs
(A) Surface deposition of CXCL1 on ECs after stimulation with nLDL (200 µg/ml) or mox-LDL (200 µg/ml) was quantified by surface ELISA (see chapter 2.5.2 for details). #P<0.05 versus nLDL or vehicle; *P<0.05 versus moxLDL. n=4. (B) Endothelial CXCL1 secretion after stimulation with nLDL (200 µg/ml) or moxLDL (200 µg/ml) was quantified in the medium by ELISA (see chapter 2.5.2 for details). #P<0.01 versus nLDL or vehicle; *P<0.01 versus moxLDL. n=4.

Furthermore, treatment of ECs *in vitro* with LPA20:4, but not with LPA18:0, upregulated CXCL1 mRNA expression after 60 minutes (Fig. 35). This LPA-induced CXCL1 mRNA expression was reduced by blocking LPA receptors using Ki16425 (Fig. 35), demonstrating that LPA receptors are involved in LPA20:4-mediated upregulation of CXCL1. Taken together, these results imply that unsaturated LPA triggers both the acute release of preformed CXCL1 and the transcriptional upregulation of CXCL1 resulting in a bi-phasic response of endothelial CXCL1.

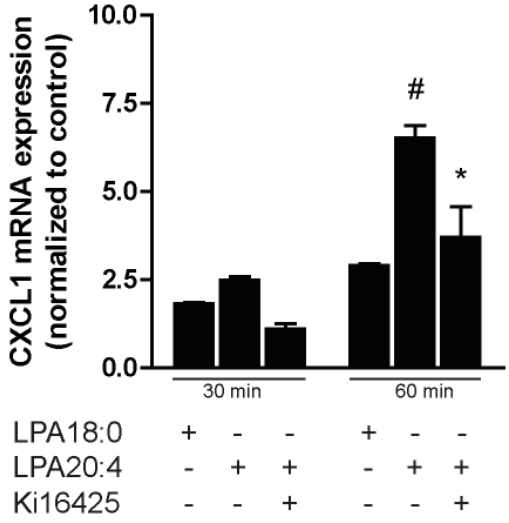

Figure 35: Unsaturated LPA induces CXCL1 expression
The CXCL1 mRNA expression was determined by qRT-PCR (see chapter 2.6.2 for details) in treated ECs that were treated for 30 or 60 min with LPA20:4 or LPA18:0 (10 µM). In addition, the effect of LPA20:4 on endothelial CXCL1 expression was studied in the presence of the LPA receptor antagonist Ki16425 (100 µM). #P<0.05 versus LPA18:0; *P<0.05 versus LPA20:4. n=4.

To study whether CXCL1 is stored in arterial endothelial cells *in vivo*, double immunostaining for vWF and CXCL1 was performed in normal mouse carotid arteries. Indeed, CXCL1-specific immunostaining was evident in vWF-positive ECs (Fig. 36A).

Chemokines need to be immobilised on the cell surface to effectively induce monocyte adhesion [63]. Therefore, the endothelial surface deposition of CXCL1 in carotid arteries upon treatment with LPA was studied *in vivo* using two-photon microscopy. Following perfusion of carotid arteries for 1 h with LPA20:4, CXCL1 was detectable by a fluorescently-labelled CXCL1 Ab on the surface of the ECs (Fig. 36B). In contrast, CXCL1-specific immunostaining on the endothelial surface was absent after treatment with control buffer (Fig. 36B).

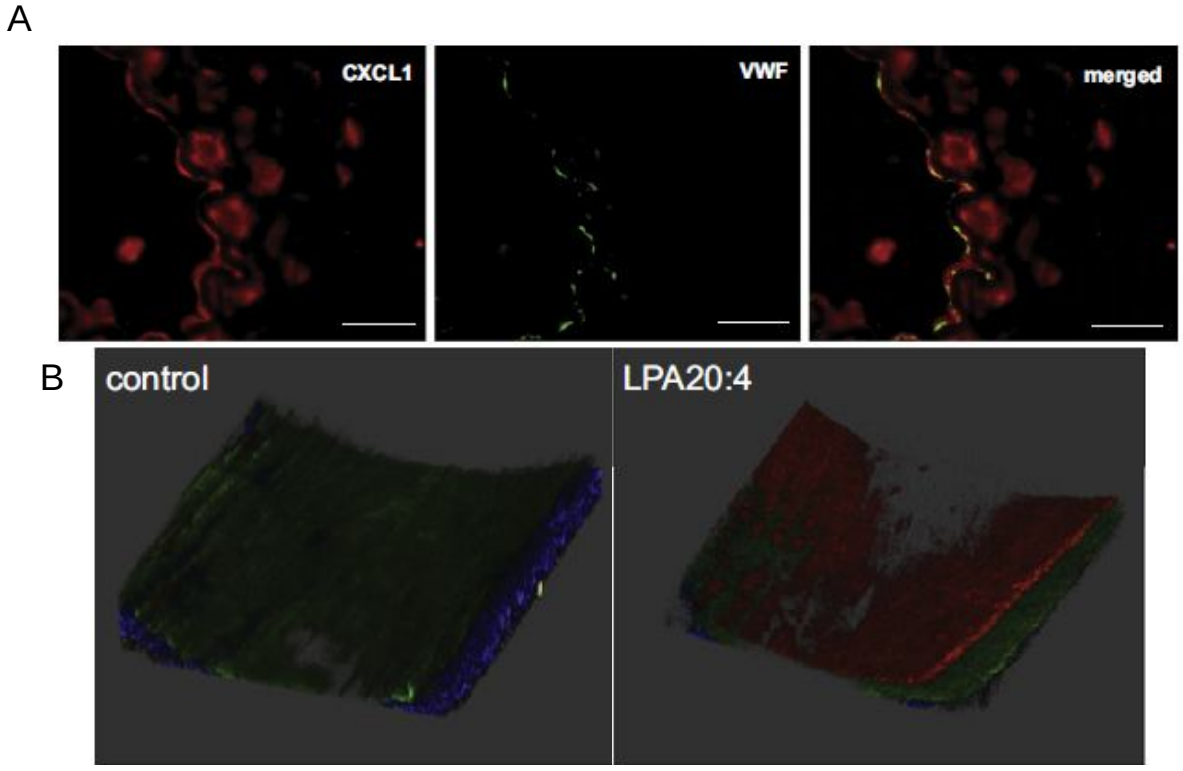

Figure 36: LPA induces deposition of preformed CXCL1 on endothelial surface
(A) Double immunostaining for CXCL1 and vWF shows the presence of CXCL1 protein in the ECs of normal mouse carotid arteries (see chapter 2.5.5 for details). Scale bars: 20 µm. (B) Two-photon microscopy was performed in mouse carotid arteries, which were perfused *ex vivo* with control buffer or LPA20:4 (10 µM). Using a fluorescently-labelled Ab (red), CXCL1 was detected in 3-D reconstructions of the z-stack images (see chapter 2.5.6 for details). Green; elastic laminae, blue; collagen.

3.2.3 Expression of LPA_1 and LPA_3 in atherosclerotic plaques

The expression of LPA_1 mRNA in normal mouse arteries is almost twice as high as LPA_2 and LPA_3 (Fig.18). QRT PCR was performed to study the differential regulation of the LPA receptors by hyperlipidemia. Following two months of a HFD, the LPA_2 mRNA expression was reduced by

38% in the aorta of ApoE$^{-/-}$ mice as compared to a normal diet (Fig. 37). In contrast, LPA_3 expression increased between 1 month and 2 months of a HFD, whereas the LPA_1 mRNA expression remained unchanged (Fig. 37). These results demonstrate that the expression of LPA_1 and LPA_3 predominate in the aortic wall during hyperlipidemia.

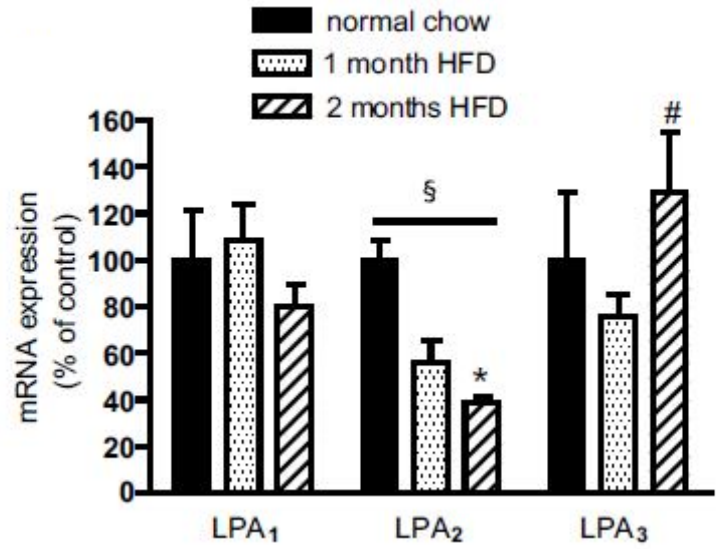

Figure 37: Regulation of LPA receptor expression during hyperlipidemia
LPA_1, LPA_2 and LPA_3 mRNA expression in the aortas of ApoE$^{-/-}$ mice that were fed a normal diet or a HFD for 1 or 2 months was analysed by qRT PCR (see chapter 2.6.2 for details). *P<0.05 versus normal diet; #P<0.05 versus 1 month HFD; §P<0.001 for linear trend. n=3-4 mice.

To identify the cell types in atherosclerotic plaques that express LPA receptors, double immunofluorescence staining was performed. In aortic root lesions of ApoE$^{-/-}$ mice that were fed a HFD for 3 months, both Mac-2-positive macrophages and vWF-positive ECs expressed LPA_1 as well as LPA_3 (Fig. 38A-B).

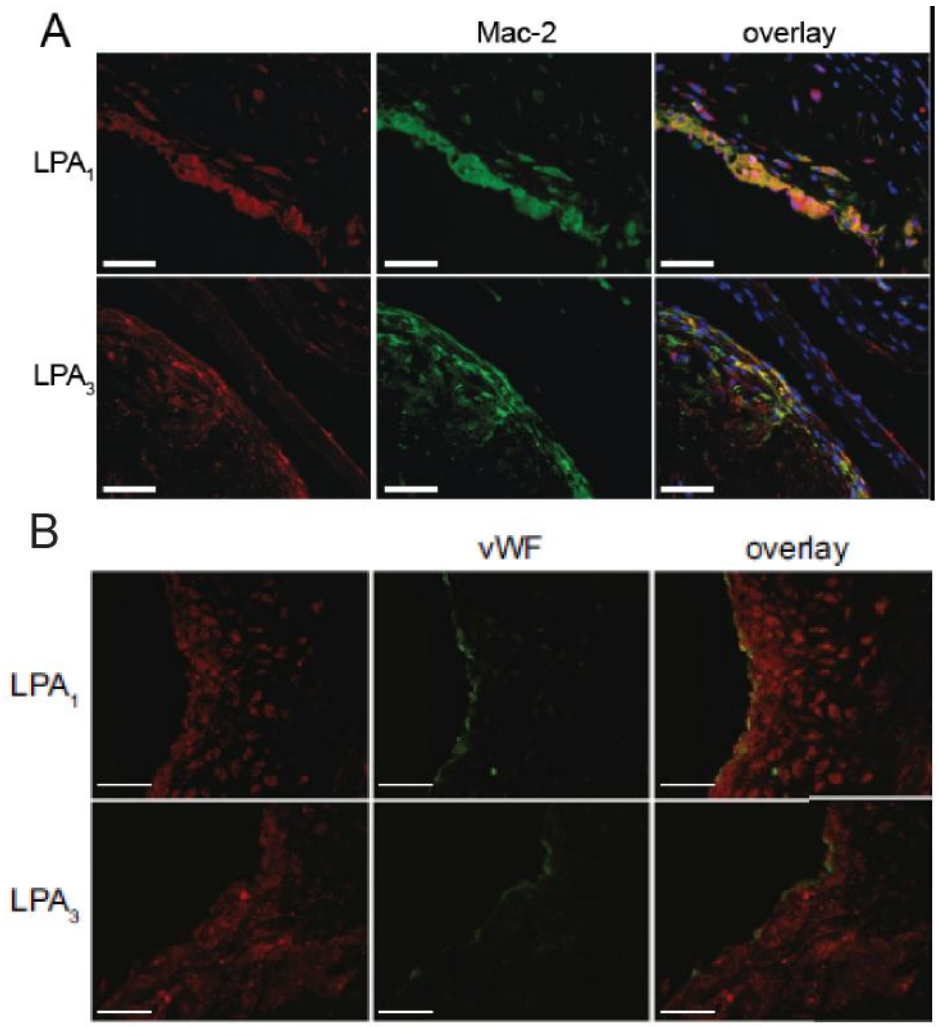

Figure 38: Expression of LPA_1 and LPA_3 in mouse atherosclerotic plaques
(A) Double immunostaining for Mac-2 and for either LPA_1 or LPA_3 was performed in aortic root sections from $ApoE^{-/-}$ mice on a HFD for 3 months (see chapter 2.5.5 for details). Scale bars: 50 µm. (B) Double immunostaining for vWF and for either LPA_1 or LPA_3 was performed in aortic root plaques of $ApoE^{-/-}$ mice (see chapter 2.5.5 for details). Scale bars: 20 µm.

To compare the cellular LPA receptor expression between mouse and human atherosclerotic plaques, double immunostaining for vWF and either LPA_1 or LPA_3 was performed in sections from human carotid artery plaques (Fig. 39). LPA_1 and LPA_3 were expressed in vWF-positive endothelial cells of human plaques. Moreover, additional cell types in the lesions also expressed LPA_1 and LPA_3. This demonstrates that the LPA receptor expression in lesional endothelial cells is similar in mice and humans.

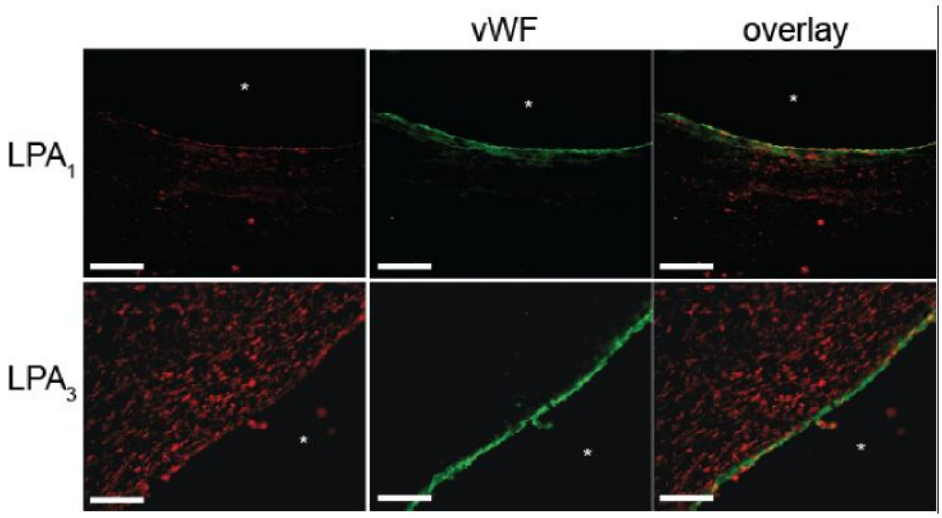

Figure 39: Expression of LPA_1 and LPA_3 in human atherosclerotic plaques
Double immunostaining for vWF and either LPA_1 or LPA_3 was performed in sections of human atherosclerotic plaques from carotid arteries (see chapter 2.5.5 for details). Scale bars: 100 µm. Stars indicate the lumen.

3.2.4 LPA induces arterial recruitment of leukocytes via LPA_1 and LPA_3

Hyperlipidemia-induced arterial leukocyte adhesion in $ApoE^{-/-}$ mice is inhibited by treatment with Ki16425 [123], which preferentially blocks LPA_1 and LPA_3 [106]. To identify the roles of LPA_1 and LPA_3 in hyperlipidemia-induced leukocyte adhesion independently, LPA receptors were silenced. LPA receptor-specific siRNA was applied locally to the carotid artery of $ApoE^{-/-}$ mice that were fed a HFD for 4 weeks. The leukocyte adhesion to the carotid artery was analysed 4 d after treatment with non-targeting siRNA, LPA_1-, LPA_2- or LPA_3-specific siRNA by intravital microscopy. In contrast to the treatment with LPA_2-specific siRNA, LPA_1- or LPA_3-specific siRNA reduced the hyperlipidemia-induced leukocyte adhesion to the arterial wall (Fig. 40A). The leukocyte adhesion to the vessel wall fully recovered 14 days following LPA_1- or LPA_3-specific siRNA treatment (Fig. 40B). Taken together, these results demonstrate that both LPA_1 and LPA_3 mediate independently hyperlipidemia-induced arterial leukocyte adhesion *in vivo*.

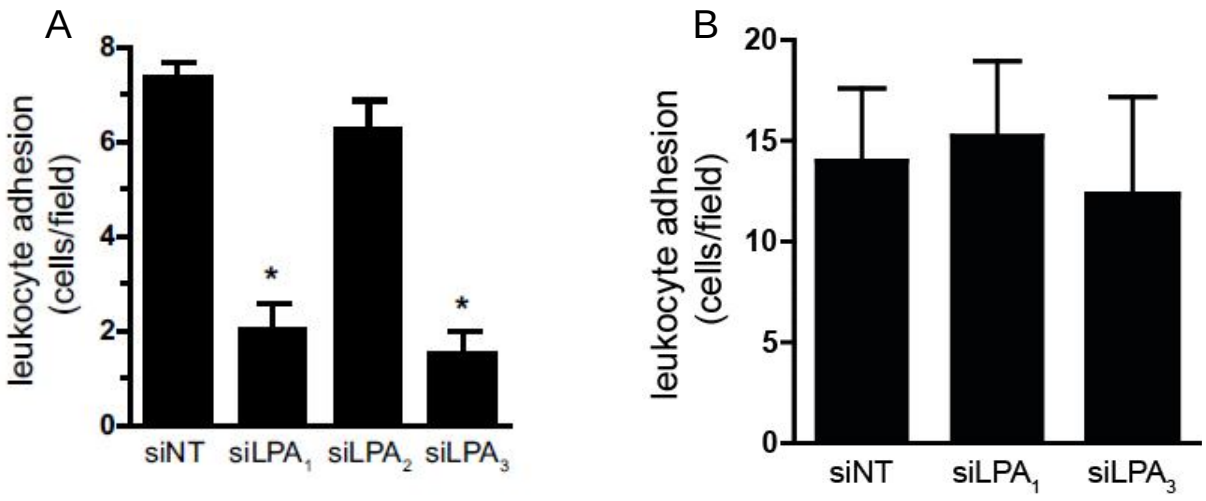

Figure 40: LPA_1 and LPA_3 independently mediate hyperlipidemia-induced leukocyte adhesion
(A) IVM was performed to study leukocyte adhesion to carotid arteries in $ApoE^{-/-}$ mice 4 days following treatment with non-targeting siRNA (siNT), LPA_1-, LPA_2- or LPA_3-specific siRNA (see chapter 2.4.8 for details). *P<0.05 versus siNT and LPA_2-siRNA. n=3-4 mice. (B) Leukocyte adhesion in $ApoE^{-/-}$ mice was studied by IVM 14 days after treatment with LPA_1-, siNT- or LPA_3-specific siRNA (see chapter 2.4.8 for details). n=3-4 mice.

3.2.5 Unsaturated LPA promotes the progression of atherosclerosis

The effect of LPA on the progression of atherosclerosis was studied in $ApoE^{-/-}$ mice that were fed a HFD by systemic administration of LPA20:4, LPA18:0 or vehicle for 4 weeks. No significant differences in the lipid levels were detectable between the three groups (Table.16). Treatment with LPA20:4 increased the lipid deposition in the aorta and the plaque area in the aortic root compared to vehicle (Fig. 41A-B). This atherogenic effect is most likely due to enhanced recruitment of monocytes, since LPA20:4-treatment increased the lesional macrophage number as well as the Mac-2-immunopositive area (Fig. 41C). In contrast, LPA18:0 did neither affect the lipid deposition, the plaque area nor the plaque macrophage content (Fig. 41A-C). Therefore, only unsaturated LPAs, such as LPA20:4, enhance atherogenesis.

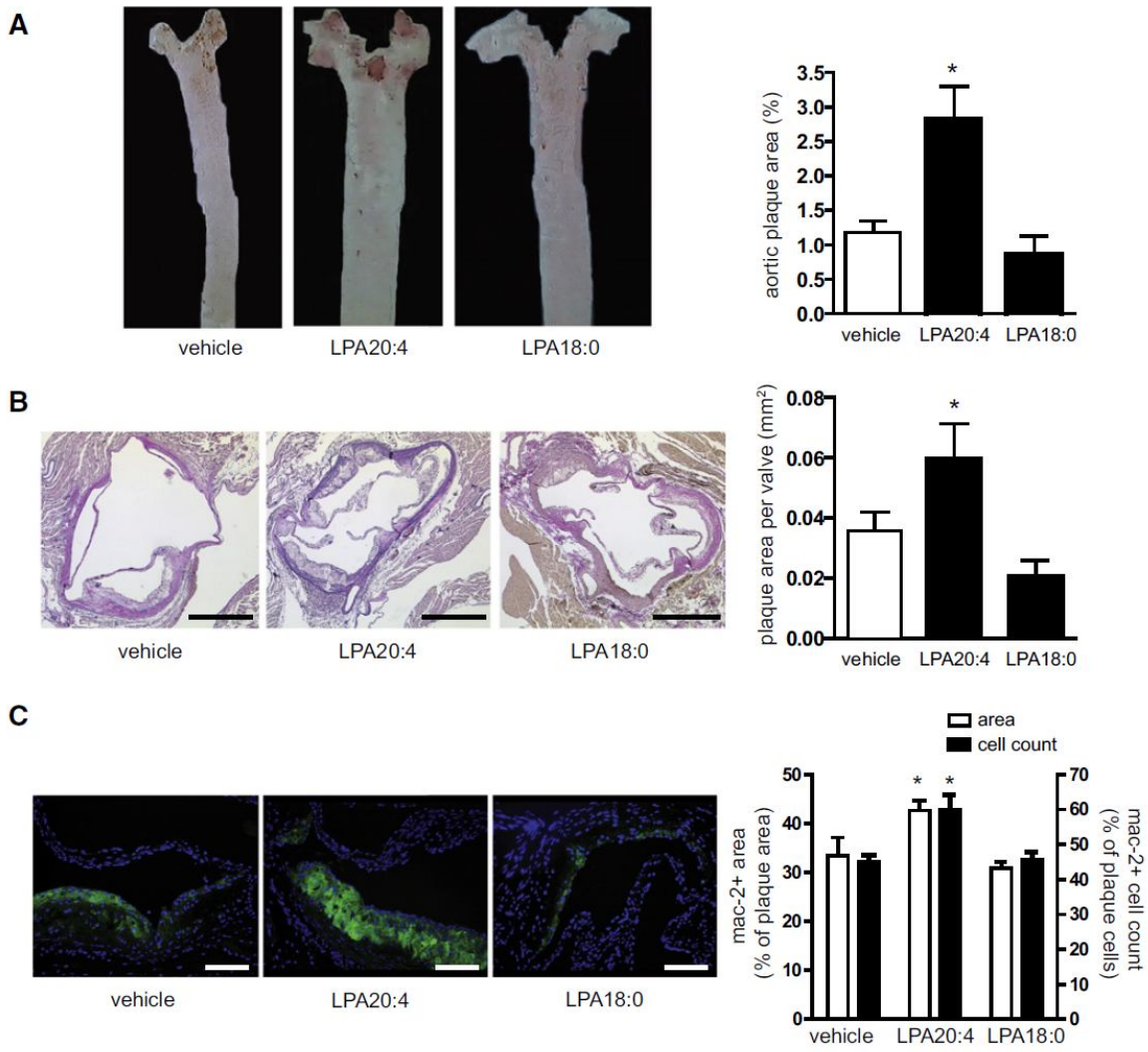

Figure 41: LPA20:4 induces progression of atherosclerosis

ApoE$^{-/-}$ mice on a HFD were treated with LPA20:4, LPA18:0 (both 2 nmol/mouse, twice weekly, IP) or vehicle (PBS, IP) for 4 weeks. (A) The lipid deposition in the aorta was quantified by Oil red O staining (see chapter 2.5.4 for details). *P<0.05 versus all other groups. n=5-6 mice. (B) The plaque area in the aortic valve was quantified by EVG staining (see chapter 2.5.4 for details). Scale bars: 500 µm. *P<0.05 versus all other groups. n=4-6 mice. (C) The Mac-2-immunopositive area and the Mac-2 positive cell number were quantified (see chapter 2.5.5 for details). Scale bars: 100 µm. *P<0.05 versus all other groups. n=5-7 mice.

	Vehicle	LPA20:4	LPA18:0	p value
Cholesterol (mmol/L)	16.85±1.05 (n=6)	16.48±1.15 (n=8)	16.70±1.20 (n=5)	0.97
Triglycerides (mmol/L)	0.58±0.04 (n=6)	0.69±0.11 (n=6)	0.58±0.01 (n=5)	0.49

Table 16: Serum biochemistry of ApoE$^{-/-}$ mice treated with LPA20:4, LPA18:0 or vehicle (see chapter 2.5.7 for details).

Oxidation of LDL primarily occurs in the vessel wall and not in the circulation [28, 124]. Therefore, the local effect of LPA inside the arterial wall on atherogenesis was studied. Accelerated plaque formation was induced locally by partial carotid ligation, which acutely reduces blood flow velocity and shear stress. In hyperlipidemic mice, partial carotid ligation leads to formation of atherosclerotic plaques in the CCA within 6 weeks [107]. 2 weeks after partial ligation, carotid arteries were treated with LPA20:4 by weekly perivascular application of pluronic gel. This treatment with LPA20:4 increased the plaque size in the carotid artery 4 weeks after partial ligation as compared to vehicle (Fig. 42A). This enhanced plaque formation by local LPA20:4 applications were associated with increased accumulation of macrophages compared with vehicle-treated carotid arteries (Fig. 42B).

This demonstrates that in addition to circulating LPA, increased levels of unsaturated LPA in the vessel wall also promote atherosclerotic plaque progression and the accumulation of macrophages.

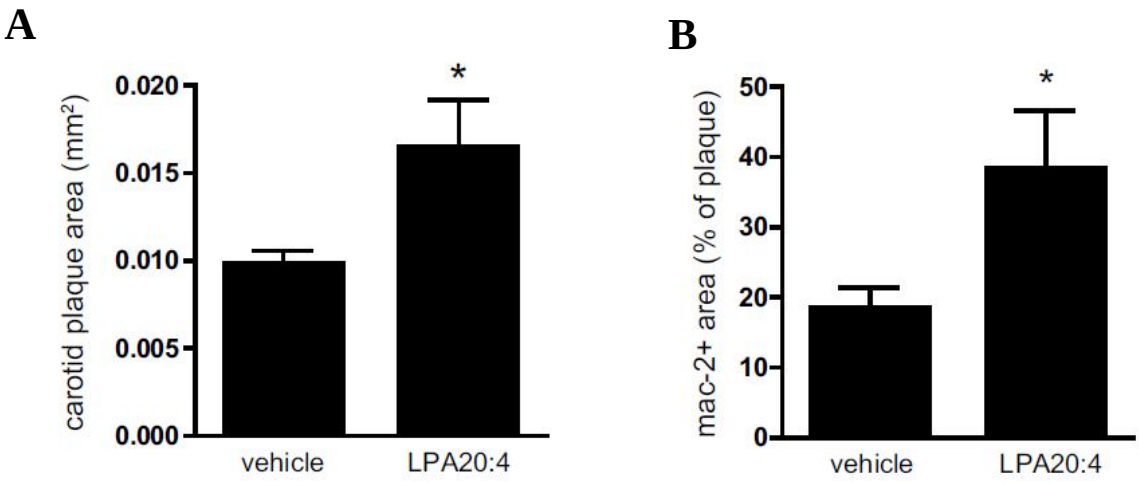

Figure 42: Increased LPA20:4 in the vessel wall results in increased plaque progression
Carotid arteries of ApoE$^{-/-}$ mice were treated weekly with LPA20:4 (2 nmol/mouse) or vehicle (PBS) by perivascular application following 2 weeks after partial ligation. (A) The plaque area was quantified by EVG staining 4 weeks after partial carotid ligation (see chapter 2.5.4 for details). *P<0.05. n=3-4 mice. (B) The neointimal Mac-2 immunopositive area was determined 4 weeks after partial carotid ligation (see chapter 2.5.5 for details). *P<0.05. n=3-4 mice.

3.2.6 Diet-induced atherosclerosis is suppressed by blocking LPA_1 and LPA_3

The role of LPA receptors in diet-induced atherosclerosis was studied by treating ApoE$^{-/-}$ mice on HFD with Ki16425 for 3 months by daily injections. Serum biochemistry parameters were determined after 3 months of Ki16425 treatment to determine potential adverse effects on renal function. The creatinine levels in the serum were not significantly different from vehicle-treated

mice (Table.17). Furthermore, chronic Ki16425 application did not affect the cholesterol, triglyceride and CRP levels in ApoE$^{-/-}$ mice (Table.17).

	Vehicle	**Ki16425**	**P value**
Cholesterol (mmol/L)	18.77±0.80 (n=4)	17.58±1.13 (n=3)	0.41
Triglycerides (mmol/L)	0.46±0.06 (n=4)	0.48±0.06 (n=3)	0.88
Creatinine (µmol/L)	16.00±1.47 (n=4)	18.00±2.19 (n=4)	0.47
CRP (mg/L)	1.50±0.86 (n=4)	1.25±1.25 (n=4)	0.87

Table 17: Serum biochemistry of ApoE$^{-/-}$ mice treated with Ki16425 or vehicle for 3 months (see chapter 2.5.7 for details).

Atherosclerosis was quantified in ApoE$^{-/-}$ mice by Oil red O staining of the *en face* prepared thoracoabdominal aorta and in sections of the aortic root by planimetry. Treatment with Ki16425 reduced the lipid deposition in the aorta by 38% compared to control buffer-treated mice (Fig. 43A). Accordingly, the plaque area in the aortic root was reduced by 35% in the Ki16425-treated mice (Fig. 43B).

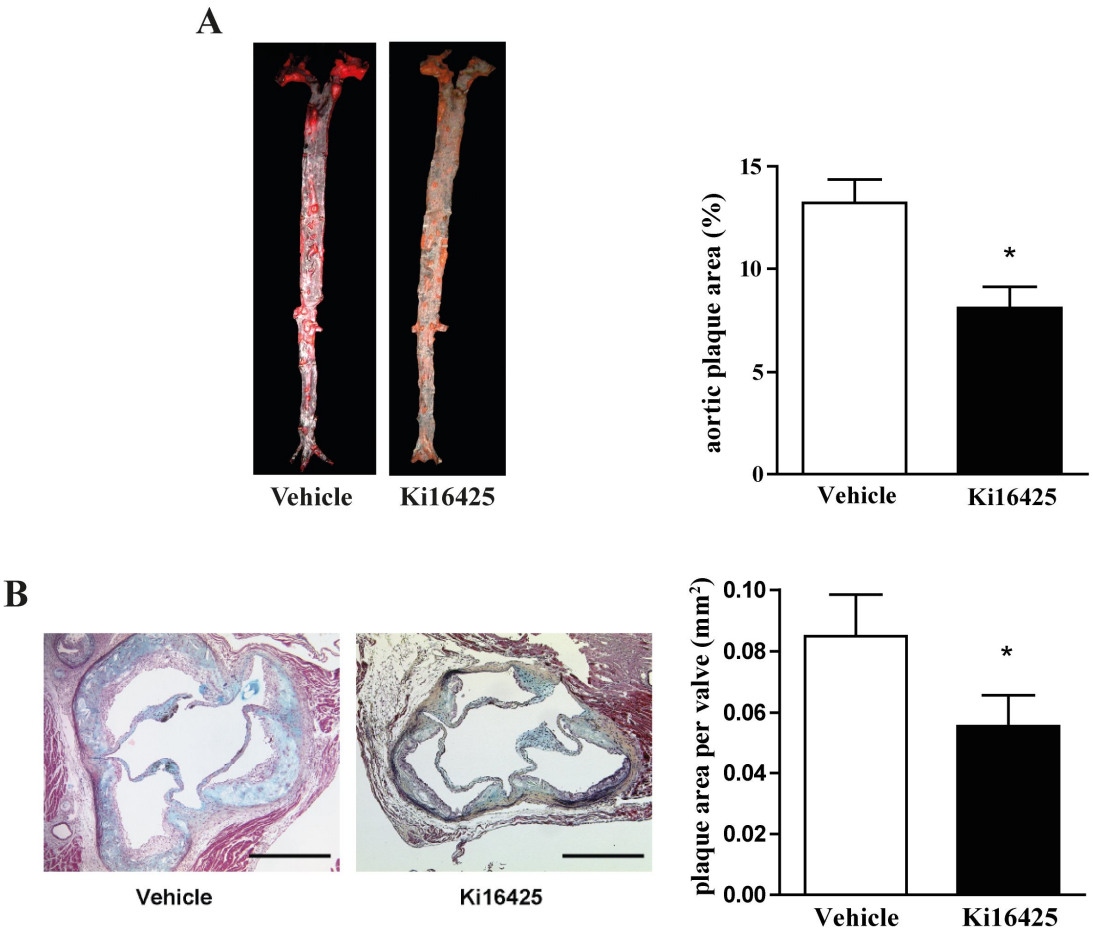

Figure 43: Effect of Ki16425 on diet-induced plaque formation
ApoE$^{-/-}$ mice on HFD were treated with Ki16425 (5 mg/Kg/day) or vehicle (10% DMSO in PBS) for 3 months by daily injections (IP) (see 2.4.3 for details). (A) The lipid deposition in the aorta was quantified in the *en face* prepared thoracoabdominal aorta by Oil red O staining (see chapter 2.5.4 for details). *P<0.05. n=4 mice. (B) The plaque size in the aortic root was determined in sections that were stained with Movats' pentachrome or EVG (see chapter 2.5.4 for details). *P<0.05. Scale bars: 500 µm. n=3 mice.

The effect of Ki16425 on the cellular composition of the atherosclerotic plaques was studied by cell-specific immunostainings of aortic root sections. The diminished plaque size in the aortic root was associated with a reduced macrophage accumulation in Ki16425-treated as compared to vehicle-treated mice, as detected by Mac-2 immunostaining (Fig. 44A). Moreover, the Mac-2-positive cell number in the plaque was reduced by Ki16425 treatment, indicating impaired recruitment of monocytes (Fig. 44A). In contrast, the SMC content of the plaque was unaltered in Ki16425-treated as compared to vehicle-treated mice (Fig. 44B).

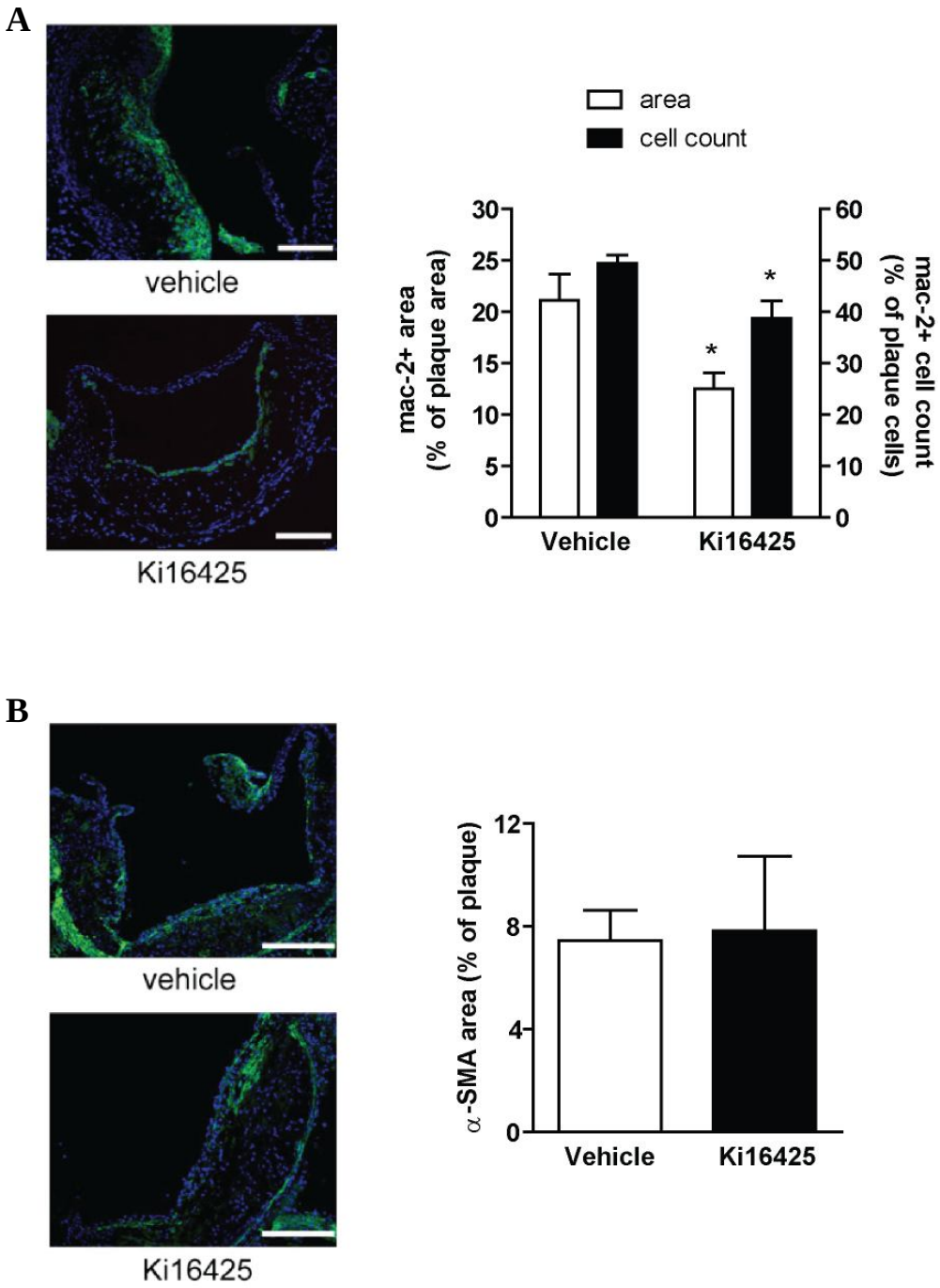

Figure 44: Effect of Ki16425 on macrophage and SMC accumulation in atherosclerotic plaques

ApoE$^{-/-}$ mice on a HFD were treated with Ki16425 (5 mg/Kg/day) or vehicle (10% DMSO in PBS) for 3 months by daily injections (IP) (see chapter 2.4.3 for details). (A) The macrophage content in the plaque was studied by analysing the Mac-2 immunopositive area and the Mac-2 positive cell number (see chapter 2.5.5 for details). Scale bar: 200 µm. *P<0.05. n=3-4 mice. (B) The SMC content in the plaque was studied by immunostaining for α-SMA (see chapter 2.5.5 for details). Scale bar: 200 µm. P=NS. n=4 mice.

To study the effect of Ki16425 on CXCL1 expression in atherosclerotic lesions, immunostaining for CXCL1 was performed. In Ki16425-treated mice, the CXCL1-immunopositive area per plaque area was reduced by 35% compared to control buffer-treated mice (Fig. 45).

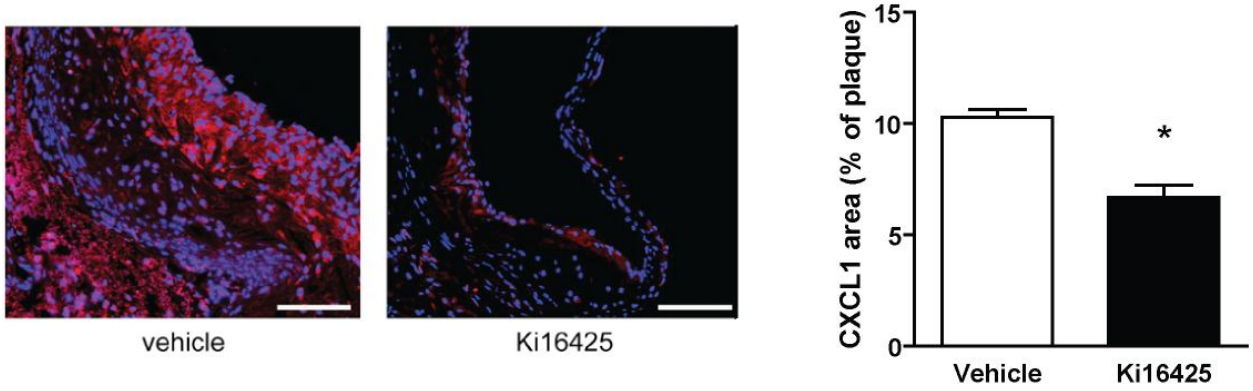

Figure 45: Role of LPA receptors on CXCL1 expression in atherosclerotic plaque
ApoE$^{-/-}$ mice on a HFD were treated with Ki16425 (5 mg/Kg/day) or vehicle (10% DMSO in PBS) for 3 months by daily injections (IP) (see chapter 2.4.3 for details). Immunostaining for CXCL1 (red) was performed in aortic root sections. The CXCL1-immunopositive area per plaque area was quantified (see chapter 2.5.5 for details). Scale bar: 100 µm. n=2-4 mice. *P<0.05.

To assess the effect of Ki16425 on the expression of other chemokines which are known to play a role in atherosclerosis, such as CCL2, CCL5, and CX3CL1, quantitative real time RT-PCR was performed in plaque samples obtained from ApoE$^{-/-}$ mice on HFD for 3 months. Treatment with Ki16425 did not affect the expression of CCL2, CCL5 or CX_3CL1 in atherosclerotic lesions compared to vehicle (Fig. 46). This indicates that the inhibitory effect of Ki16425 on CXCL1 expression is rather specific for this chemokine.

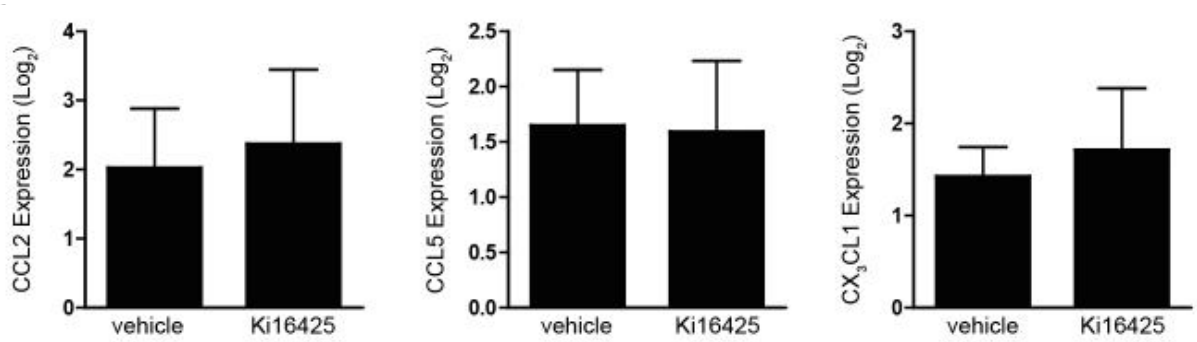

Figure 46: Effect of Ki16425 on chemokine expression
ApoE$^{-/-}$ mice on HFD were treated with Ki16425 (5 mg/Kg/day) or vehicle (10% DMSO in PBS) for 3 months by daily injections (IP) (see chapter 2.4.3 for details). The expression of CCL2, CCL5 and CX_3CL1 in the plaque was studied by qRT-PCR (see chapter 2.6.2 for details). P=NS. n=4.

To further verify that CXCL1 mediates the pro-atherogenic effects of LPA receptors, the role of Ki16425 on atherosclerosis was studied in ApoE$^{-/-}$ mice on HFD in which CXCL1 was inhibited by blocking antibody. In mice treated with CXCL1 Ab, the plaque size and the lesional macrophage accumulation was not decreased by treatment with Ki16425 as compared to vehicle (Fig. 47). This strongly suggests that the anti-atherogenic effects of Ki16425 are mediated by an impaired function of CXCL1.

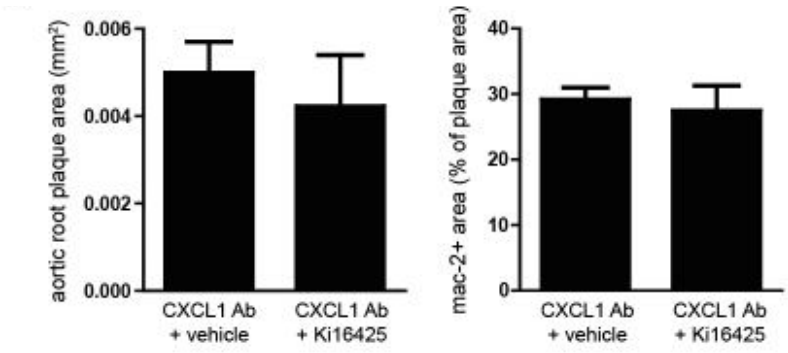

Figure 47: Effect of Ki16425 on atherosclerotic plaques

ApoE$^{-/-}$ mice on HFD were treated with CXCL1 Ab (50 µg/mouse/twice weekly) with or without Ki16425 (5 mg/Kg/day, see chapter 2.4.3 for details). After 4 weeks, the plaque size in the aortic root and the lesional macrophage accumulation were studied by EVG staining and Mac-2 immunostaining, respectively (see chapter 2.5.4 and 2.5.5 for details). n=4-6. P=NS.

4. Discussion

4.1 LPA receptors: Differential regulation in vascular diseases

LPA exerts its functions via 7 G protein-coupled receptors [1, 3, 4], of which LPA_1, LPA_2, and LPA_3 belong to the EDG family of receptors [7]. LPA_1 is highly expressed in rat carotid arteries, whereas LPA_2 and LPA_3 mRNA are not detectable [5]. In contrast to the LPA receptor expression profile in rats, we found that the uninjured carotid arteries of C57BL/6 mice express LPA_1, LPA_2, and LPA_3 mRNA. Cheng and co-workers reported that the expression of LPA_1 mRNA in the carotid arteries of C57BL/6 mice is significantly higher than that of LPA_2 and LPA_3 [6]. Similar to this study, we found that LPA_1 mRNA expression in the murine carotid artery is approximately 2 times higher than LPA_2 and LPA_3 expression. Following carotid ligation, Panchatcharam and co-workers found that LPA_1 and LPA_2 are upregulated, and LPA_3 remains unaltered [125]. However, we found that LPA_1 mRNA expression was downregulated and that of LPA_2 and LPA_3 were upregulated 1 week after wire-induced carotid injury. The difference in the injury models used and the time point at which the LPA receptor expression was studied could explain the contrasting results between our study and the study by Panchatcharam and colleagues [125]. We found predominant expression of LPA_1 in the endothelial cells and of LPA_3 in the macrophages of the neointima. The substantial loss of endothelial cells following wire-induced carotid injury could explain the reduction of LPA_1 mRNA 1 week following injury. Cultured macrophages exhibit high expression of LPA_2 and LPA_3 mRNA [123]. The increase in LPA_2 and LPA_3 mRNA at 1 week after vessel injury might have been due to the macrophage accumulation in the neointima. As compared to the expression of LPA_1 and LPA_2 mRNA 1 week after injury, that at 2 weeks after injury was downregulated.

Previous studies demonstrate that monocytes and macrophages express LPA_1, LPA_2, and LPA_3 mRNA [123, 126], whereas human umbilical ECs (HUVECS) produce mainly LPA_1 and LPA_3 [12]. We detected LPA_1 and LPA_3 protein expression in the ECs and macrophages of atherosclerotic plaques from hyperlipidemic mice. LPA_1 and LPA_3 proteins were also detected in the ECs of human atherosclerotic plaques. In the vessel wall, hyperlipidemia induced downregulation of LPA_2 mRNA expression, upregulation of LPA_3 mRNA expression and no change in LPA_1 mRNA expression.

Regulation of the various LPA receptors in the vessel wall differed between wire-induced endothelial denudation, atherosclerosis, hyperlipidemia, and carotid ligation. Our results indicate that LPA_1 and LPA_3 are prominently expressed in the vessel wall in murine atherosclerosis and

vascular injury models. The cell-specific expression of LPA receptors in atherosclerotic plaques between mice and humans is similar.

4.2 LPA-induced neointima formation via CXCL12

4.2.1 Role of LPA receptors in neointima formation

Several reports have shown that uninjured carotid arteries incubated with unsaturated LPA such as LPA18:1 or LPA20:4 develop neointimal lesions [5, 105]. Similar to these previous results, we found that incubation of mouse carotid arteries with unsaturated LPA20:4 and the LPA analogue 1-AGP18:1 resulted in neointima formation. This LPA-induced neointima formation was blocked by local pharmacological inhibition of LPA_1 and LPA_3 in the vessel wall. In contrast, neointima formation after carotid ligation was increased in $LPA_1^{-/-}$ mice [125]. However, this was associated with an enhanced migratory activity of $LPA_1^{-/-}$ SMCs due to the compensatory upregulation of LPA_3 [125]. Therefore, increased LPA_3 expression might cause aggravated neointimal hyperplasia in $LPA_1^{-/-}$ mice.

A further study in $LPA_1^{-/-}$ mice showed that treatment of the carotid artery with 1-AGP induces neointima formation similar to that of wild-type mice [6]. We found that LPA_1 and LPA_3 independently mediated LPA-induced neointima formation, as demonstrated by the silencing of LPA_1 and LPA_3 in the carotid artery. Thus, we avoided the problem of using $LPA_1^{-/-}$ mice, which overexpress LPA_3, and were able to study the effects of LPA_1 and LPA_3 on neointima formation independently.

Furthermore, LPA receptor knockout mice, except $LPA_2^{-/-}$ mice, display phenotypic changes which may affect neointima formation [3, 8]. Approximately 50% of LPA_1 knockout mice die perinatally, and the surviving mice are characterised by reduced body size, reduced brain mass, a suckling defect, and craniofacial dysmorphism [3]. The genetic deletion of LPA_3 results in delayed embryo implantation, altered embryo spacing, and reduced litter size [3, 8]. Although LPA_2 knockout mice do not exhibit any obvious phenotypic changes, a reduction of LPA-induced phospholipase C (PLC) activation and Ca^{2+} mobilisation is evident in embryonic fibroblasts from $LPA_2^{-/-}$ mice [8]. Therefore, other methods of studying the function of LPA receptors, such as pharmacological inhibitors or RNA interference, might be more reliable than involving the use of knockout mice. In addition to LPA receptor subtype-specific siRNA, we applied the pharmacological inhibitor Ki16425, which selectively inhibits LPA_1 and LPA_3 with a Ki value of 0.34 µM and 0.93 µM, respectively [106]. To a lesser extent, Ki16425 also inhibits LPA_2 with a Ki

value of 6.5 µM [106]. Since LPA_1, LPA_2, and LPA_3 are also expressed on macrophages, the effect of Ki16425 on macrophage LPA receptors cannot be excluded [123]. Ki16425 does not alter the actions of other receptor agonists such as sphingosine-1-phosphate, sphingosylphosphorylcholine, psychosine, 2-arachidonoylglycerol, PAF, lysophosphatidylcholine, A1 adenosine receptor agonist, bradykinin, epidermal growth factor, and platelet-derived growth factor [106]. Although Ki16425 has a high selectivity towards LPA_1 and LPA_3, the possibility of it binding to other receptors cannot be completely excluded. Ki16425 has been used in previous studies for *in vivo* experiments [127, 128], and our results demonstrated no toxic effects in mice treated with Ki16425. Therefore, there is substantial evidence that renders Ki16425 acceptable for *in vivo* experiments.

Dioctylglycerol pyrophosphate (DGPP) is an LPA receptor antagonist that blocks predominantly LPA_3 but also LPA_1 [129]. In line with our results, LPA-induced neointima formation in rats lackingLPA_3 expression in the vessel wall is partially blocked by treatment with DGPP, indicating that LPA_1 is involved in neointima formation [5]. The reason for the partial inhibition of neointima formation could be explained by the incomplete inhibition of LPA_1 through DGPP.

PPAR-γ is a nuclear receptor belonging to the nuclear hormone receptor superfamily and regulates genes that control cellular differentiation, development, and energy metabolism [130]. PPAR-γ is an intracellular receptor for LPA [130]. In rats, LPA-induced neointima formation is blocked by co-incubation with the PPARγ antagonist GW9662 [5]. Moreover, 1-AGP-induced neointima formation is completely inhibited in conditional PPAR-γ knockout mice [6]. Conversely, treatment of carotid arteries with the PPAR-γ agonist rosiglitazone causes neointima formation similar to that caused by unsaturated LPA [5]. LPA20:4-induced activation of PPAR-γ is partially inhibited by the $LPA_{1/3}$ antagonist DGPP, suggesting that $LPA_{1/3}$ may be involved in activating PPAR-γ [5]. Moreover, HIF-1α-induced activation of PPAR-γ is described in cardiac hypertrophy, indicating that LPA activates PPAR-γ by LPA receptor-mediated upregulation of HIF-1α [131]. Interestingly, treatment with rosiglitazone following balloon injury of carotid arteries in rats reduces neointima formation in contrast to 1-AGP [6]. Rosiglitazone has opposite effects on neointima formation in uninjured and injured carotid arteries, indicating that the role of PPAR-γ is not directly related to LPA [6].

In summary, our results clearly demonstrate that both LPA_1 and LPA_3 independently mediate LPA-induced neointima formation and that pharmacological inhibition of LPA receptors might be of therapeutic value in the prevention of neointimal hyperplasia.

4.2.2 LPA in neointima formation: Role of SPCs

BM-derived progenitor cells characterised by the expression of the stem cell marker Sca-1 and absence of lineage (lin) markers are increased in the circulation following vascular injury [98]. These progenitor cells are recruited to the neointima and differentiate into SMMHC-expressing SMCs after systemic injection into mice with carotid injury, suggesting that this population of Sca-1^+/lin^- progenitor cells contain SPCs [98]. In a study using mice that were transplanted with BM cells that express LacZ, β-galactosidase-positive SMCs were detected in the neointima, indicating that endogenous SPCs reside in the BM [132]. Following vascular injury, blocking LPA_1 and LPA_3 using Ki16425 inhibits the neointimal expression of CXCL12 and HIF-1α, the mobilisation of SPCs, and neointima formation [121]. However, it is unclear whether the LPA receptor-mediated SPC mobilisation leads to SMC accumulation in the neointima. We found that blocking LPA_1 and LPA_3 following vascular injury reduced the neointimal accumulation of SMCs and macrophages. Moreover, this SMC population expresses Sca-1, indicating that LPA receptors mediate the recruitment of SPCs to the neointima. However, these results do not directly demonstrate the role of LPA_1 and LPA_3 in the recruitment of BM-derived SPCs to the neointima. Intraluminal incubation of the carotid artery with LPA20:4 or 1-AGP induced the mobilisation of Sca-1^+/lin^- cells into the circulation and neointima formation via LPA_1 and LPA_3. Thus, BM-derived SPCs are recruited to the neointima and differentiate into SMCs. LPA induces SPC mobilisation and neointima formation via LPA_1 and LPA_3.

4.2.3 Role of SPCs in vascular diseases

The role of SPCs in vascular diseases is a controversial issue. Following mechanical vascular injury in female mice transplanted with male BM cells, 44% of the neointimal SMCs were derived from the BM [133]. In another study, wire-induced injury of the femoral artery was performed in mice that were subjected to BM transplantation with cells that express the LacZ gene. Double immunostaining for LacZ and α-SMA shows that BM-derived SPCs are recruited to the neointima following injury [132].

The type of vascular injury, for example wire-induced injury, ligation injury, or cuff placement, determines the extent of BM-derived SPC recruitment to the neointima. The percentage of neointimal cells derived from the BM is the highest following wire-induced vascular injury [134]. Conversely, following vascular ligation or cuff placement, only a small number of BM-derived SPCs are detected in the neointima [134]. These differences in the extent of neointimal SPC recruitment correlates with the degree of injury-induced apoptosis of vascular cells [134].

Furthermore, lesional recruitment of SPCs appears to be infrequent in diet-induced atherosclerosis, which might be explained by the low rate of apoptosis in plaque cells as compared to medial cells after vascular injury [132, 135]. However, inducing apoptosis of endogenous SPCs that have been recruited to atherosclerotic lesions reduces plaque size, indicating that SPCs also play a role in diet-induced atherosclerosis [136].

Several studies also show that neointimal SMCs are not derived from circulating SPCs after vascular injury [137-139]. The inability to detect SPC-derived SMCs in the neointima may be due to methodological difficulties. Detection of LacZ expression by X-gal staining, for instance, is performed in fixed tissues and requires the enzymatic cleavage of X-gal. Overfixation of the tissue with paraformaldehyde can result in the inactivity of β-galactosidase and thus lead to false-negative results. We developed a new method to detect BM-derived SMCs in vital, *ex vivo*-perfused carotid arteries by TPLSM, which is highly sensitive and reliable. We transplanted BM cells from mice that express LacZ under the control of a SMC-specific promoter into wild-type mice and studied the β-galactosidase activity in the carotid artery 4 weeks after LPA incubation using a fluorescent substrate. This technique enables the investigation of β-galactosidase activity in live, BM-derived SMCs in the vessel wall and avoids false-negative results due to overfixation. Moreover, this method avoids the problems related to immunostaining, which might not be sufficiently sensitive if the SMC marker expression is low. Thus, we were able to clearly demonstrate SMC-specific LacZ activity in BM-derived cells of the LPA-treated vessel wall, i.e. in SPCs. This SMC-specific LacZ activity is almost absent if the LPA receptors are blocked, demonstrating that LPA treatment induces the neointimal recruitment of SPCs via LPA_1 and LPA_3.

Therefore, the extent of neointimal SPC recruitment depends on the type of vascular injury and is correlated with the degree of apoptotic vascular cells. Studying the reporter gene expression under a SMC-specific promoter is currently the most advanced technique to identify the recruitment of SPCs to the neointima. We have convincingly demonstrated that LPA induces the recruitment of BM-derived SPCs to the neointima via LPA_1 and LPA_3.

4.2.4 LPA-induced HIF-1α/CXCL12 axis in vascular injury

The transcription factor HIF-1α is upregulated following vascular injury and regulates the expression of CXCL12 in the vessel wall [104]. CXCL12 induces the mobilisation and recruitment of BM-derived SPCs to the site of injury, where the SPCs contribute to neointima formation [97, 98]. HIF-1α silencing following vascular injury reduces the neointimal expression of CXCL12 and blocks SPC mobilisation and neointima formation [104]. HIF-1α upregulates CXCL12, which

promotes SPC-mediated neointima formation following vascular injury. However, the trigger for HIF-1α activation following injury is unknown. In this context, 2 separate studies have shown that carotid artery incubation with unsaturated LPA induces neointimal hyperplasia containing mostly SMCs [5, 105]. Moreover, blocking the LPA receptors LPA_1 and LPA_3 following vascular injury inhibits neointima formation, SPC mobilisation, and neointimal expression of HIF-1α and CXCL12, suggesting that LPA may activate the HIF-1α/CXCL12 axis following vascular injury, resulting in neointima formation [121]. Moreover, the neointimal expression of HIF-1α and CXCL12 is elevated 4 weeks following intraluminal incubation of the carotid artery with LPA20:4 or 1AGP18:1 [121]. However, HIF-1α and CXCL12 need to be upregulated at earlier time points in order to induce the recruitment of SPCs to the neointima. Our findings demonstrated that HIF-1α and CXCL12 were elevated as early as 1 day following intraluminal incubation with LPA20:4. Subsequently, the levels of HIF-1α and CXCL12 in the vessel wall remained elevated throughout neointima formation. Moreover, we demonstrated that HIF-1α and CXCL12 were co-localised within the same neointimal cell, indicating that HIF-1α regulates the expression of CXCL12. These results are in line with previous studies and support the concept that LPA activates HIF-1α to induce CXCL12-mediated SPC recruitment, leading to neointima formation. Mechanistically, we showed that the increased CXCL12 expression in the LPA20:4-treated vessel wall was responsible for SPC mobilisation and neointima formation, because silencing of CXCL12 in the vessel wall prevented the effects of LPA. Furthermore, blocking LPA_1 and LPA_3 during LPA incubation inhibited CXCL12-mediated SPC mobilisation and neointima formation.

Heterodimer formation of LPA receptors has been shown, including LPA_1 with LPA_3 [140]. We found that selective knockdown of either LPA_1 or LPA_3 in the vessel wall is sufficient to prevent LPA20:4-induced SPC mobilisation and neointima formation, which can be explained by the functional interaction of LPA_1 with LPA_3, for example, as heterodimers [140]. Therefore, blocking either one of these LPA receptors is sufficient to inhibit the effects induced by LPA. Moreover, activation of a particular receptor heterodimer may lead to a specific signalling pathway compared to the activation of monomers. Taken together, LPA acts independently via LPA_1 and LPA_3 to activate the HIF-1α/CXCL12 axis that induces the mobilisation and recruitment of SPCs and results in neointimal hyperplasia (Fig. 48).

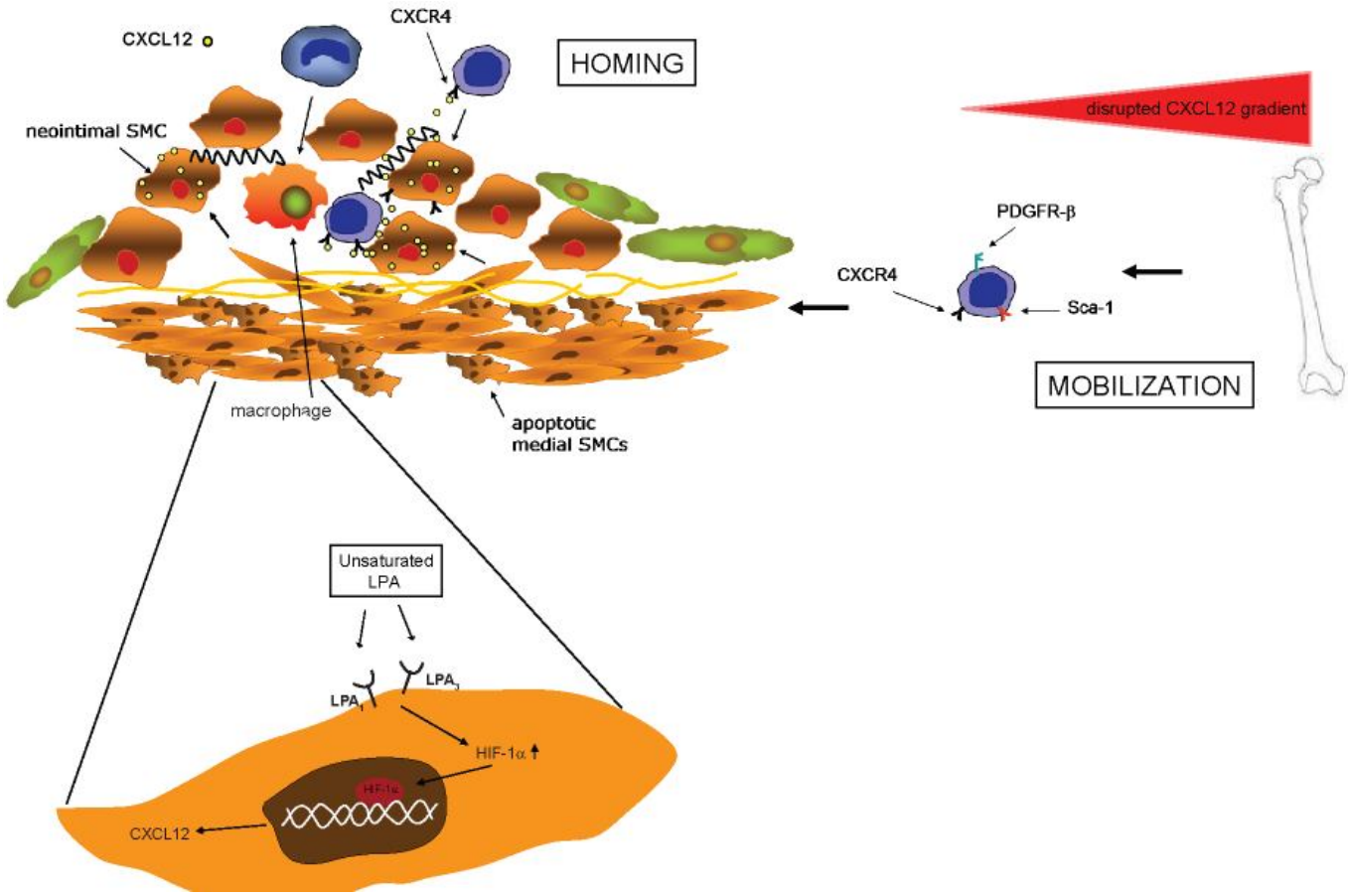

Figure 48: LPA-induced HIF-1α/CXCL12 axis in neointima formation
Following vascular injury, unsaturated LPA acts via LPA_1 and LPA_3 to induce HIF-1α-mediated CXLC12 expression in medial SMCs. CXCL12 induces the mobilisation of $Sca1^+/lin^-$ SPCs to the circulation and these SPCs are subsequently recruited to the site of injury via the CXCL12 receptor, CXCR4 (modified according to Schober 2008).

4.2.5 Sources of LPA following vascular injury

Following vascular injury, LPA can be produced in a number of ways such as from activated platelets or apoptotic cells [1, 141, 142]. Soon after vessel injury, platelets bind to the injured surface via the platelet-specific receptor glycoprotein 1b and its ligand vWF and are activated [143]. LPA is generated in a 2-step process after platelet activation. First, membrane phospholipids of the activated platelets are converted to LPLs by the enzymes secretory-type PL-A_2 and PS-specific PLA_1 and then, these LPLs are converted to LPA by ATX [1, 142]. In particular, activated platelets are an important source of LPA20:4 precursors [144] and may substantially increase the concentration of unsaturated LPA in the vessel wall immediately after endothelial denudation.

Apoptosis leads to the release of microvesicles, which are characterised by the translocation of LPA precursors such as PS or PA from the inner to the outer leaflet of the plasma membrane [141, 145]. This translocation of LPA precursors makes them accessible to enzymes involved in LPA

synthesis [141, 145]. For example, PA can be further converted to LPA by PLA_1 or PLA_2-type enzymes [1].

Following vascular injury, a large proportion of the medial SMCs become apoptotic, and apoptotic bodies produced from injured SMCs induce CXCL12 expression in uninjured SMCs [97]. Moreover, blocking the apoptosis of medial SMCs after vascular injury reduced the CXCL12 expression *in vivo* [97]. Apoptotic microvesicles from medial SMCs might play an important role in generating LPA, which in turn mediates the upregulation of CXCL12 by apoptotic SMCs.

Neointima formation induced by vessel ligation upregulates ATX [125]. ATX hydrolyses LPLs to generate LPA and is a major LPA-producing enzyme in the blood [1]. The combined upregulation of precursors for LPA and ATX may lead to enhanced LPA generation following vascular injury.

4.3 LPA-induced monocyte recruitment via CXCL1

4.3.1 MoxLDL-derived LPA in monocyte adhesion

Although LDL plays an essential role in cholesterol transport in the blood, increased levels of circulating LDL cholesterol are associated with an increased risk for atherosclerotic cardiovascular disease [28, 32, 34]. LDL consists of a core made up of esterified cholesterol and triglycerides that are surrounded by a shell of phospholipids, free cholesterol, and apolipoprotein B100 (ApoB100) [28]. Accumulation of circulating LDL in the intima via binding of ApoB100 to extracellular matrix-derived proteoglycans [146, 147] is important in the initiation of atherogenesis [148]. In the sub-endothelium, LDL can be oxidatively modified by myeloperoxidase, lipoxygenases, or reactive oxygen species such as HOCl, phenoxyl radical intermediates, or peroxynitrite, which are generated in the intima during inflammation [28, 34, 42]. Depending on the degree of oxidation, oxidised LDL can be functionally divided into minimally modified LDL (mmLDL)/mildly oxidised LDL (moxLDL), and profoundly oxidised LDL (oxLDL) [149]. In addition to oxidation, products of other processes such as glycation or desialylation are also called mmLDL [149]. Therefore, the effects of mmLDL may differ from that of moxLDL. Similar to LDL, mmLDL and moxLDL are recognised by the LDL receptor but not by most of the scavenger receptors [149]. In contrast, oxLDL is not recognised by the LDL receptor due to extensive oxidation of the ApoB component. However, oxLDL is a ligand for various scavenger receptors, which leads to uncontrolled uptake of oxLDL by macrophages [149]. Modified LDL induces the expression of various adhesion molecules and cytokines in ECs, which mediates the recruitment of circulating

monocytes to the sub-endothelial space [32, 34, 35], a crucial step in early atherogenesis [34, 35]. Moreover, LPA is produced during mild oxidation of LDL [5, 10] and has been shown to induce monocyte adhesion to the endothelium under static conditions *in vitro* by increasing the endothelial expression of adhesion molecules and chemokines [12, 13].

According to our results, moxLDL-induced monocyte rolling and adhesion requires endothelial LPA receptors and ATX activity, indicating that moxLDL-derived LPA induces monocyte adhesion to the endothelium (Fig. 49). Moreover, the presence of ATX activity in the medium of cultured endothelial cells has been demonstrated, further suggesting that ATX derived from endothelial cells generates LPA from moxLDL [123]. In contrast to blocking the endothelial LPA receptors, inhibiting ATX activity did not completely prevent monocyte adhesion, which could be due to an insufficient dose of the ATX inhibitor or to LPA derived from a source that does not require endothelial ATX activity. Similar to moxLDL, LPA20:4 also promotes monocyte rolling and adhesion to the endothelium. In contrast to LPA20:4, LPA18:0 does not promote monocyte rolling or adhesion, suggesting that the type of fatty acid chain determines the functional differences of LPA species in monocyte adhesion [123].

CXCL1 is the main chemokine for the VCAM-1-mediated adhesion of monocytes to the endothelium of atherosclerotic arteries [61, 150]. Here, we show that the CXCL1/CXCR2 axis plays an essential role in monocyte recruitment induced by moxLDL, because blocking endothelial CXCL1 or monocyte-specific CXCR2 inhibits moxLDL-induced monocyte rolling and adhesion in carotid arteries perfused *ex vivo* (Fig. 49). Similar to our results, a previous study showed that CXCL1 mediates mmLDL-induced monocyte adhesion to cultured endothelial cells under static conditions [62]. Our finding that blocking the LPA receptors completely inhibits moxLDL-induced monocyte adhesion suggests that the moxLDL-dependent activation of LPA receptors is closely linked to the effects of CXCL1 as an adhesion chemokine. Moreover, LPA20:4-induced monocyte adhesion is exclusively mediated via the CXCL1/CXCR2 axis, implying that LPA20:4 is crucial for moxLDL to induce CXCL1-dependent monocyte arrest. However, the contribution of other LPA species such as 1AGP18:1 in inducing CXCL1-mediated monocyte arrest following moxLDL treatment cannot be excluded [123]. Other LPA species may promote moxLDL-induced monocyte adhesion in a CXCL1-independent manner since blocking CXCL1, in contrast to the inhibition of LPA receptors, reduces the monocyte adhesion following moxLDL treatment by only 50%.

Furthermore, we demonstrated that hyperlipidemia-induced leukocyte adhesion in $ApoE^{-/-}$mice is also mediated by LPA_1 and LPA_3 expressed in the vessel wall. These findings confirm the crucial role of these LPA receptors in monocyte adhesion in a mouse model of atherosclerosis and imply that LPA is involved in hyperlipidemia-induced monocyte recruitment. Notably,

hyperlipidemia results in enhanced LPA formation likely due to upregulation of ATX [14, 151]. Similar to humans, lipoprotein oxidation, especially minimally oxidised LDL, has been demonstrated in ApoE$^{-/-}$ mice and causally linked to atherogenesis [152, 153]. Although it is unclear whether oxidised LDL is instrumental in hyperlipidemia-induced leukocyte adhesion in ApoE$^{-/-}$ mice, our results are compatible with the concept that LPA derived from lipoprotein oxidation also determines atherogenic leukocyte recruitment in this mouse model. However, we cannot exclude the possibility that other mechanisms of LPA synthesis play a role in hyperlipidemia-induced leukocyte adhesion, e.g. increased ATX expression and activity [14, 151]. Notably, inhibition of either LPA_1 or LPA_3 signalling is sufficient to block hyperlipidemia-induced leukocyte adhesion, which could be due to the formation of heterodimers between LPA_1 and LPA_3 (see section 4.2.4 for details).

Surface immobilisation via glycosaminoglycans of CXCL1 released from endothelial cells is a prerequisite for the efficient adhesion of monocytes [62, 63]. We provide the first evidence for a secretagogue effect of LPA on endothelial CXCL1, because blocking the LPA receptors inhibited the moxLDL-induced release of CXCL1 from endothelial cells and its subsequent deposition on the endothelial surface (Fig. 49). The finding that LPA20:4 induces CXCL1 secretion from endothelial cells indicates that LPA20:4 might be involved in moxLDL-induced release of CXCL1 [123]. Moreover, we demonstrated that LPA20:4 promotes the surface deposition of CXCL1 in carotid arteries, which might be due to its enhanced release from endothelial cells. In addition to the release of CXCL1 [123], LPA20:4, but not LPA18:0, upregulates CXCL1 mRNA expression in endothelial cells. In contrast to the ROCK signalling pathway that mediates only the release of CXCL1, activation of NF-κB by LPA20:4 induces the expression of CXCL1 in endothelial cells [123]. In addition to our results, LPA18:1 has been shown to release pentraxin-3 from endothelial cells, resulting in enhanced monocyte migration; however, a role for pentraxin-3 in inducing monocyte adhesion has not been reported [154].

Although CXCL1 appears to play an essential role in moxLDL-induced monocyte adhesion, blocking monocytic CXCR2 results in a more pronounced reduction of monocyte adhesion than inhibition of endothelial cell-derived CXCL1, suggesting that other CXCR2 ligands such as macrophage migration inhibitory factor (MIF) may also be involved in this process. A role of MIF in oxLDL-induced monocyte adhesion to endothelial cells has been described *in vitro* [155] and MIF mediates monocyte adhesion via CXCR2 in *ex vivo*-perfused carotid arteries of hyperlipidemic ApoE$^{-/-}$ mice [156]. Thus, our results would be in agreement with a role of MIF in LPA-mediated leukocyte adhesion, because inhibition or silencing of LPA_1 and LPA_3 completely prevented the moxLDL- and hyperlipidemia-induced monocyte adhesion. LPA20:4-induced

monocyte adhesion was solely due to the effects of CXCL1 (at least at a low dose of 10 µM), indicating that a different LPA species derived from the oxidation of LDL might affect MIF. However, currently, there is no evidence to prove a functional interaction of MIF with any LPA species. Notably, prolonged treatment (3 h) of carotid arteries with a high dose of LPA20:4 (40 µM) induces monocyte adhesion also via CXCR4 in addition to CXCR2. This CXCR4-dependent monocyte adhesion may be mediated by MIF, since MIF can trigger leukocyte adhesion via CXCR4 and CXCR2 [156]. However, such high LPA20:4 concentrations (40 µM) have not been observed *in vivo* during hyperlipidemia, thus it is unlikely that there is a dose-dependent effect of this LPA species on MIF-dependent leukocyte adhesion *in vivo*.

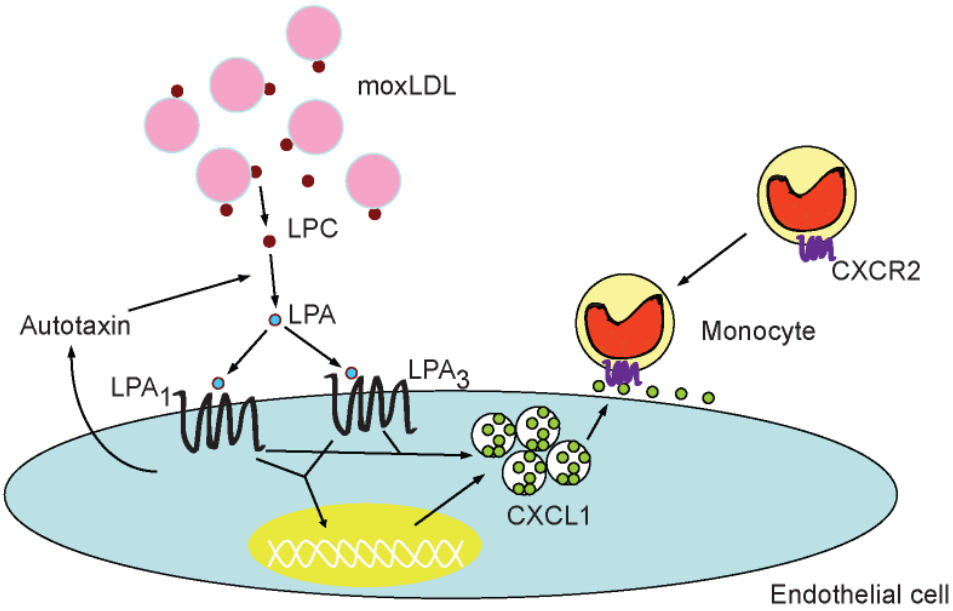

Figure 49: LPA-induced monocyte recruitment via CXCL1
LPA generated during mild oxidation of LDL via endothelial cell-derived ATX activates LPA_1 and LPA_3 on ECs. This activation of LPA_1 and LPA_3 induces the transcriptional upregulation of CXCL1 and the release of preformed CXCL1 from the endothelium resulting in monocyte adhesion [123]. LPA-lysophosphatidic acid, LPC- lysophosphatidylcholine, moxLDL-mildly oxidised LDL.

4.3.2 LPA effects on CXCL1: A 2-phase model

Our results demonstrate that moxLDL induces CXCL1-dependent monocyte adhesion to the endothelium via LPA receptors following short-term treatment (1 h) of the carotid arteries, indicating that LPA-dependent release of endothelial CXCL1 may account for moxLDL-induced monocyte adhesion. Similarly, LPA20:4 enhances monocyte rolling and adhesion to the

endothelium following short-term treatment in a CXCL1-dependent manner [123]. In contrast to LPA20:4, monocyte rolling and adhesion is absent following treatment with LPA18:0, indicating that only particular LPA species mediate this effect [123]. The presence of pre-formed CXCL1 protein in endothelial cells could be deduced because short-term treatment (1 h) with LPA20:4 was sufficient to induce monocyte adhesion. Accordingly, we detected CXCL1 expression in the ECs of normal mouse carotid arteries. Notably, it has been shown that pre-formed CXCL1 is stored in non Weibel-Palade body (WPB) secretory vesicles in the ECs [157, 158]. Further evidence for the release of endothelial CXCL1 by LPA was obtained from *in vitro* experiments: both LPA20:4 [123] and moxLDL induced the release of CXCL1 via LPA_1 and LPA_3 from cultured endothelial cells following short-term treatment. Furthermore, we clearly demonstrated the endothelial surface deposition of CXCL1 following stimulation of the carotid artery with LPA20:4. Therefore, this LPA20:4-induced release of CXCL1 accounts for an immediate response of the endothelial cells, resulting in monocyte adhesion.

In addition to releasing pre-formed CXCL1, LPA can also upregulate CXCL1 mRNA expression. We showed that treatment of cultured ECs with LPA20:4 induced CXCL1 mRNA expression in a LPA_1- and LPA_3-dependent manner, whereas LPA18:0 did not affectCXCL1 mRNA expression. Furthermore, a sustained effect of LPA20:4 on CXCL1-mediated leukocyte adhesion was observed *in vivo* even 3 days following treatment, although plasma LPA levels were not increased at this time, indicating that a transient rise in LPA20:4 after injection triggers a long-term response, for instance by enhancing CXCL1 mRNA expression [123]. Moreover, reduced expression of CXCL1 in the plaque following LPA receptor antagonist treatment may be due to impaired CXCL1 transcription. Therefore, we postulate that LPA exerts a 2-phase response of CXCL1, including the acute release of pre-formed CXCL1 and a more chronic upregulation of CXCL1 mRNA expression. This 2-phase model might explain the profound and long-lasting effect of even trace amounts of LPA in inducing monocyte recruitment.

4.3.3 Role of LPA and LPA receptors in atherosclerosis

Via G protein-coupled LPA receptors, LPA promotes various biological processes associated with atherosclerosis [159]. For example, LPA induces the expression of chemoattractants and adhesion molecules such as CCL2, IL8, ICAM-1, VCAM-1, and E-selectin in cultured endothelial cells, resulting in enhanced monocyte adhesion under static conditions [12, 13, 160, 161]. In SMCs, LPA mediates moxLDL-induced CCL20 expression, which is increased in the circulation of patients with atherosclerosis [162] and induces a synthetic phenotype characterised by reduced

expression of contractile proteins and an increased proliferation rate [163]. Furthermore, LPA is responsible for the activation of monocytes, platelets, and endothelial cells by modified LDL [10, 164]. Despite these atherogenic properties *in vitro*, the role of LPA and LPA receptors in atherosclerotic plaque development has not been studied.

To our knowledge, this is the first report providing evidence for the role of LPA receptors in atherosclerosis. According to our results, pharmacological inhibition of LPA_1 and LPA_3 reduces hyperlipidemia-induced plaque formation. This effect of the LPA receptor antagonist, which is highly specific for LPA_1 and LPA_3, suggests that these 2 LPA receptors play an important role in plaque formation [106]. In contrast to diet-induced atherosclerosis, enhanced plaque formation was observed after carotid ligation in $LPA_1^{-/-}$ mice [125]. Furthermore, combined LPA_1 and LPA_2 deficiency partially prevented ligation-induced lesion development, whereas genetic deletion of only LPA_2 was ineffective [125]. Carotid ligation is primarily characterised by vascular remodelling due to the response of SMCs to the cessation of flow but not by macrophage accumulation as in diet-induced atherosclerosis [165]. Therefore, the underlying mechanisms of lesion formation are fundamentally different between these 2 animal models, and the effects of targeting LPA receptors cannot be compared. Accordingly, increased lesion formation in LPA_1-deficient mice has been attributed to the enhanced migration of SMCs due to the overexpression of LPA_3 [125]. Our finding that the LPA receptor antagonist reduced the macrophage cell number in the plaque likely accounts for the diminished plaque size. The plaque macrophage content is primarily determined by the recruitment of circulating monocytes [166]. Our finding that endothelial LPA_1 and LPA_3 are crucial for atherogenic monocyte adhesion (See Section 4.3.1 for details), the first step in the recruitment of monocytes, implies that blocking LPA receptors reduces atherosclerosis via diminished monocyte recruitment. LPA receptor-mediated monocyte adhesion depends on the release of CXCL1 from the endothelium (See section 4.3.1 for details). In agreement with a prominent role of LPA receptor-mediated monocyte adhesion in plaque formation, we found that inhibiting LPA receptors reduced CXCL1 expression in the plaque and blocking CXCL1 offset the effect of the LPA receptor antagonist in atherogenesis. Moreover, the expression of other chemokines such as CX3CL1, CCL2, and CCL5, known to be involved in monocyte accumulation in plaques, was not affected by blocking LPA_1 and LPA_3. Of note, we demonstrate LPA_1 and LPA_3 expression in endothelial cells of mouse and human atherosclerotic plaques indicating that LPA receptor-mediated atherogenic monocyte recruitment also occurs in humans. In contrast, we have no evidence for a crucial role for endothelial LPA_2 in atherosclerosis because suppression of LPA_2 in the vessel wall does not affect atherogenic leukocyte adhesion, and hyperlipidemia downregulates LPA_2 in the aorta. However, we cannot exclude the possibility

that LPA_2, which is highly expressed in macrophages, also contributes to plaque development [123]. In addition to establishing an important role of LPA_1 and LPA_3, the effects of the LPA receptor antagonist on atherosclerosis also implies that LPA generated during hyperlipidemia promotes plaque formation.

Further evidence for the role of LPA in plaque development was obtained by LPA treatment. In line with the results of the LPA receptor antagonist, LPA20:4 enhanced plaque formation and monocyte recruitment. However, LPA18:0 did not affect atherosclerosis, demonstrating that pro-atherogenic effects depend on the LPA species. Similar to the effects of LPA receptors, treatment with LPA20:4 induces leukocyte adhesion to the endothelium in a CXCL1-dependent manner, indicating that LPA-dependent monocyte recruitment is also instrumental in LPA20:4-induced plaque formation [123]. Although the endothelium appearsto be the main source of CXCL1 in LPA-induced monocyte recruitment following LPA injection, activated platelets may be an additional source of CXCL1 contributing to plaque formation [167, 168]. We showed that enhanced monocyte recruitment plays a prominent role in LPA-induced plaque formation. Alternatively, LPA inhibits reverse transendothelial migration of monocyte-derived cells *in vitro*, indicating that LPA enhances macrophage retention within the plaque [169]. However, the role of macrophage emigration in lesion regression is under debate [169, 170].

LPA accumulates in atherosclerotic plaques and progressively increases during lesion development, suggesting that vessel-derived LPA plays an important role in atherogenesis [10, 171]. Similar to the results obtained after LPA injection, treatment of the carotid artery with LPA20:4 promoted atherosclerotic lesion development by enhanced macrophage accumulation, indicating that LPA directly acts on the vessel wall cells to enhance atherogenesis. The mechanism of macrophage accumulation induced by vessel wall-derived LPA appears to be similar to that induced by circulating LPA, because local treatment with LPA20:4, like injection of LPA20:4, promotes leukocyte adhesion to the endothelium in a CXCL1-dependent manner [123]. Thus, we could prove the pro-atherogenic function of vessel wall-derived LPA. However, the atherosclerosis-promoting effect of increased circulating LPA levels observed following systemic LPA injection might also be involved in human atherogenesis, as plasma LPA levels are elevated during hypercholesterolemia (Dohi, Miyauchi et al. 2012). Moreover, the formation of LPA through LDL oxidation may also occur in the circulation because plasma concentrations of oxLDL are elevated during atherosclerosis [172]. Taken together, we showed that both vessel wall-derived and circulating LPAs can be pro-atherogenic; however, further studies are required to determine the relative contribution of LPA from different origins to atherosclerosis.

4.3.4 The sources of LPA in atherosclerosis

Various studies from different groups have demonstrated that LPA is generated during mild oxidation of LDL [5, 10]. Initially, it was reported that the total LPA level increases after copper-mediated (640 µmol/L, 20 h copper treatment) or spontaneous oxidation of LDL and mediates moxLDL-induced platelet activation [10]. A following study demonstrated that the alkyl ether analogues of LPA but not the acyl LPA species are selectively increased in moxLDL compared to nLDL [5]. In contrast, very mild oxidation of LDL (100 µmol/L, 4 h copper treatment) does not result in LPA generation but increases the LPC content [123]. Although these differences might be explained by a varying degree of LDL oxidation, the precise mechanism by which LPA is produced during oxidation of LDL is unclear. LDL oxidation generates oxidised phosphatidylcholine, which is effectively converted by the lipoprotein-associated phospholipase A_2 into LPC [122]. LDL-derived ATX activity may be postulated from the above mentioned finding that LPA is generated during LDL oxidation in the absence of exogenous ATX activity [5, 10]. Our data strongly suggest that moxLDL-derived LPC can also be converted to LPA, for example, via ATX derived from endothelial cells because moxLDL-induced monocyte adhesion was inhibited by blocking the endothelial ATX activity in carotid arteries perfused *ex vivo*. In agreement, LPC-induced lymphocyte adhesion to ECs requires the expression and secretion of ATX, indicating that LPA mediates the effects of LPC on lymphocyte adhesion [173]. Furthermore, endothelial cell-derived ATX has been linked to lymphocyte homing to lymph nodes [174].

Therefore, we propose a 2-step process of LPA generation from oxidised LDL, where PLA_2 produces LPC which is further converted to LPA by ATX. This mechanism of LPA synthesis from oxidised LDL might be a significant source of LPA during atherogenesis. Hyperlipidemia increases the plasma LPC levels, followed by its accumulation in the aorta and serum ATX activity [14, 175]. The accumulation of LPC during plaque formation precedes the increase of LPA [171]. In addition, ATX is expressed in vascular lesions and may convert LPC to LPA in developing atherosclerotic plaques [125].

Although LDL is believed to be protected from oxidation in the plasma, owing to the presence of antioxidants, several animal and human studies describe increased plasma concentrations of oxLDL during atherosclerosis, indicating that LDL is either oxidised in the circulation or that oxLDL generated in the vessel wall leaks into the circulation [172, 176, 177]. In humans, plasma LPA levels are positively correlated with LPC, ATX, and LDL levels, indicating that LPA may also be generated from oxidised LDL in the circulation [178]. LPA levels in the circulation are further elevated in patients with acute coronary syndrome, which may be due to the activation of

platelets [178]. Platelets play an important role in atherogenesis, and activated platelets are a source for LPA; therefore, activated platelets may additionally contribute to LPA generation during atherosclerosis [1]. However, the role of platelet-derived LPA in plaque formation remains to be determined.

4.3.5 Role of CXCL1 in atherosclerosis

Chemokines play an important role in leukocyte recruitment during atherogenesis [179]. This monocyte recruitment is crucial for the accumulation of lesional macrophages through different stages of atheroma formation [170, 180].

Studies have shown that genetic deletion of the CC chemokine CCL2 or its receptor CCR2 reduces atherosclerosis due to reduced macrophage accumulation, suggesting that the CCL2/CCR2 axis may induce monocyte recruitment during atherosclerosis [181-183]. In addition, CCL2 and CCR2 are increased in SMCs and monocytes during hyperlipidemia [184, 185]. Moreover, CCL2 and CXCL1 work together in promoting monocyte recruitment via an inflamed endothelium [63]. CXCL1 is immobilised on the endothelial surface and induces monocyte adhesion via CXCR2, whereas CCL2 is secreted in a soluble form and contributes to monocyte shape change, spreading, and trans-endothelial migration via CCR2 [63]. In addition, the CCL2/CCR2 axis is involved in monocyte homeostasis and hyperlipidemia-induced monocytosis, as demonstrated in CCR2 and CCL2-deficient mice [186]. Therefore, the pro-atherogenic role of the CCL2/CCR2 axis can be addressed both to monocyte mobilisation during hyperlipidemia and to increased monocyte recruitment.

Genetic deletion of the CCL5 receptor CCR5 impairs atherosclerotic plaque formation and produces a more stable plaque phenotype with reduced macrophages/T cells and increased SMC accumulation [187]. Platelet-derived CCL5 and CXCL4 can be deposited and immobilised on the activated endothelium or lesions, resulting in enhanced monocyte recruitment [188, 189]. However, the effects of platelet-derived chemokines such as CCL5 and CXCL4 may not be functional during the initial stages of plaque development, where platelet activation is sparse. Moreover, blocking CCL5 using an antagonist inhibits the progression of established atherosclerotic lesions by blocking the recruitment of leukocytes to the plaque [190].

Furthermore, genetic deletion of the CX_3CL1 receptor CX_3CR1 inhibits atherosclerotic lesion development [191]. CX_3CL1 induces monocyte and T cell arrest to the endothelium via CX_3CR1 in an integrin-dependent manner [192]. Most importantly, the CX_3CL1/CX_3CR1 interaction is essential for the survival of monocytes and macrophages within the plaque [193]. In humans,

polymorphisms in the CX_3CR1 gene have been identified as a risk factor for coronary artery disease and atherosclerosis [194, 195].

Combined inhibition of CCL2, CX_3CR1, and CCR5 almost completely inhibits atherosclerosis in $ApoE^{-/-}$ mice, which is attributed to declined levels of circulating monocytes [196]. In contrast to CCL2 deficiency, which reduces the levels of both the $Ly6C^{hi}$ (inflammatory subtype) and $Ly6C^{lo}$ (non-inflammatory subtype) monocyte subsets in the circulation, the absence of CX_3CR1 only reduces the $Ly6C^{lo}$ subset, suggesting that CCL2 and CX_3CR1 limit plaque formation by reducing different monocyte subsets in the circulation [196]. Alternatively, increased apoptosis of plaque cells due to the absence of CX_3CR1 signalling may also account for the reduced plaque size in CX_3CR1-deficient mice [193]. Moreover, the combined inhibition of CCL2, CX_3CR1, and CCR5 axes results in an even more profound reduction of $Ly6C^{hi}$ and $Ly6C^{lo}$ monocyte subsets than in CCL2 and CX_3CR1-deficient mice, further suggesting that the reduced plaque size is due to the declined number of circulating monocytes [196]. Of note, $Ly6C^{hi}$ monocytes require CCR2 and CX_3CR1 whereas the $Ly6C^{lo}$ monocytes require CCR5 for plaque entry, indicating that reduced monocyte entry into the plaque may additionally account for the abrogated atherosclerotic lesion development in CCL2/CX_3CR1-deficient mice treated with a CCR5 antagonist [197]. Therefore, the study by Combadiere and co-workers demonstrates an additive effect on the inhibition of atherosclerosis compared to the studies where only one of the chemokine axes is blocked, suggesting that the contribution of each chemokine to plaque formation is distinct and not redundant [181, 187, 191]. Although combined inhibition of the CCL2, CX_3CR1, and CCR5 axes almost completely abolishes plaque formation, the essential role of CXCL1, which induces leukocyte arrest to the endothelium, in atherogenesis cannot be overlooked [61, 196]. It is possible to envision that CXCL1-induced monocyte adhesion is no longer essential for plaque development if circulating monocytes are greatly reduced, as seen in CCL2/CX_3CR1-deficient mice treated with a CCR5 antagonist [196]. We showed that CXCL1 is crucial for LPA-induced plaque development because blocking CXCL1 abolished the atheroprotective effect of the LPA receptor antagonist. Furthermore, pharmacological inhibition of LPA_1 and LPA_3 did not only impair plaque formation but also reduced, in contrast to CCL2, CCL5, and CX_3CL1, the lesional expression of CXCL1. The pro-atherogenic effect of CXCL1 appears to be more important in early atherosclerosis, because inhibition of CXCL1 in mice with advanced lesion formation was not associated with a regression of atherosclerosis, although there was a tendency towards impaired lesion progression [156].

4.4 Saturated versus unsaturated LPA in vascular diseases

Hypercholesterolemia is associated with increased serum levels of LPC and ATX activity [14]. ATX exhibits a substrate specificity for unsaturated over saturated LPC in hypercholesterolemic rabbits [14]. In contrast to saturated LPA, incubation of carotid arteries with unsaturated LPA induces neointima formation even in the absence of injury [5, 105]. Among a variety of unsaturated LPAs, LPA20:4 and 1AGP18:1 are most effective in stimulating neointimal growth [5]. Moreover, unsaturated LPA but not saturated LPA switches the phenotype of VSMCs from a differentiated to a dedifferentiated state, which is involved in atherosclerosis [163], and induces the activation of atheroprotective PPAR-γ *in vitro* [5].

Taken together, these studies suggest that only unsaturated LPA plays an important role in vascular diseases. We found that preferentially unsaturated LPA20:4 and 1AGP18:1 induced the HIF-1α-mediated CXCL12/CXCR4 axis, resulting in SPC mobilisation and neointima formation. However, this HIF-1α-mediated SPC recruitment was not observed when the arteries were treated with saturated LPA18:0 [121]. In contrast to LPA18:0, LPA20:4 induces monocyte adhesion and rolling via the CXCL1/CXCR2 axis [123]. Moreover, treatment of hyperlipidemic mice with LPA20:4 induced the progression of atherosclerosis, whereas LPA18:0 did not have any effect on plaque progression.

One reason for the differential effects of the various LPA species may be due to differences in receptor specificity towards unsaturated and saturated LPA [198]. For instance, LPA_3 shows a higher affinity towards unsaturated LPA than saturated LPA, whereas LPA_1 and LPA_2 have broad ligand specificity [198]. However, our finding that both LPA_1 and LPA_3 mediate LPA-induced neointima formation and monocyte adhesion makes LPA receptor specificity towards different LPA species an unlikely explanation for the exclusive effects of unsaturated LPA. Compared to saturated fatty acids, unsaturated fatty acid chains are more susceptible to oxidation, and this may influence the receptor-binding properties of various LPA species. Unfortunately, the level of oxidation in saturated and unsaturated LPA is currently unknown. Further studies are required to accurately determine the underlying cause for the atherogenic properties of unsaturated LPA.

4.5 Dual roles of LPA in vascular diseases

The current study demonstrates that LPA plays a crucial role in 2 distinct disease mechanisms of vascular lesion formation. In neointima formation, which is characterised by the accumulation of SMCs, LPA induces SPC recruitment by upregulating CXCL12 in SMCs. However, in

macrophage-rich atherosclerotic lesion formation, LPA recruits monocytes via endothelial CXCL1.

Our results suggest that the concentration of LPA shapes the type of vascular response because, in contrast to high LPA concentrations (40 µM), low levels of LPA (10 µM) did not affect SMC accumulation in vascular lesions. Both platelet activation and apoptosis of SMCs after vascular injury may transiently lead to an exceptionally high local LPA concentration in the vessel wall that triggers the CXCL12-induced SPC mobilisation, similar to incubation of the carotid artery with 40 µM LPA. However, high as well as low LPA levels increase the adhesion of monocytes in arteries perfused *ex vivo*, indicating that high LPA concentrations can also promote monocyte recruitment.

Alternatively, cell type-specific effects on endothelial cells and SMCs may underlie the dual role of LPA in vascular diseases. During carotid incubation, LPA has been shown to enter the vessel wall and to localise in the media [105]. In addition, endothelial denudation after vascular injury allows direct access of LPA to medial SMCs. Therefore, LPA may induce a SMC-specific response after vascular injury that is characterised by CXCL12-mediated recruitment of SPCs. During atherogenesis, our results showed that LPA mediates adhesion of monocytes via CXCL1, which is stored in endothelial cells [157].

Of note, the differential effects of LPA in the vasculature are not because of the activation of different LPA receptors. In fact, we found that the effects of LPA on both CXCL12-mediated SPC recruitment and CXCL1-dependent atherogenesis can be prevented by silencing LPA_1 or LPA_3. Therefore, drugs that inhibit either LPA_1 or LPA_3 might be a promising for the treatment and prevention of both atherosclerosis and restenosis. The LPA_1 antagonist AM152 has been tested in phase 1/2 clinical trials for the treatment of idiopathic pulmonary fibrosis; unfortunately, no results of these trials are available [199]. In principle, drugs targeting the LPA receptors can be administered via drug-eluting stents, to inhibit restenosis or systemically to treat atherosclerosis. Additionally, the enzymes critically involved in LPA synthesis are attractive therapeutic targets in vascular diseases. Currently, the lipoprotein-associated phospholipase A2 inhibitor darapladib is being investigated in phase 3 trials for its effect in atherosclerotic cardiovascular disease [200]. Further studies are required to establish the clinical value of drugs that target LPA receptors or LPA synthesis in the treatment of cardiovascular diseases.

5 Summary

LPA and vascular diseases

The CXCL12/CXCR4 axis directs the SPC mediated vascular repair following injury [97-99]. The mechanism that induces CXCL12 following vessel injury and thus leads to neointima formation through SPC recruitment was unknown. Of note, short-term incubation of uninjured carotid arteries with unsaturated LPA, which is produced upon platelet activation, results in intimal SMC accumulation [5, 105, 201]. Furthermore, unsaturated LPA induces CXCL12 expression in a LPA_1- and LPA_3-dependent manner *in vitro* [15]. Following vascular injury, blocking LPA_1 and LPA_3 inhibits the mobilisation of SPC, neointima formation and neointimal expression of HIF-1α and CXCL12 [121]. Moreover, blocking CXCR4 suppressed LPA-induced neointima formation [121]. LPA may activate the CXCL12/CXCR4 axis resulting in SPC-mediated neointima formation. However, there is no direct evidence which shows that LPA induces neointima formation by the recruitment of BM-derived SPCs. In addition, it is not known whether LPA_1 and LPA_3 have differential functions in LPA-induced neointima formation.

LPA receptor expression was differentially regulated following vascular injury. LPA_1, which was primarily detectable in ECs, was reduced, whereas LPA_2 and LPA_3 were transiently increased, e.g. macrophages. Blocking LPA_1 and LPA_3 following injury reduced the neointimal SMCs, which express the stem cell marker Sca-1 and macrophage content with no difference in the T-cell content and re-endothelialisation. This suggests that LPA promotes neointima formation by the recruitment of SPCs. Of note short-term incubation with unsaturated LPA induces a sustained upregulation of HIF-1α together with CXCL12 in neointimal cells. Knockdown of LPA-induced CXCL12 expression in the vessel wall blocked the SPC mobilisation and neointima formation. This indicates that LPA activates the HIF-1α/CXCL12 axis and thus SPC-mediated vascular repair. Furthermore, the mobilisation of SPCs and the neointima formation following incubation with unsaturated LPA was inhibited by blocking LPA_1 and LPA_3. This provides additional evidence that the effect of blocking LPA_1 and LPA_3 on neointima formation after vascular injury is due to a reduced SPC recruitment. In mice, which express a SMC-specific reporter gene only in BM cells, reporter gene activity was found in neointimal cells following LPA incubation. Blocking LPA_1 and LPA_3 during LPA incubation inhibited the recruitment of BM-derived cells which express the SMC-specific reporter gene. This clearly demonstrates that LPA via LPA_1 and/or LPA_3 promotes neointima formation by the recruitment of BM-derived SPCs. Silencing of each of the LPA receptors, LPA_1 and LPA_3, in the vessel wall blocked LPA-induced SPC mobilisation and

neointima formation. LPA-induced SPC recruitment and neointima formation can be mediated independently by either LPA_1 or LPA_3. Although the LPA-mediated recruitment of SPCs explains the reduced neointimal SMC content after blocking LPA_1 and LPA_3, it remains unclear how LPA is involved in the accumulation of macrophages.

Lesional macrophages are derived from circulating monocytes, which are recruited into the vessel wall via activated ECs. LDL that is modified in the sub-endothelial space plays a central role in the proatherogenic activation of ECs by inducing CXCL1 [34, 62]. Noteworthy, mild oxidation of LDL leads to the synthesis of LPA and high concentrations of LPA is present in the core of the atherosclerotic lesions [10]. Moreover, LPA induces the adhesion of monocytes to ECs by increasing the expression of endothelial chemokines and adhesion molecules [12, 13]. Therefore, LPA_1 and LPA_3 may mediate monocyte recruitment that is induced by modified LDL-derived LPA. We studied the role of LPA in modified LDL-induced monocyte recruitment and atherosclerosis.

Ex vivo perfusion experiments of the carotid artery revealed that moxLDL increases monocyte adhesion to the endothelium via CXCL1, which is mediated by endothelial LPA_1 and LPA_3 and requires the release of ATX from ECs. Accordingly, the moxLDL-induced surface expression and secretion of CXCL1 from ECs is mediated by LPA_1 and LPA_3. This indicates that LPA is of crucial importance in the moxLDL-induced monocyte adhesion. Treatment with LPA20:4, indeed, increased the adhesion of monocytes to the endothelium via CXCL1. In the endothelium of murine carotid arteries, pre-formed CXCL1 was found which was released and immobilised on the cell surface following LPA20:4-stimulation. Moreover, unsaturated LPA20:4 but not saturated LPA18:0 increased the CXCL1 mRNA expression in ECs in a LPA_1- and LPA_3-dependent manner. MoxLDL-derived LPA induces monocyte adhesion to ECs by stimulating the release and transcription of CXCL1.

Hyperlipidemia induces differential regulation of LPA receptor expression in the aorta of $ApoE^{-/-}$ mice characterised by a reduced LPA_2 expression, an increased LPA_3 expression and an unchanged LPA_1 expression. Immunofluorescence staining demonstrates that both LPA_1 and LPA_3 are expressed in macrophages and ECs of mouse atherosclerotic plaques. In addition, LPA_1 and LPA_3 are also present in ECs of human atherosclerotic plaques. LPA_1 and LPA_3 are predominantly expressed during atherosclerosis which indicates that they may play an important role in atherogenesis. Accordingly, silencing of either LPA_1 or LPA_3 in the artery blocked the hyperlipidemia-induced leukocyte adhesion to the endothelium. However, knockdown of LPA_2 did not have any effect on leukocyte adhesion. LPA_1 and LPA_3 independently play a role in hyperlipidemia-induced leukocyte adhesion. Systemic or local treatment of hyperlipidemic mice

with LPA20:4 increased the plaque size due to enhanced macrophage accumulation whereas systemic treatment with LPA18:0 had no effect on the progression of atherosclerosis. Conversely, pharmacological inhibition of LPA_1 and LPA_3 by Ki16425 in hyperlipidemic mice reduced the plaque size due to diminished macrophage accumulation. This effect was absent in mice that were treated with a blocking CXCL1 Ab in addition to Ki16425. Moreover, the expression of CXCL1, but not of CCL2, CCL5 and CX_3CL1, was reduced in the plaque after treatment with the LPA receptor antagonist. Endogenous LPA induces macrophage accumulation and atherosclerosis via CXCL1 in hyperlipidemic mice.

6 References

1. Aoki, J., A. Inoue, and S. Okudaira, *Two pathways for lysophosphatidic acid production.* Biochim Biophys Acta, 2008. **1781**(9): p. 513-8.

2. Mills, G.B. and W.H. Moolenaar, *The emerging role of lysophosphatidic acid in cancer.* Nat Rev Cancer, 2003. **3**(8): p. 582-91.

3. Choi, J.W., et al., *LPA receptors: subtypes and biological actions.* Annual review of pharmacology and toxicology, 2010. **50**: p. 157-86.

4. Lin, M.E., D.R. Herr, and J. Chun, *Lysophosphatidic acid (LPA) receptors: signaling properties and disease relevance.* Prostaglandins Other Lipid Mediat, 2010. **91**(3-4): p. 130-8

5. Zhang, C., et al., *Lysophosphatidic acid induces neointima formation through PPARgamma activation.* J Exp Med, 2004. **199**(6): p. 763-74.

6. Cheng, Y., et al., *Lysophosphatidic acid-induced arterial wall remodeling: requirement of PPARgamma but not LPA1 or LPA2 GPCR.* Cellular signalling, 2009. **21**(12): p. 1874-84.

7. Berdichevets, I.N., et al., *Lysophosphatidic acid is a lipid mediator with wide range of biological activities. Biosynthetic pathways and mechanism of action.* Biochemistry (Mosc), 2010. **75**(9): p. 1088-97.

8. Choi, J.W., C.W. Lee, and J. Chun, *Biological roles of lysophospholipid receptors revealed by genetic null mice: an update.* Biochim Biophys Acta, 2008. **1781**(9): p. 531-9.

9. Murakami, M., et al., *Identification of the orphan GPCR, P2Y(10) receptor as the sphingosine-1-phosphate and lysophosphatidic acid receptor.* Biochem Biophys Res Commun, 2008. **371**(4): p. 707-12.

10. Siess, W., et al., *Lysophosphatidic acid mediates the rapid activation of platelets and endothelial cells by mildly oxidized low density lipoprotein and accumulates in human atherosclerotic lesions.* Proc Natl Acad Sci U S A, 1999. **96**(12): p. 6931-6.

11. Rother, E., et al., *Subtype-selective antagonists of lysophosphatidic Acid receptors inhibit platelet activation triggered by the lipid core of atherosclerotic plaques.* Circulation, 2003. **108**(6): p. 741-7.

12. Lin, C.I., et al., *Lysophosphatidic acid regulates inflammation-related genes in human endothelial cells through LPA1 and LPA3.* Biochem Biophys Res Commun, 2007. **363**(4): p. 1001-8.

13. Rizza, C., et al., *Lysophosphatidic acid as a regulator of endothelial/leukocyte interaction.* Lab Invest, 1999. **79**(10): p. 1227-35.

14. Tokumura, A., et al., *Increased formation of lysophosphatidic acids by lysophospholipase D in serum of hypercholesterolemic rabbits.* The Journal of Lipid Research, 2002. **43**(2): p. 307-15.

15. Jeon, E.S., et al., *Cancer-derived lysophosphatidic acid stimulates differentiation of human mesenchymal stem cells to myofibroblast-like cells.* Stem Cells, 2008. **26**(3): p. 789-97.

16. Tokumura, A., et al., *Lysophosphatidic acids induce proliferation of cultured vascular smooth muscle cells from rat aorta.* Am J Physiol, 1994. **267**(1 Pt 1): p. C204-10.

17. Charo, I.F. and R.M. Ransohoff, *The many roles of chemokines and chemokine receptors in inflammation.* N Engl J Med, 2006. **354**(6): p. 610-21.

18. Allen, S.J., S.E. Crown, and T.M. Handel, *Chemokine: receptor structure, interactions, and antagonism.* Annu Rev Immunol, 2007. **25**: p. 787-820.

19. Viola, A. and A.D. Luster, *Chemokines and their receptors: drug targets in immunity and inflammation.* Annu Rev Pharmacol Toxicol, 2008. **48**: p. 171-97.

20. Johnson, Z., A.E. Proudfoot, and T.M. Handel, *Interaction of chemokines and glycosaminoglycans: a new twist in the regulation of chemokine function with opportunities for therapeutic intervention.* Cytokine Growth Factor Rev, 2005. **16**(6): p. 625-36.

21. Schall, T.J. and A.E. Proudfoot, *Overcoming hurdles in developing successful drugs targeting chemokine receptors.* Nat Rev Immunol, 2011. **11**(5): p. 355-63.

22. Fernandez, E.J. and E. Lolis, *Structure, function, and inhibition of chemokines.* Annu Rev Pharmacol Toxicol, 2002. **42**: p. 469-99.

23. Zlotnik, A. and O. Yoshie, *Chemokines: a new classification system and their role in immunity.* Immunity, 2000. **12**(2): p. 121-7.

24. Moser, B. and K. Willimann, *Chemokines: role in inflammation and immune surveillance.* Ann Rheum Dis, 2004. **63 Suppl 2**: p. ii84-ii89.

25. Bacon, K., et al., *Chemokine/chemokine receptor nomenclature.* J Interferon Cytokine Res, 2002. **22**(10): p. 1067-8.

26. Baggiolini, M., *Chemokines and leukocyte traffic.* Nature, 1998. **392**(6676): p. 565-8.

27. Charo, I.F. and M.B. Taubman, *Chemokines in the pathogenesis of vascular disease.* Circ Res, 2004. **95**(9): p. 858-66.

28. Hansson, G.K. and A. Hermansson, *The immune system in atherosclerosis.* Nat Immunol, 2011. **12**(3): p. 204-12

29. Mackay, J. and G. Mensah, *The Atlas of heart disease and stroke*2004, Geneva: World Health Organization.

30. Hansson, G.K., A.K. Robertson, and C. Soderberg-Naucler, *Inflammation and atherosclerosis.* Annu Rev Pathol, 2006. **1**: p. 297-329

31. Ross, R., *The pathogenesis of atherosclerosis: a perspective for the 1990s.* Nature, 1993. **362**(6423): p. 801-9

32. Ross, R., *Atherosclerosis--an inflammatory disease.* N Engl J Med, 1999. **340**(2): p. 115-26.

33. Lahoute, C., et al., *Adaptive immunity in atherosclerosis: mechanisms and future therapeutic targets.* Nat Rev Cardiol, 2011. **8**(6): p. 348-58

34. Glass, C.K. and J.L. Witztum, *Atherosclerosis. the road ahead.* Cell, 2001. **104**(4): p. 503-16.

35. Hansson, G.K., *Inflammation, atherosclerosis, and coronary artery diesease.* N Engl J Med, 2005. **352**(16): p. 1685-95.

36. Hansson, G.K. and P. Libby, *The immune response in atherosclerosis: a double-edged sword.* Nature Reviews Immunology, 2006. **6**(7): p. 508-19.

37. Weber, C., A. Zernecke, and P. Libby, *The multifaceted contributions of leukocyte subsets to atherosclerosis: lessons from mouse models.* Nature Reviews Immunology, 2008. **8**(10): p. 802-15.

38. Libby, P., *Inflammation in atherosclerosis.* Nature, 2002. **420**(6917): p. 868-74.

39. Libby, P., M. DiCarli, and R. Weissleder, *The vascular biology of atherosclerosis and imaging targets.* J Nucl Med, 2010. **51 Suppl 1**: p. 33S-37S

40. Schwenke, D.C. and T.E. Carew, *Initiation of atherosclerotic lesions in cholesterol-fed rabbits. I. Focal increases in arterial LDL concentration precede development of fatty streak lesions.* Arteriosclerosis, 1989. **9**(6): p. 895-907.

41. Williams, K.J. and I. Tabas, *The response-to-retention hypothesis of atherogenesis reinforced.* Curr Opin Lipidol, 1998. **9**(5): p. 471-4.

42. Stocker, R. and J.F. Keaney, Jr., *Role of oxidative modifications in atherosclerosis.* Physiol Rev, 2004. **84**(4): p. 1381-478.

43. Ley, K., et al., *Getting to the site of inflammation: the leukocyte adhesion cascade updated.* Nature Reviews Immunology, 2007. **7**(9): p. 678-89.

44. Johnston, B. and E.C. Butcher, *Chemokines in rapid leukocyte adhesion triggering and migration.* Semin Immunol, 2002. **14**(2): p. 83-92.

45. Langer, H.F. and T. Chavakis, *Leukocyte-endothelial interactions in inflammation.* J Cell Mol Med, 2009. **13**(7): p. 1211-20.

46. Mestas, J. and K. Ley, *Monocyte-endothelial cell interactions in the development of atherosclerosis.* Trends Cardiovasc Med, 2008. **18**(6): p. 228-32.

47. Marshall, B.T., et al., *Direct observation of catch bonds involving cell-adhesion molecules.* Nature, 2003. **423**(6936): p. 190-3.

48. Finger, E.B., et al., *Adhesion through L-selectin requires a threshold hydrodynamic shear.* Nature, 1996. **379**(6562): p. 266-9.

49. Lawrence, M.B., et al., *Threshold levels of fluid shear promote leukocyte adhesion through selectins.* J Cell Biol, 1997. **136**(3): p. 717-27.

50. Constantin, G., et al., *Chemokines trigger immediate beta2 integrin affinity and mobility changes: differential regulation and roles in lymphocyte arrest under flow.* Immunity, 2000. **13**(6): p. 759-69.

51. Shamri, R., et al., *Lymphocyte arrest requires instantaneous induction of an extended LFA-1 conformation mediated by endothelium-bound chemokines.* Nat Immunol, 2005. **6**(5): p. 497-506.

52. Shattil, S.J., *Integrins and Src: dynamic duo of adhesion signaling.* Trends Cell Biol, 2005. **15**(8): p. 399-403.

53. Giagulli, C., et al., *The Src family kinases Hck and Fgr are dispensable for inside-out, chemoattractant-induced signaling regulating beta 2 integrin affinity and valency in neutrophils, but are required for beta 2 integrin-mediated outside-in signaling involved in sustained adhesion.* J Immunol, 2006. **177**(1): p. 604-11.

54. Engelhardt, B. and H. Wolburg, *Mini-review: Transendothelial migration of leukocytes: through the front door or around the side of the house?* Eur J Immunol, 2004. **34**(11): p. 2955-63.

55. Richmond, A., et al., *Molecular characterization and chromosomal mapping of melanoma growth stimulatory.* Embo J, 1988. **7**(7): p. 2025-33.

56. Anisowicz, A., L. Bardwell, and R. Sager, *Constitutive overexpression of a growth-regulated gene in transformed Chinese hamster and human cells.* Proc Natl Acad Sci U S A, 1987. **84**(20): p. 7188-92.

57. Zernecke, A., E. Shagdarsuren, and C. Weber, *Chemokines in atherosclerosis: an update.* Arterioscler Thromb Vasc Biol, 2008. **28**(11): p. 1897-908.

58. Geiser, T., et al., *The interleukin-8-related chemotactic cytokines GRO alpha, GRO beta, and GRO gamma activate human neutrophil and basophil leukocytes.* J Biol Chem, 1993. **268**(21): p. 15419-24.

59. Jinquan, T., et al., *Recombinant human growth-regulated oncogene-alpha induces T lymphocyte chemotaxis. A process regulated via IL-8 receptors by IFN-gamma, TNF-alpha, IL-4, IL-10, and IL-13.* J Immunol, 1995. **155**(11): p. 5359-68.

60. Boisvert, W.A., et al., *Up-regulated expression of the CXCR2 ligand KC/GRO-alpha in atherosclerotic lesions plays a central role in macrophage accumulation and lesion progression.* Am J Pathol, 2006. **168**(4): p. 1385-95.

61. Huo, Y., et al., *The chemokine KC, but not monocyte chemoattractant protein-1, triggers monocyte arrest on early atherosclerotic endothelium.* J Clin Invest, 2001. **108**(9): p. 1307-14.

62. Schwartz, D., et al., *Role of the GRO family of chemokines in monocyte adhesion to MM-LDL-stimulated endothelium.* J Clin Invest, 1994. **94**(5): p. 1968-73.

63. Weber, K.S., et al., *Differential immobilization and hierarchical involvement of chemokines in monocyte arrest and transmigration on inflamed endothelium in shear flow.* Eur J Immunol, 1999. **29**(2): p. 700-12.

64. Randolph, G.J. and M.B. Furie, *A soluble gradient of endogenous monocyte chemoattractant protein-1 promotes the transendothelial migration of monocytes in vitro.* J Immunol, 1995. **155**(7): p. 3610-8.

65. Weintraub, W.S., *The pathophysiology and burden of restenosis.* Am J Cardiol, 2007. **100**(5A): p. 3K-9K.

66. Jukema, J.W., et al., *Restenosis after PCI. Part 1: pathophysiology and risk factors.* Nat Rev Cardiol, 2011.

67. Bauters, C. and J.M. Isner, *The biology of restenosis.* Prog Cardiovasc Dis, 1997. **40**(2): p. 107-16.

68. Garg, S. and P.W. Serruys, *Coronary stents: current status.* J Am Coll Cardiol, 2010. **56**(10 Suppl): p. S1-42.

69. Barragan, P., et al., *Ticlopidine and subcutaneous heparin as an alternative regimen following coronary stenting.* Cathet Cardiovasc Diagn, 1994. **32**(2): p. 133-8.

70. Schomig, A., et al., *A randomized comparison of antiplatelet and anticoagulant therapy after the placement of coronary-artery stents.* N Engl J Med, 1996. **334**(17): p. 1084-9.

71. Cutlip, D.E., et al., *Acute and nine-month clinical outcomes after "suboptimal" coronary stenting: results from the STent Anti-thrombotic Regimen Study (STARS) registry.* J Am Coll Cardiol, 1999. **34**(3): p. 698-706.

72. Welt, F.G. and C. Rogers, *Inflammation and restenosis in the stent era.* Arterioscler Thromb Vasc Biol, 2002. **22**(11): p. 1769-76.

73. Dangas, G. and V. Fuster, *Management of restenosis after coronary intervention.* Am Heart J, 1996. **132**(2 Pt 1): p. 428-36

74. Nobuyoshi, M., et al., *Restenosis after percutaneous transluminal coronary angioplasty: pathologic observations in 20 patients.* J Am Coll Cardiol, 1991. **17**(2): p. 433-9.

75. Farb, A., et al., *Morphological predictors of restenosis after coronary stenting in humans.* Circulation, 2002. **105**(25): p. 2974-80.

76. Tung, R., et al., *Narrative review: drug-eluting stents for the management of restenosis: a critical appraisal of the evidence.* Ann Intern Med, 2006. **144**(12): p. 913-9.

77. Al-Lamee, R., et al., *Comparison of Long-Term Clinical and Angiographic Outcomes Following Implantation of Bare Metal Stents and Drug-Eluting Stents in Aorto-Ostial Lesions.* Am J Cardiol, 2011.

78. Maisel, W.H., *Unanswered questions--drug-eluting stents and the risk of late thrombosis.* N Engl J Med, 2007. **356**(10): p. 981-4.

79. Eisenstein, E.L., et al., *Clopidogrel use and long-term clinical outcomes after drug-eluting stent implantation.* Jama, 2007. **297**(2): p. 159-68.

80. Finn, A.V., et al., *Pathological correlates of late drug-eluting stent thrombosis: strut coverage as a marker of endothelialization.* Circulation, 2007. **115**(18): p. 2435-41.

81. Joner, M., et al., *Pathology of drug-eluting stents in humans: delayed healing and late thrombotic risk.* J Am Coll Cardiol, 2006. **48**(1): p. 193-202.

82. Chitkara, K. and K. Pujara, *Drug-eluting Stents in Acute Coronary Syndrome: Is There a Risk of Stent Thrombosis with Second-Generation Stents?* Eur J Cardiovasc Med, 2010. **1**(2): p. 20-24

83. Curfman, G.D., et al., *Drug-eluting coronary stents--promise and uncertainty.* N Engl J Med, 2007. **356**(10): p. 1059-60.

84. Nagasawa, T., H. Kikutani, and T. Kishimoto, *Molecular cloning and structure of a pre-B-cell growth-stimulating factor.* Proc Natl Acad Sci U S A, 1994. **91**(6): p. 2305-9.

85. Schober, A., et al., *SDF-1alpha-mediated tissue repair by stem cells: a promising tool in cardiovascular medicine?* Trends Cardiovasc Med, 2006. **16**(4): p. 103-8.

86. Tashiro, K., et al., *Signal sequence trap: a cloning strategy for secreted proteins and type I membrane proteins,* in *Science*1993. p. 600-3.

87. Aiuti, A., et al., *The chemokine SDF-1 is a chemoattractant for human CD34+ hematopoietic progenitor cells and provides a new mechanism to explain the mobilization of CD34+ progenitors to peripheral blood.* J Exp Med, 1997. **185**(1): p. 111-20.

88. Hartmann, T.N., et al., *A crosstalk between intracellular CXCR7 and CXCR4 involved in rapid CXCL12-triggered integrin activation but not in chemokine-triggered motility of human T lymphocytes and CD34+ cells.* J Leukoc Biol, 2008. **84**(4): p. 1130-40

89. Janowski, M., *Functional diversity of SDF-1 splicing variants.* Cell Adh Migr, 2009. **3**(3): p. 243-9.

90. Sierra, M.D., et al., *Differential processing of stromal-derived factor-1 {alpha} and {beta} explains functional diversity.* Blood, 2003.

91. Yu, L., et al., *Identification and expression of novel isoforms of human stromal cell-derived factor 1.* Gene, 2006. **374**: p. 174-9.

92. Shirozu, M., et al., *Structure and chromosomal localization of the human stromal cell-derived factor 1 (SDF1) gene.* Genomics, 1995. **28**(3): p. 495-500.

93. Nagasawa, T., et al., *Defects of B-cell lymphopoiesis and bone-marrow myelopoiesis in mice lacking the CXC chemokine PBSF/SDF-1.* Nature, 1996. **382**(6592): p. 635-8.

94. Zou, Y.R., et al., *Function of the chemokine receptor CXCR4 in haematopoiesis and in cerebellar development.* Nature, 1998. **393**(6685): p. 595-9.

95. Hattori, K., et al., *Plasma elevation of stromal cell-derived factor-1 induces mobilization of mature and immature hematopoietic progenitor and stem cells.* Blood, 2001. **97**(11): p. 3354-60.

96. Keating, G.M., *Plerixafor: a review of its use in stem-cell mobilization in patients with lymphoma or multiple myeloma.* Drugs, 2011. **71**(12): p. 1623-47.

97. Zernecke, A., et al., *SDF-1alpha/CXCR4 axis is instrumental in neointimal hyperplasia and recruitment of smooth muscle progenitor cells.* Circ Res, 2005. **96**(7): p. 784-91.

98. Schober, A., et al., *Crucial role of stromal cell-derived factor-1alpha in neointima formation after vascular injury in apolipoprotein E-deficient mice.* Circulation, 2003. **108**(20): p. 2491-7.

99. Schober, A., *Chemokines in vascular dysfunction and remodeling.* Arterioscler Thromb Vasc Biol, 2008. **28**(11): p. 1950-9.

100. Karshovska, E., et al., *A small molecule CXCR4 antagonist inhibits neointima formation and smooth muscle progenitor cell mobilization after arterial injury.* J Thromb Haemost, 2008. **6**(10): p. 1812-5.

101. Hellwig-Burgel, T., et al., *Review: hypoxia-inducible factor-1 (HIF-1): a novel transcription factor in immune reactions.* J Interferon Cytokine Res, 2005. **25**(6): p. 297-310.

102. Zarember, K.A. and H.L. Malech, *HIF-1alpha: a master regulator of innate host defenses?* J Clin Invest, 2005. **115**(7): p. 1702-4.

103. Sharp, F.R. and M. Bernaudin, *HIF1 and oxygen sensing in the brain.* Nat Rev Neurosci, 2004. **5**(6): p. 437-48.

104. Karshovska, E., et al., *Expression of HIF-1alpha in injured arteries controls SDF-1alpha mediated neointima formation in apolipoprotein E deficient mice.* Arterioscler Thromb Vasc Biol, 2007. **27**(12): p. 2540-7.

105. Yoshida, K., et al., *Vascular remodeling induced by naturally occurring unsaturated lysophosphatidic acid in vivo.* Circulation, 2003. **108**(14): p. 1746-52.

106. Ohta, H., et al., *Ki16425, a subtype-selective antagonist for EDG-family lysophosphatidic acid receptors.* Mol Pharmacol, 2003. **64**(4): p. 994-1005.

107. Nam, D., et al., *Partial carotid ligation is a model of acutely induced disturbed flow, leading to rapid endothelial dysfunction and atherosclerosis.* American Journal of physiology. Heart and circulatory physiology, 2009. **297**(4): p. H1535-43.

108. Moessler, H., et al., *The SM 22 promoter directs tissue-specific expression in arterial but not in venous or visceral smooth muscle cells in transgenic mice.* Development, 1996. **122**(8): p. 2415-25.

109. Escobar-Chavez, J.J., et al., *Applications of thermo-reversible pluronic F-127 gels in pharmaceutical formulations.* J Pharm Pharm Sci, 2006. **9**(3): p. 339-58.

110. Koenen, R.R., et al., *Disrupting functional interactions between platelet chemokines inhibits atherosclerosis in hyperlipidemic mice.* Nat Med, 2009. **15**(1): p. 97-103.

111. Ramos, C.L., et al., *Direct demonstration of P-selectin- and VCAM-1-dependent mononuclear cell rolling in early atherosclerotic lesions of apolipoprotein E-deficient mice.* Circ Res, 1999. **84**(11): p. 1237-44.

112. Ziegler-Heitbrock, H.W., et al., *Establishment of a human cell line (Mono Mac 6) with characteristics of mature monocytes.* Int J Cancer, 1988. **41**(3): p. 456-61.

113. Sakly, N., et al., *Anti-endothelial cell antibodies determination by cyto-ELISA: a comparative study between three cell types used as substrates.* Ann N Y Acad Sci, 2005. **1050**: p. 201-9.

114. So, P.T., et al., *Two-photon excitation fluorescence microscopy.* Annu Rev Biomed Eng, 2000. **2**: p. 399-429.

115. Megens, R.T., et al., *Two-photon microscopy of vital murine elastic and muscular arteries. Combined structural and functional imaging with subcellular resolution.* J Vasc Res, 2007. **44**(2): p. 87-98.

116. Vandesompele, J., et al., *Accurate normalization of real-time quantitative RT-PCR data by geometric averaging of multiple internal control genes.* Genome Biol, 2002. **3**(7): p. RESEARCH0034.

117. Suh, S.H., et al., *Characterisation of explanted endothelial cells from mouse aorta: electrophysiology and Ca2+ signalling.* Pflugers Arch, 1999. **438**(5): p. 612-20.

118. Ferguson, C.G., et al., *Fluorogenic phospholipid substrate to detect lysophospholipase D/autotaxin activity.* Org Lett, 2006. **8**(10): p. 2023-6.

119. Esterbauer, H., et al., *Continuous monitoring of in vitro oxidation of human low density lipoprotein.* Free Radic Res Commun, 1989. **6**(1): p. 67-75.

120. Qiu, G. and J.S. Hill, *Endothelial lipase enhances low density lipoprotein binding and cell association in THP-1 macrophages.* Cardiovasc Res, 2007. **76**(3): p. 528-38.

121. Subramanian, P., et al., *Lysophosphatidic acid receptors LPA1 and LPA3 promote CXCL12-mediated smooth muscle progenitor cell recruitment in neointima formation.* Circ Res, 2010. **107**(1): p. 96-105.

122. Steinbrecher, U.P., et al., *Modification of low density lipoprotein by endothelial cells involves lipid peroxidation and degradation of low density lipoprotein phospholipids.* Proc Natl Acad Sci U S A, 1984. **81**(12): p. 3883-7.

123. Zhou, Z., et al., *Lipoprotein-Derived Lysophosphatidic Acid Promotes Atherosclerosis by Releasing CXCL1 from the Endothelium.* Cell metabolism, 2011. **13**(5): p. 592-600.

124. Williams, K.J. and I. Tabas, *The response-to-retention hypothesis of early atherogenesis.* Arterioscler Thromb Vasc Biol, 1995. **15**(5): p. 551-61.

125. Panchatcharam, M., et al., *Lysophosphatidic acid receptors 1 and 2 play roles in regulation of vascular injury responses but not blood pressure.* Circ Res, 2008. **103**(6): p. 662-70.

126. Fueller, M., et al., *Activation of human monocytic cells by lysophosphatidic acid and sphingosine-1-phosphate.* Cellular signalling, 2003. **15**(4): p. 367-75.

127. Pradere, J.P., et al., *LPA1 receptor activation promotes renal interstitial fibrosis.* J Am Soc Nephrol, 2007. **18**(12): p. 3110-8.

128. Zhao, J., et al., *Lysophosphatidic acid receptor 1 modulates lipopolysaccharide-induced inflammation in alveolar epithelial cells and murine lungs.* Am J Physiol Lung Cell Mol Physiol, 2011. **301**(4): p. L547-56.

129. Fischer, D.J., et al., *Short-chain phosphatidates are subtype-selective antagonists of lysophosphatidic acid receptors.* Mol Pharmacol, 2001. **60**(4): p. 776-84.

130. McIntyre, T.M., et al., *Identification of an intracellular receptor for lysophosphatidic acid (LPA): LPA is a transcellular PPARgamma agonist.* Proc Natl Acad Sci U S A, 2003. **100**(1): p. 131-6.

131. Krishnan, J., et al., *Activation of a HIF1alpha-PPARgamma axis underlies the integration of glycolytic and lipid anabolic pathways in pathologic cardiac hypertrophy.* Cell metabolism, 2009. **9**(6): p. 512-24.

132. Sata, M., et al., *Hematopoietic stem cells differentiate into vascular cells that participate in the pathogenesis of atherosclerosis.* Nat Med, 2002. **8**(4): p. 403-9.

133. Han, C.I., G.R. Campbell, and J.H. Campbell, *Circulating bone marrow cells can contribute to neointimal formation.* J Vasc Res, 2001. **38**(2): p. 113-9

134. Tanaka, K., et al., *Diverse contribution of bone marrow cells to neointimal hyperplasia after mechanical vascular injuries.* Circ Res, 2003. **93**(8): p. 783-90.

135. Bentzon, J.F., et al., *Smooth muscle cells in atherosclerosis originate from the local vessel wall and not circulating progenitor cells in ApoE knockout mice.* Arterioscler Thromb Vasc Biol, 2006. **26**(12): p. 2696-702.

136. Yu, H., et al., *Bone marrow-derived smooth muscle-like cells are infrequent in advanced primary atherosclerotic plaques but promote atherosclerosis.* Arterioscler Thromb Vasc Biol, 2011. **31**(6): p. 1291-9.

137. Groenewegen, H.C., et al., *Non-bone marrow origin of neointimal smooth muscle cells in experimental in-stent restenosis in rats.* J Vasc Res, 2008. **45**(6): p. 493-502.

138. Rodriguez-Menocal, L., et al., *The origin of post-injury neointimal cells in the rat balloon injury model.* Cardiovasc Res, 2009. **81**(1): p. 46-53.

139. Daniel, J.M., et al., *Time-course analysis on the differentiation of bone marrow-derived progenitor cells into smooth muscle cells during neointima formation.* Arterioscler Thromb Vasc Biol, 2010. **30**(10): p. 1890-6.

140. Zaslavsky, A., et al., *Homo- and hetero-dimerization of LPA/S1P receptors, OGR1 and GPR4.* Biochim Biophys Acta, 2006. **1761**(10): p. 1200-12.

141. Fourcade, O., et al., *Secretory phospholipase A2 generates the novel lipid mediator lysophosphatidic acid in membrane microvesicles shed from activated cells.* Cell, 1995. **80**(6): p. 919-27.

142. Sano, T., et al., *Multiple mechanisms linked to platelet activation result in lysophosphatidic acid and sphingosine 1-phosphate generation in blood.* J Biol Chem, 2002. **277**(24): p. 21197-206.

143. Davi, G. and C. Patrono, *Platelet activation and atherothrombosis.* N Engl J Med, 2007. **357**(24): p. 2482-94.

144. Gerrard, J.M. and P. Robinson, *Identification of the molecular species of lysophosphatidic acid produced when platelets are stimulated by thrombin.* Biochim Biophys Acta, 1989. **1001**(3): p. 282-5.

145. Williamson, P. and R.A. Schlegel, *Transbilayer phospholipid movement and the clearance of apoptotic cells.* Biochim Biophys Acta, 2002. **1585**(2-3): p. 53-63.

146. Boren, J., et al., *Identification of the principal proteoglycan-binding site in LDL. A single-point mutation in apo-B100 severely affects proteoglycan interaction without affecting LDL receptor binding.* J Clin Invest, 1998. **101**(12): p. 2658-64.

147. Tabas, I., K.J. Williams, and J. Boren, *Subendothelial Lipoprotein Retention as the Initiating Process in Atherosclerosis: Update and Therapeutic Implications.* Circulation, 2007. **116**(16): p. 1832-1844.

148. Skalen, K., et al., *Subendothelial retention of atherogenic lipoproteins in early atherosclerosis.* Nature, 2002. **417**(6890): p. 750-4.

149. Levitan, I., S. Volkov, and P.V. Subbaiah, *Oxidized LDL: diversity, patterns of recognition, and pathophysiology.* Antioxid Redox Signal, 2010. **13**(1): p. 39-75.

150. Smith, D.F., et al., *GRO family chemokines are specialized for monocyte arrest from flow.* American Journal of physiology. Heart and circulatory physiology, 2005. **289**(5): p. H1976-84.

151. Dusaulcy, R., et al., *Adipose-specific disruption of autotaxin enhances nutritional fattening and reduces plasma lysophosphatidic acid.* J Lipid Res, 2011. **52**(6): p. 1247-55.

152. Aviram, M., et al., *Lesioned low density lipoprotein in atherosclerotic apolipoprotein E-deficient transgenic mice and in humans is oxidized and aggregated.* Biochem Biophys Res Commun, 1995. **216**(2): p. 501-13.

153. Palinski, W., et al., *ApoE-deficient mice are a model of lipoprotein oxidation in atherogenesis. Demonstration of oxidation-specific epitopes in lesions and high titers of autoantibodies to malondialdehyde-lysine in serum.* Arterioscler Thromb, 1994. **14**(4): p. 605-16.

154. Gustin, C., et al., *Upregulation of pentraxin-3 in human endothelial cells after lysophosphatidic acid exposure.* Arterioscler Thromb Vasc Biol, 2008. **28**(3): p. 491-7.

155. Schober, A., et al., *Stabilization of atherosclerotic plaques by blockade of macrophage migration inhibitory factor after vascular injury in apolipoprotein E-deficient mice.* Circulation, 2004. **109**(3): p. 380-5.

156. Bernhagen, J., et al., *MIF is a noncognate ligand of CXC chemokine receptors in inflammatory and atherogenic cell recruitment.* Nat Med, 2007. **13**(5): p. 587-96.

157. Oynebraten, I., et al., *Rapid chemokine secretion from endothelial cells originates from 2 distinct compartments.* Blood, 2004. **104**(2): p. 314-20.

158. Hol, J., L. Wilhelmsen, and G. Haraldsen, *The murine IL-8 homologues KC, MIP-2, and LIX are found in endothelial cytoplasmic granules but not in Weibel-Palade bodies.* J Leukoc Biol, 2010. **87**(3): p. 501-8.

159. Smyth, S.S., et al., *Roles of lysophosphatidic acid in cardiovascular physiology and disease.* Biochim Biophys Acta, 2008. **1781**(9): p. 563-70.

160. Lee, H., et al., *Lysophospholipids increase ICAM-1 expression in HUVEC through a Gi- and NF-kappaB-dependent mechanism.* Am J Physiol Cell Physiol, 2004. **287**(6): p. C1657-66.

161. Lin, C.I., et al., *Lysophospholipids increase IL-8 and MCP-1 expressions in human umbilical cord vein endothelial cells through an IL-1-dependent mechanism.* J Cell Biochem, 2006. **99**(4): p. 1216-32.

162. Calvayrac, O., et al., *CCL20 is increased in hypercholesterolemic subjects and is upregulated by LDL in vascular smooth muscle cells: role of NF-kappaB.* Arterioscler Thromb Vasc Biol, 2011. **31**(11): p. 2733-41.

163. Hayashi, K., et al., *Phenotypic modulation of vascular smooth muscle cells induced by unsaturated lysophosphatidic acids.* Circ Res, 2001. **89**(3): p. 251-8.

164. Fueller, M., et al., *Activation of human monocytic cells by lysophosphatidic acid and sphingosine-1-phosphate.* Cell Signal, 2003. **15**(4): p. 367-75.

165. Kumar, A. and V. Lindner, *Remodeling with neointima formation in the mouse carotid artery after cessation of blood flow.* Arterioscler Thromb Vasc Biol, 1997. **17**(10): p. 2238-44.

166. Woollard, K.J. and F. Geissmann, *Monocytes in atherosclerosis: subsets and functions.* Nat Rev Cardiol, 2010. **7**(2): p. 77-86.

167. Damas, J.K., et al., *CXC-chemokines, a new group of cytokines in congestive heart failure--possible role of platelets and monocytes.* Cardiovasc Res, 2000. **45**(2): p. 428-36.

168. Holm, T., et al., *CXC-chemokines in coronary artery disease: possible pathogenic role of interactions between oxidized low-density lipoprotein, platelets and peripheral blood mononuclear cells.* J Thromb Haemost, 2003. **1**(2): p. 257-62.

169. Llodra, J., et al., *Emigration of monocyte-derived cells from atherosclerotic lesions characterizes regressive, but not progressive, plaques.* Proc Natl Acad Sci U S A, 2004. **101**(32): p. 11779-84.

170. Potteaux, S., et al., *Suppressed monocyte recruitment drives macrophage removal from atherosclerotic plaques of Apoe-/- mice during disease regression.* J Clin Invest, 2011. **121**(5): p. 2025-36.

171. Bot, M., et al., *Atherosclerotic lesion progression changes lysophosphatidic acid homeostasis to favor its accumulation.* Am J Pathol, 2010. **176**(6): p. 3073-84.

172. Wallenfeldt, K., et al., *Oxidized low-density lipoprotein in plasma is a prognostic marker of subclinical atherosclerosis development in clinically healthy men.* J Intern Med, 2004. **256**(5): p. 413-20.

173. Nakasaki, T., et al., *Involvement of the lysophosphatidic acid-generating enzyme autotaxin in lymphocyte-endothelial cell interactions.* Am J Pathol, 2008. **173**(5): p. 1566-76.

174. Kanda, H., et al., *Autotaxin, an ectoenzyme that produces lysophosphatidic acid, promotes the entry of lymphocytes into secondary lymphoid organs.* Nat Immunol, 2008. **9**(4): p. 415-23.

175. Portman, O.W., et al., *Metabolism of lysolecithin in vivo: effects of hyperlipemia and atherosclerosis in squirrel monkeys.* J Lipid Res, 1970. **11**(6): p. 596-604.

176. Frei, B., R. Stocker, and B.N. Ames, *Antioxidant defenses and lipid peroxidation in human blood plasma.* Proc Natl Acad Sci U S A, 1988. **85**(24): p. 9748-52.

177. Kato, R., et al., *Transient increase in plasma oxidized LDL during the progression of atherosclerosis in apolipoprotein E knockout mice.* Arterioscler Thromb Vasc Biol, 2009. **29**(1): p. 33-9.

178. Dohi, T., et al., *Increased circulating plasma lysophosphatidic acid in patients with acute coronary syndrome.* Clin Chim Acta, 2012. **413**(1-2): p. 207-12.

179. Weber, C., A. Schober, and A. Zernecke, *Chemokines: key regulators of mononuclear cell recruitment in atherosclerotic vascular disease.* Arterioscler Thromb Vasc Biol, 2004. **24**(11): p. 1997-2008.

180. Swirski, F.K., et al., *Monocyte accumulation in mouse atherogenesis is progressive and proportional to extent of disease.* Proc Natl Acad Sci U S A, 2006. **103**(27): p. 10340-5.

181. Boring, L., et al., *Decreased lesion formation in CCR2-/- mice reveals a role for chemokines in the initiation of atherosclerosis.* Nature, 1998. **394**(6696): p. 894-7.

182. Dawson, T.C., et al., *Absence of CC chemokine receptor-2 reduces atherosclerosis in apolipoprotein E-deficient mice.* Atherosclerosis, 1999. **143**(1): p. 205-11.

183. Guo, J., et al., *Transplantation of monocyte CC-chemokine receptor 2-deficient bone marrow into ApoE3-Leiden mice inhibits atherogenesis.* Arterioscler Thromb Vasc Biol, 2003. **23**(3): p. 447-53.

184. Yu, X., et al., *Elevated expression of monocyte chemoattractant protein 1 by vascular smooth muscle cells in hypercholesterolemic primates.* Proc Natl Acad Sci U S A, 1992. **89**(15): p. 6953-7.

185. Han, K.H., et al., *Chemokine receptor CCR2 expression and monocyte chemoattractant protein-1-mediated chemotaxis in human monocytes. A regulatory role for plasma LDL.* Arterioscler Thromb Vasc Biol, 1998. **18**(12): p. 1983-91.

186. Tsou, C.L., et al., *Critical roles for CCR2 and MCP-3 in monocyte mobilization from bone marrow and recruitment to inflammatory sites.* J Clin Invest, 2007. **117**(4): p. 902-9.

187. Braunersreuther, V., et al., *Ccr5 but not Ccr1 deficiency reduces development of diet-induced atherosclerosis in mice.* Arterioscler Thromb Vasc Biol, 2007. **27**(2): p. 373-9.

188. von Hundelshausen, P., et al., *RANTES deposition by platelets triggers monocyte arrest on inflamed and atherosclerotic endothelium.* Circulation, 2001. **103**(13): p. 1772-7.

189. Huo, Y., et al., *Circulating activated platelets exacerbate atherosclerosis in mice deficient in apolipoprotein E.* Nat Med, 2003. **9**(1): p. 61-7.

190. Braunersreuther, V., et al., *A novel RANTES antagonist prevents progression of established atherosclerotic lesions in mice.* Arterioscler Thromb Vasc Biol, 2008. **28**(6): p. 1090-6.

191. Combadiere, C., et al., *Decreased atherosclerotic lesion formation in CX3CR1/apolipoprotein E double knockout mice.* Circulation, 2003. **107**(7): p. 1009-16.

192. Fong, A.M., et al., *Fractalkine and CX3CR1 mediate a novel mechanism of leukocyte capture, firm adhesion, and activation under physiologic flow.* J Exp Med, 1998. **188**(8): p. 1413-9.

193. Landsman, L., et al., *CX3CR1 is required for monocyte homeostasis and atherogenesis by promoting cell survival.* Blood, 2009. **113**(4): p. 963-72.

194. Moatti, D., et al., *Polymorphism in the fractalkine receptor CX3CR1 as a genetic risk factor for coronary artery disease.* Blood, 2001. **97**(7): p. 1925-8.

195. McDermott, D.H., et al., *Association between polymorphism in the chemokine receptor CX3CR1 and coronary vascular endothelial dysfunction and atherosclerosis.* Circ Res, 2001. **89**(5): p. 401-7.

196. Combadiere, C., et al., *Combined inhibition of CCL2, CX3CR1, and CCR5 abrogates Ly6C(hi) and Ly6C(lo) monocytosis and almost abolishes atherosclerosis in hypercholesterolemic mice.* Circulation, 2008. **117**(13): p. 1649-57.

197. Tacke, F., et al., *Monocyte subsets differentially employ CCR2, CCR5, and CX3CR1 to accumulate within atherosclerotic plaques.* J Clin Invest, 2007. **117**(1): p. 185-94.

198. Bandoh, K., et al., *Lysophosphatidic acid (LPA) receptors of the EDG family are differentially activated by LPA species. Structure-activity relationship of cloned LPA receptors.* FEBS Lett, 2000. **478**(1-2): p. 159-65.

199. *Orphan drug status for LPA1 antagonist AM152 for treatment of idiopathic pulmonary fibrosis* http://www.science20.com/news_articles/orphan_drug_status_lpa1_antagonist_am152_treatment_idiopathic_pulmonary_fibrosis-78315, 2011.

200. Charo, I.F. and R. Taub, *Anti-inflammatory therapeutics for the treatment of atherosclerosis.* Nat Rev Drug Discov, 2011. **10**(5): p. 365-76.

201. Aoki, J., et al., *Serum lysophosphatidic acid is produced through diverse phospholipase pathways.* J Biol Chem, 2002. **277**(50): p. 48737-44.

7 Acknowledgement

I would like to express my gratitude to everyone who has supported me throughout the process of this work. First, I would like to thank my supervisor, Prof. Dr. Andreas Schober for giving me the opportunity to work in this institute on an interesting topic. This thesis would not have been possible without his support, advice and the good discussions. I am very thankful to Prof. Dr. Jürgen Bernhagen for taking the time to review this thesis as a co-examiner and to Dr. Schlaich for being my third examiner.

I would like to thank my colleuges, Xiaofeng, Mali, Shamima, Yuanyuan and Zhou Zhe for providing a pleasant environment in the lab. I would like to thank Mali and Shamina for the fruitful discussions, exchange of ideas and for being a good friend. Furthermore, I want to express my gratitude to Kathrin, Anna and Yvonne Jansen for the excellent technical assistance and help with the immunostainings. I would also like to thank Remco Megens for helping me with the two-photon microscopy experiments. In addition, I want to thank Dr. Jerold Chun for providing the sections from LPA receptor knock out mouse and Zhou Zhe for helping me with the *ex vivo* perfusion and intravital microscopy experiments. I also want to thank Prof. Dr. Christian Weber and all the colleagues of IMCAR.

I want to express my gratitude to Dr. Dhandapany for all the guidance throughout the years and my best friends, Raghav and Bineep for their encouragement. Last but not least, I would like to thank my mom and my sister for their constant love and support.

This study was funded by Deutsche Forschungsgemeinschaft (SCHO1056/3-1, WE1913/7-2, WE1913/11-1), a grant from the Interdisciplinary Centre for Clinical Research “BIOMAT” within the faculty of Medicine at the RWTH Aachen University and by the “Munchner Medizinischen Wochenschrift”.

8 Curriculum Vitae

PERSONAL DATA:

Name:	Pallavi Subramanian
Date of birth:	22.06.1986
Place of birth:	Pondicherry, India
Nationality:	Indian
Gender:	Female

EDUCATION:

2001-2003:	High school education, G.R.G matriculation higher secondary school in Coimbatore, India.
2003-2006:	B.Sc. Biotechnology, Dr. G.R.D College of science, Coimbatore, India.
2006-2008:	M.Sc. Biotechnology, P.S.G College of arts and science, Coimbatore, India.
2008-2012:	PhD, University hospital RWTH Aachen, Institute for Molecular Cardiovascular Research (IMCAR), Aachen, Germany.

PUBLICATIONS:

Hamesch K, **Subramanian P**, Li X, Dembowsky K, Chevalier E, Weber C, Schober A. The CXCR4 antagonist POL5551 is equally effective as sirolimus in reducing neointima formation without impairing re-endothelialisation. Thromb Haemost, 2012;107:356-368.

Zhou Z*****, **Subramanian P***, Sevilmis G, Globke B, Soehnlein O, Karshovska E, Megens RT, Heyll K, Chun J, Saulnier-Blache J, Reinholz M, van Zandvoort M, Weber C, Schober A. Lipoprotein-derived lysophosphatidic acid promotes atherosclerosis by releasing CXCL1 from the endothelium. Cell Metabolism, 2011;13:592-600. *** Equal contribution**

Subramanian P*, Karshovska E*****, Reinhard P, Megens RT, Zhou Z, Akhtar S, Schumann U, Li X, van Zandvoort M, Ludin C, Weber C, Schober A. Lysophosphatidic acid receptors LPA_1 and LPA_3 promote CXCL12-mediated smooth muscle progenitor cell recruitment in neointima formation. Circ Res. 2010;107:96-105. *** Equal contribution**

Subramanian P, Schober A. Neointima formation after vascular injury: Is it all about cd39? Thromb Haemost. 2010;103:257-258.

L.V.K.S. Bhaskar, K. Thangaraj, **Subramanian P**, P.S Dandapani, S. F. D. Paul. Molecular genetic analysis of Neuropeptide Y (NPY) gene in patients with cardiac arrhythmia. Sri Ramachandra Journal of medicine, August 2008, 8-13.

CONFERENCES:

Oral presentation- 'LPA induced chemokine functions in vascular disease' at **Frontiers in Vascular Biology, Minerva School, Jerusalem, Israel (2010)**

Oral presentation- 'Lysophosphatidic acid induces CXCL12 dependent recruitment of smooth muscle progenitor cells for vascular repair through $LPA_{1/3}$' at **16th International Vascular Biology Meeting, Los Angeles, USA (2010)**

Poster presentation- 'Lysophosphatidic acid induces CXCL12 dependent recruitment of smooth muscle progenitor cells for vascular repair through $LPA_{1/3}$' at **Frontiers in Cardiovascular Biology, Berlin, Germany (2010)**

Poster presentation- 'Smooth muscle cell specific deletion of HIF-1alpha results in an unstable plaque phenotype after vascular injury in ApoE deficient mice' at **European Society of Cardiology, Paris, France (2011)**

Poster presentation- ‘Smooth muscle cell specific deletion of HIF-1alpha results in an unstable plaque phenotype after vascular injury in ApoE deficient mice’ at **Joint meeting European Society of Microcirculation (ESM) and German Society of Microcirculation and Vascular Biology (GfMVB), Munich, Germany (2011)**